STUDY OF A SPACECRAFT EQUIPPED WITH A LARGE APERTURE ANTENNA FOR MOBILE-SATELLITE SERVICE

ADIAN ASTRONAUTICS LIMITED

CANADIAN ASTRONAUTICS LIMITED

Suite 201, 1024 Morrison Drive, Ottawa, Ontario K2H 8K7
(613) 820-8280

STUDY OF A SPACECRAFT EQUIPPED WITH A LARGE APERTURE ANTENNA FOR MOBILE-SATELLITE SERVICE

Prepared Under DOC Contract 15ST.36100-8-4003

September 1979

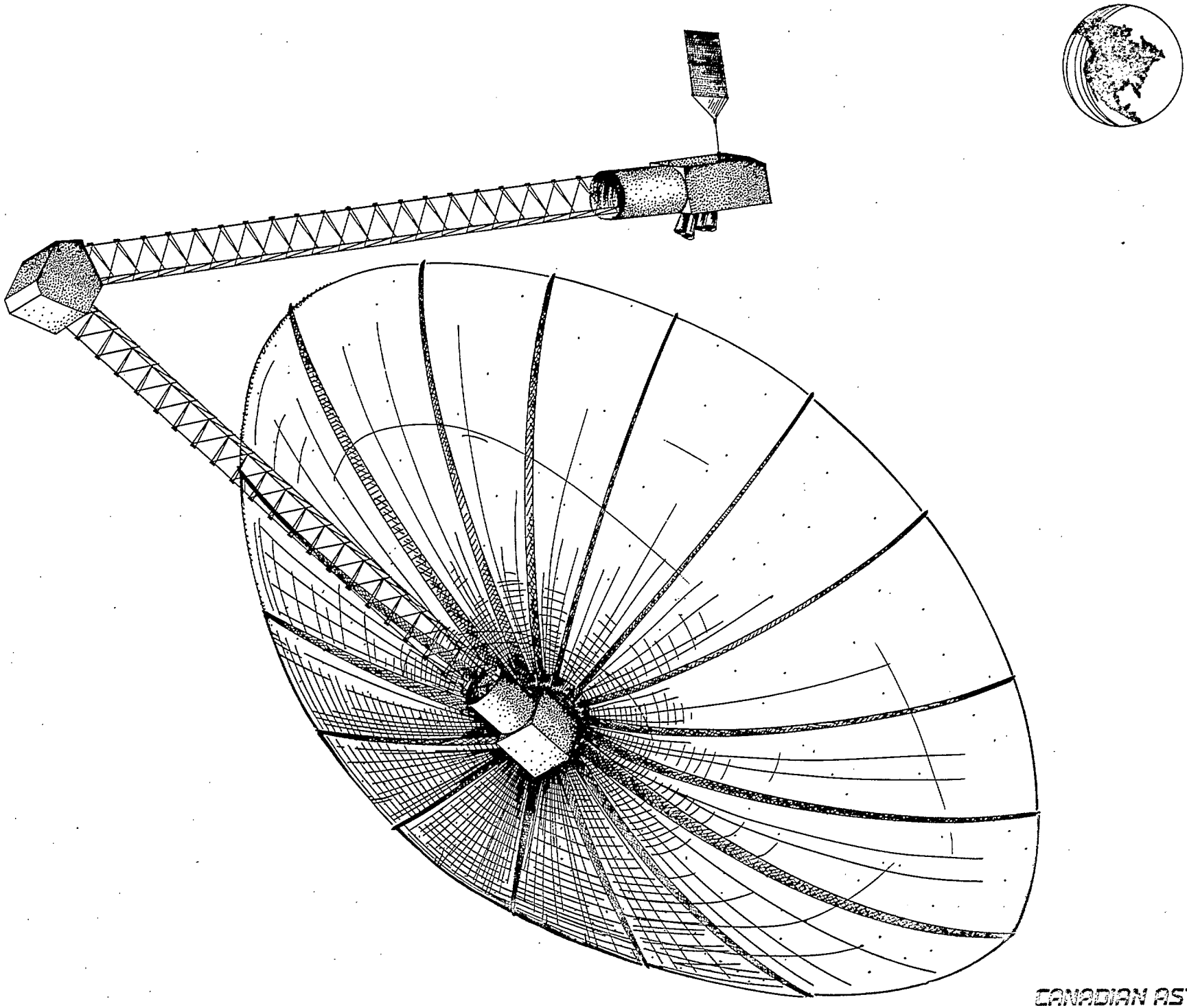

CANADIAN ASTRONAUTICS LIMITED
OTTAWA CANADA

CANADIAN ASTRONAUTICS LIMITED

Suite 201, 1024 Morrison Drive, Ottawa, Ontario K2H 8K7
(613) 820-8280

EXECUTIVE SUMMARY

This report describes a conceptual design for a mobile satellite communications system providing two-way voice service to a large number of mobile transceivers located anywhere within the Canadian boundaries. This system employs a spacecraft equipped with a large aperture antenna, thus permitting the mobile radio telephones to be simple, inexpensive low power units. The report defines the performance requirements for such a system, then identifies the range of system parameters available to the designer. A discussion of the selection of a baseline for the system parameters then follows and a conceptual baseline system design is presented, starting with the system design, and followed by a description of the space and ground-segment elements. The system cost is estimated using, in part, a modified version of the CAL satellite cost model. A detailed interference analysis completes the report. In this section, the baseline system is used to calculate the mutual interference between this new satellite-based service and other services with the same radio-frequency allocation. This analysis provides input for determining the frequency allocations for Mobile Satellite Communications Service, to be discussed at the upcoming 1979 WARC.

The baseline design chosen for evaluation is able to provide two-way full duplex voice service for up to 26,800 users generating 124 x 10^6 min/yr of traffic. By employing twenty-four beams, and reusing three frequency bands 8 times, the Canadian region is fully covered. Each beam contains 58 channels, which is adequate to provide 99% system availability for the estimated peak traffic projection. The system requires 1.35 MHz of bandwidth for

each frequency band on the uplink and the same for each downlink. With guard-bands, the following UHF frequencies are used:

	Uplink	Downlink	
Band 1	824 - 822	860 - 862	MHz
Band 2	822 - 820	862 - 864	MHz
Band 3	820 - 818	864 - 866	MHz

The system thus requires a total of 6 MHz for the uplink and 6 MHz for the downlink, the same as for a standard TV broadcast channel.

Existing TV stations will interfere with the proposed system, but very few UHF stations are in use in the proposed coverage region. Proper frequency co-ordination and satellite beam shaping will permit the operation of this system with other mobile services such as the (experimental) cellular mobile system. For this system to operate, the frequency allocation for the uplinks cannot be shared by broadcast services.

The spacecraft is unusual because it is dominated by a 26 meter (85 ft.) diameter reflector. Several manufacturers have the capability of producing such a sub-system, using technology similar to ATS-6. The UHF frequencies do not require exceptionally high dimensional tolerances on this large structure, thus lowering the development costs. A novel phased-array-feed approach is proposed which will permit mechanical distortion and movement of the reflector without affecting the communication system. Other than the antenna, the subsystems for power, RF generation and attitude control are similar to existing designs. A shuttle launch is used for the baseline.

The total system capital cost, including spares, ground stations and user terminals, and interest charges, is estimated (in 1990 dollars) to be $613,689 K. The operating costs, repayment of principal, and interest charges per year are projected as $89,893 K. The projected revenue over ten years for the system is $1,167,500 K. This is based on typical growth curve for users, and permits a payback with profit in less than ten years.

Further study is recommended in the areas of electrical and mechanical design of specific large antenna structures, and in a detailed system design of a baseline system.

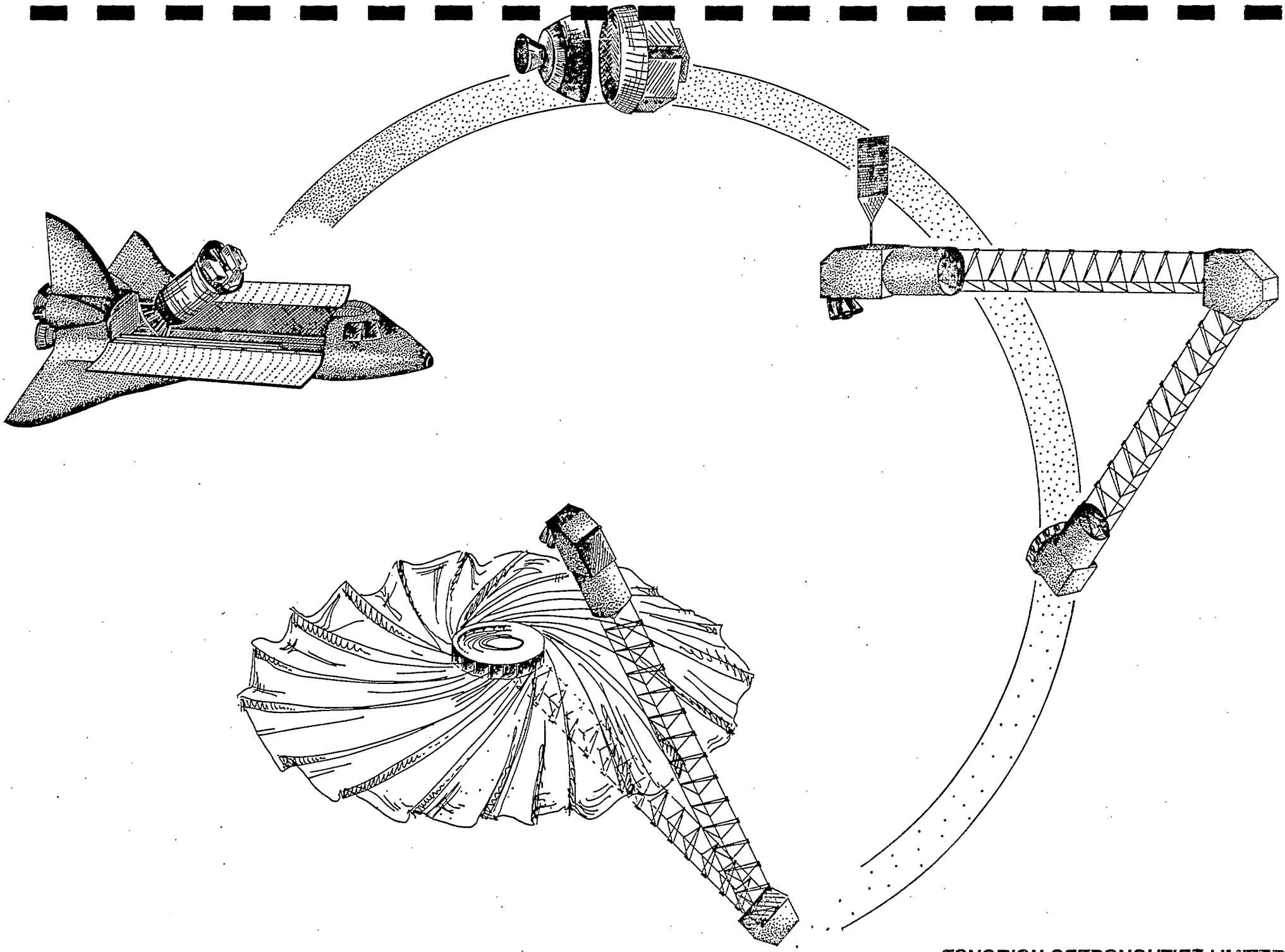

CANADIAN ASTRONAUTICS LIMITED
OTTAWA CANADA

TABLE OF CONTENTS

1.0 INTRODUCTION

This report describes a conceptual design for a typical second generation mobile satellite communications system, including an analysis of interference with other services using the same frequencies. A unique feature of this system is a spacecraft utilizing a very large aperture antenna, permitting communications capability to a large number of mobile tranceivers located anywhere within the Canadian land mass.

The report first defines the performance requirements for such a system, then identifies the range of system parameters available to the designer. A discussion of the selection of a baseline for the system parameters then follows, with brief consideration of the effects upon the resulting dependent system parameters.

A conceptual baseline system design is then presented, starting with the system design, followed by a description of the space and ground segment elements. The system cost is estimated using, in part, a modified version of the CAL satellite cost model.

A detailed interference analysis completes the report. In this section, the baseline system is used to calculate the mutual interference between this new satellite-based service and other services with the same radio-frequency allocation. This analysis provides input for determining the frequency allocations for Mobile Satellite Communications Service, to be discussed at the upcoming 1979 WARC.

2.0 SYSTEM ANALYSIS

2.1 System Requirements

This section contains the performance requirements identified for a communication system consisting of an ensemble of mobile radio telephones linked by means of a geostationary satellite.

2.1.1 Purpose

The system shall provide toll-grade full duplex voice communications to mobile transceivers located within the area defined in Paragraph 2.1.2.

2.1.2 Coverage Area

The system shall provide communications coverage to all regions of Canada. This coverage shall be approximated by a rectangle centered on Canada and subtending 3^{o} north-south by 8^{o} east-west from geosynchronous distance.

2.1.3 Frequencies

The transmissions between the satellite and the mobile users shall be at UHF frequencies compatible with Canadian frequency allocation proposals.

2.1.4 Compatibility

The system shall be compatible with and complimentary to the regular general land radio mobile radio system (GLMRS) and the newer cellular mobile radio systems (CMRS). As a goal, it would be desirable for the system to be interoperable with the CMRS.

2.1.5 Launch Date, Design Life

The program shall require first launch in 1990 and the initial spacecraft will have a design life of 10 years.

2.1.6 Number of Users, Utilization

The system shall support the number of Canadian users projected by a traffic growth model for the year 2000. The system availability shall be 99%.

2.1.7 Orbit Slot

The nominal orbit slot shall be taken as 110^{o} W longitude, with 0^{o} inclination.

2.1.8 Launch Vehicle

The space segment (satellite) shall be launched using the Space shuttle Transportation System (STS).

2.2 Range of System Parameters

The initial range of parameters available to establish the system design is very large. This section lists these parameters and identifies the particular set which have been chosen for the conceptual baseline model.

2.2.1 Frequencies

The following UHF frequency bands have been suggested for use by a future mobile-satellite system:

2.2.1 Frequencies (Cont'd.)

UPLINK	DOWNLINK
380 MHz	250 MHz
400 MHz	900 MHz
600 MHz	900 MHz
800 MHz	900 MHz
1600 MHz	1500 MHz

The 800 to 900 MHz band has been used for the initial analysis because this frequency band is presently the least congested of the choices. In addition, some recent work in the U.S. has been done in this band and it is thus interesting to see if these frequencies can be used in Canada as well.

For some system configurations, it is necessary to provide a 'backhaul' link to a central station for signal switching and control. This will probably be at SHF frequencies, and for the purpose of this study is chosen in the 7 and 8 GHz bands. There is no reason why 4 and 6 or 12 and 14 GHz links could not be used instead.

2.2.2 Modulation Schemes

Present mobile systems use analogue narrow band FM for their transmission. For this study, the same type of modulation scheme will be used to establish the link margins for the system. It is expected, however, that digital modulation of voice transmissions will be preferred in future systems. In general, using the margins required for analogue FM represents a conservative approach to the link design.

2.2.2 Modulation Schemes (Cont'd.)

Digital modulation of voice signals is accomplished in two steps as follows:

a) Analogue to digital conversion using a pulse coding scheme such as PCM or DM.

b) Modulation of the digital bit stream on a carrier (such as SCPC) using a scheme such as: BPSK, QPSK, DPSK, FSK, FFSK.

The selection of the overall digital modulation scheme thus involves a minimum of two tradeoffs; one for A/D conversion and the other for carrier modulation.

For voice transmission at marginal signal conditions DM is better than PCM since DM has a lower threshold level. In addition, a data rate required for voice A/D conversion delta modulation provides a higher signal-to-quantization distortion ratio than an equivalent PCM system (Ref: CCIR Report 509-2).

These factors, coupled with ease of implementation of DM compared to PCM, suggest the use of DM as the pulse coding scheme for voice transmission.

The question of carrier modulation in an SCPC system is more difficult due to the variety of schemes, each with varying characteristics regarding interference susceptibility, necessary RF bandwidth, demodulator threshold levels (bit error rate versus E_b/N_o), etc.

2.2.2 Modulation Schemes (Cont'd.)

The CCIR draft report (8/519) discusses briefly the question of carrier modulation and suggests that new modulation techniques such as Fast FSK (FFSK) and Tamed FM (TFM) may be superior to the phase shift keyed (PSK) schemes in a crowded spectral environment of a UHF Mobile-Satellite System. (i.e., 25 KHz channel spacing.)

Based on these considerations an overall digital modulation scheme consisting of DM/FFSK may be the most suitable; particularly in a potentially heavy interference environment. Further data is required regarding FFSK to assign to DM/FFSK a threshold C/N_o and a corresponding level of intelligibility of voice transmission - in order to make a choice.

Further overall considerations regarding either analogue or digital transmission of voice are the use of either for data transmission such as fascmile. The CCIR suggests that a mobile-satellite voice circuit be capable of supporting a 2.4 Kbit data rate. In addition, the use of voice activation and companding reduces the required ground to satellite transmission EIRP for a given uplink C/N_o.

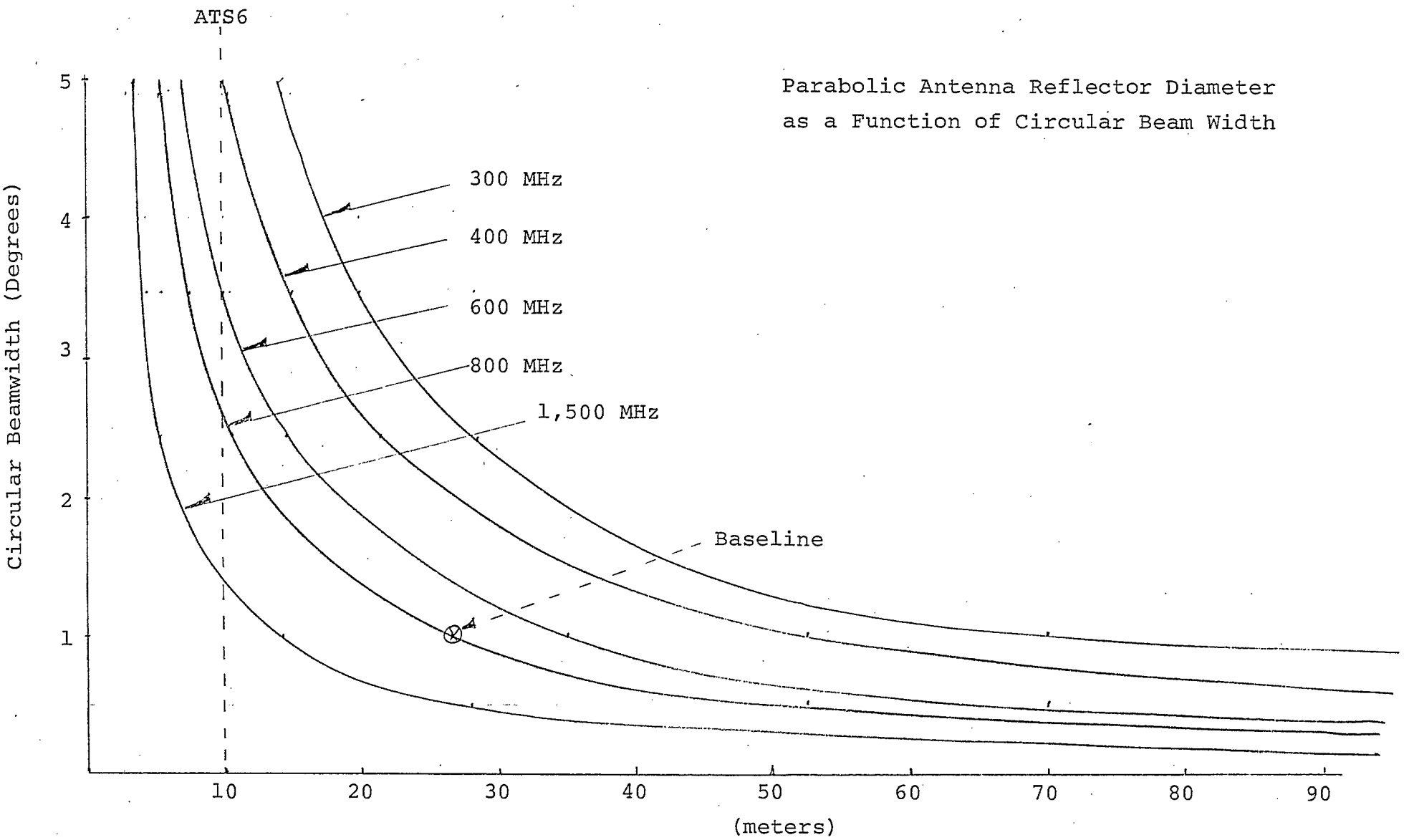
ATS6
Parabolic Antenna Reflector Diameter
as a Function of Circular Beam Width
Circular Beamwidth (Degrees)
5
4
3
2
1
300 MHz
400 MHz
600 MHz
800 MHz
1,500 MHz
Baseline
10
20
30
40
50
60
70
80
90
(meters)

Figure 2.2-0

2.2.3 Coverage Patterns for Antennas

The area to be covered is specified in Section 2.1.2. At the outset of the study, it was required to investigate the implication of providing this coverage by beams of $8^{o} \times 3^{o}$, $4^{o} \times 3^{o}$, $2^{o} \times 3^{o}$, $1^{o} \times 1^{o}$ and $\frac{1}{2}^{o} \times \frac{1}{2}^{o}$. The required parabolic reflector diameter for each of these beam sizes is shown in Figure 2.2-0 for the different frequencies. As the shuttle payload bay diameter is approximately 3 meters, all of these reflectors must be deployed in some manner after launch. Note also the line showing the diameter of the ATS-6 antenna reflector in relation to the range of existing designs.

The ground transceivers will usually be mounted on mobile platforms such as automobiles or trucks and thus will be equipped with very simple antennas. The polarization of these simple antennas is difficult to control and the orientation is constantly changing. For these reasons, the UHF receive and transmit antennas on the spacecraft will be circularly polarized.

2.2.4 Traffic Model

Appendix A contains a description of the approach used to determine the number of users and the total number of minutes per year of traffic that the system must support. This analysis projects the following traffic for the year 2000:

number of users	26,800
total traffic	124×10^{6} min/yr.

2.2.5 System Sizing Based on Capacity

Appendix B is an analysis of the channel capacity required to provide 99% availability for a system with the traffic loading of section 2.4, and a variable number of

channels/beam. Table 2.4 summarizes the results of this analysis.

# OF USERS 26,800 TOTAL TRAFFIC 124 x 10^6 MIN/YR					
# of beams, n	1	2	3	24	96
Traffic/Beam x 10^6 min/yr	124	62	31	5.17	1.29
# User/Beam x 10^3	26.8	13.4	6.7	1.12	0.28
% Extra Channels for 99% Avail.	8	10	13	30	60
# Channels/Beam	1147	584	300	58	18
Uplink or Downlink Band-Width/bm (MHz)	28.675	14.600	7.500	1.450	0.450
Min. # of Diff. Frequencies	1	2	2	3	3
Total bandwidth (MHz) Up or Down	28.675	29.200	15.000	4.350	1.350

NUMBER OF CHANNELS/BEAM
FOR MEAN USAGE ESTIMATE (YR 1995)

TABLE 2.4

2.2.6 RF Link Budgets

Typical link budgets are presented in Appendix C for the various up and downlink frequencies and for the range of coverage areas. The assumptions used to arrive at these budgets are:

- The required C/N_o is 53 dB Hz, for a one way link. This is greater by 1 dB than that specified in Ref. 2-8 for toll grade service.
- The ground-mobile antennas have hemispherical patterns and are circularly polarized. The maximum polarization loss is taken as 3 dB.
- No backoff of the output stage is included.
- Each channel has 25 KHz spacing and 18 KHz bandwidth. Baseband is 4 KHz.
- The gain at the edge of the coverage area of the spacecraft antenna is 4.1 dB below the peak.

3.0 CONCEPTUAL BASELINE SYSTEM DESIGN

This section describes one baseline conceptual design for a communications system utilizing a spacecraft equipped with a large aperture antenna. There are many variations of the baseline design that can be considered. These alternatives should be analyzed in a complete system design and trade-off study once the frequency allocations are internationally agreed upon.

The strawman baseline system is designed to provide communication capability by means of mobile transceivers located anywhere on the Canadian land mass. The complete system is comprized of the five elements shown in Figure 3-1, these are:

- the space segment
- a group of pilot transmitters
- an ensemble of mobile transceivers
- a central control station
- a group of regional ports.

The space segment consists of the spacecraft, which is equipped with a large aperture antenna and is optimized for launch by the Shuttle Transportation System. In the operational phase, spare spacecraft would also be deployed in orbit, in order to ensure adequate system availability.

The pilot transmitters are located on the ground and are used to direct the different antenna beams of the spacecraft at the appropriate areas of the Canadian land mass.

The mobile transmitters are similar in complexity to those currently used for general radio/telephone service. They differ in transmitting frequency and channels are automatically assigned by the central control station.

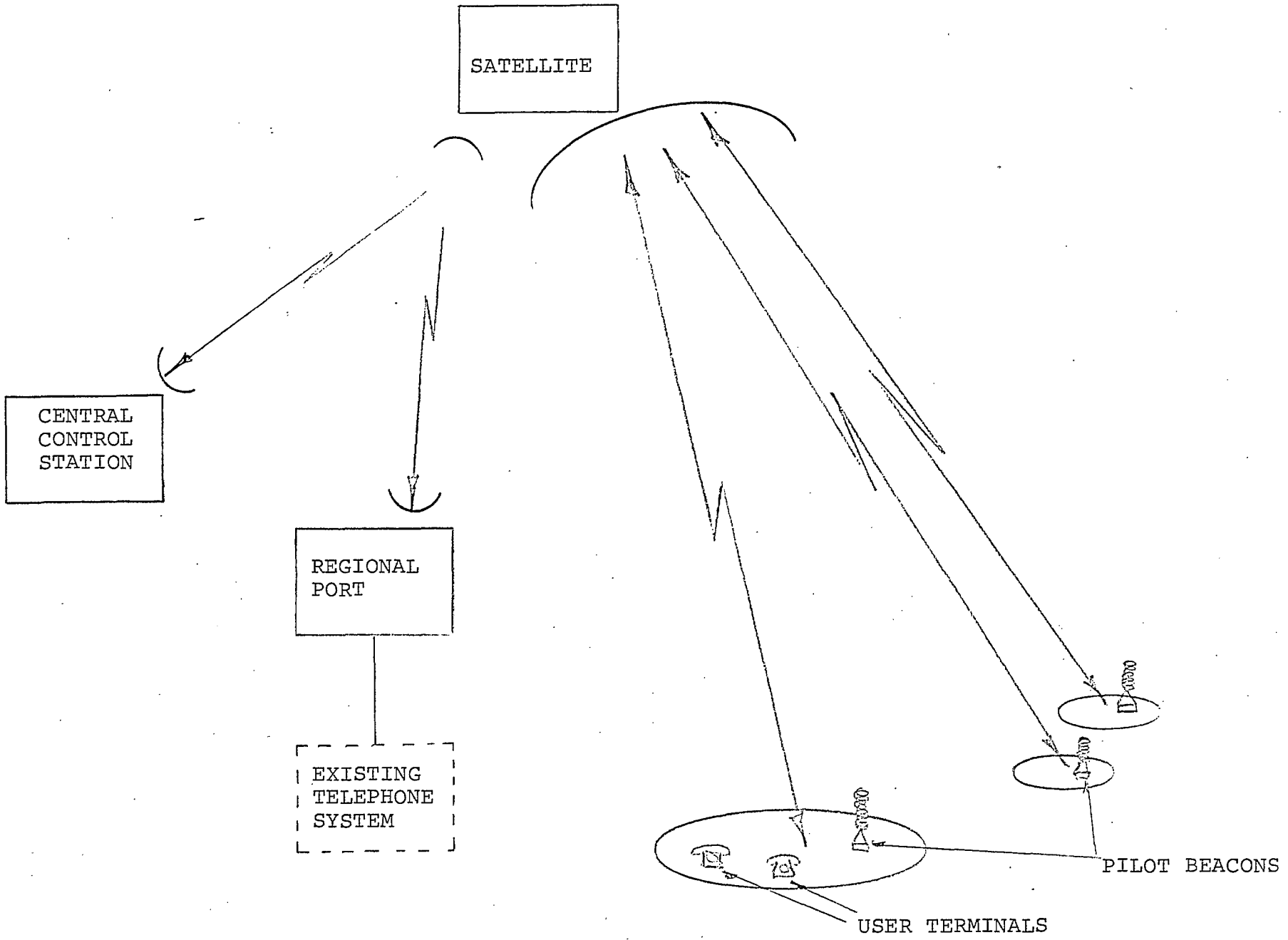

FIGURE 3.1 ELEMENTS OF THE SYSTEM

3.0 CONCEPTUAL BASELINE SYSTEM DESIGN (Cont'd.)

The central control station provides the capabilities for telemetry, tracking and command and monitors the housekeeping telemetry reports from the spacecraft. Orbit determination and stationkeeping are provided from this station. The central station provides a back-haul link at SHF for both the satellite-mobile and mobile - satellite links. The central station provides the switching capability necessary to connect any incoming call to another mobile or to the conventional telephone network. Note that this implies that any mobile user of the satellite system can communicate to a mobile user in a cellular mobile system as well. Traffic loading and billing are monitored and controlled from the central ground station.

The regional ports provide access to terrestrial systems in specific areas of Canada and are thus similar in design to the central control station but lacking the TT & C capability of the latter.

3.1 System Design

The traffic model presented in Section 2.2.4 projects the following estimates of users for the year 2000:

Total number of users	26,800
Total traffic	124,000,000 min/yr.

This estimate is for the mean value between the maximum and minimum projections. The year 2000 is chosen for system sizing because it represents the last operational year of a spacecraft with a ten year design life, in other words, a system inauguration in 1990.

3.1 System Design (Cont'd.)

The baseline system selected for this analysis has 24 contiguous 1^{o} x 1^{o} beams which tesselate the Canadian landmass into hexagonal coverage areas as shown in Figure 3-2. For this number of beams and assuming an equal number of users for each beam, the traffic model shows that 58 channels per beam are required to provide 99% availability. A minimum of three different frequency bands are required in order that no adjacent beams are served by the same frequency.

Thus the system requires a total bandwidth of:

(3 frequencies) x (25KHz/channel) X (58 channels) = 4.35 MHz

for the uplink at UHF and another 4.35 MHz for the downlinks. The arrangement of center frequencies to beams is shown in Figure 3-3, where the beams are designated by a number from 1 to 24 and the frequencies from 1 through 3. Also shown in the figure is a beam group which is defined as a set of beams, each served by a different frequency. It will be seen later that each beam group will be processed by the same local oscillators in the spacecraft transponder. It is not necessary for the three beams in the beam group to be contiguous.

For the baseline design the UHF bands have been chosen to be:

	Uplink	Downlink	
Band 1	824 - 822	860 - 862	MHz
Band 2	822 - 820	862 - 864	MHz
Band 3	820 - 818	864 - 866	MHz

The relationship of these bands to some other users in the 806 - 890 MHz band are shown in Figure 3.4.

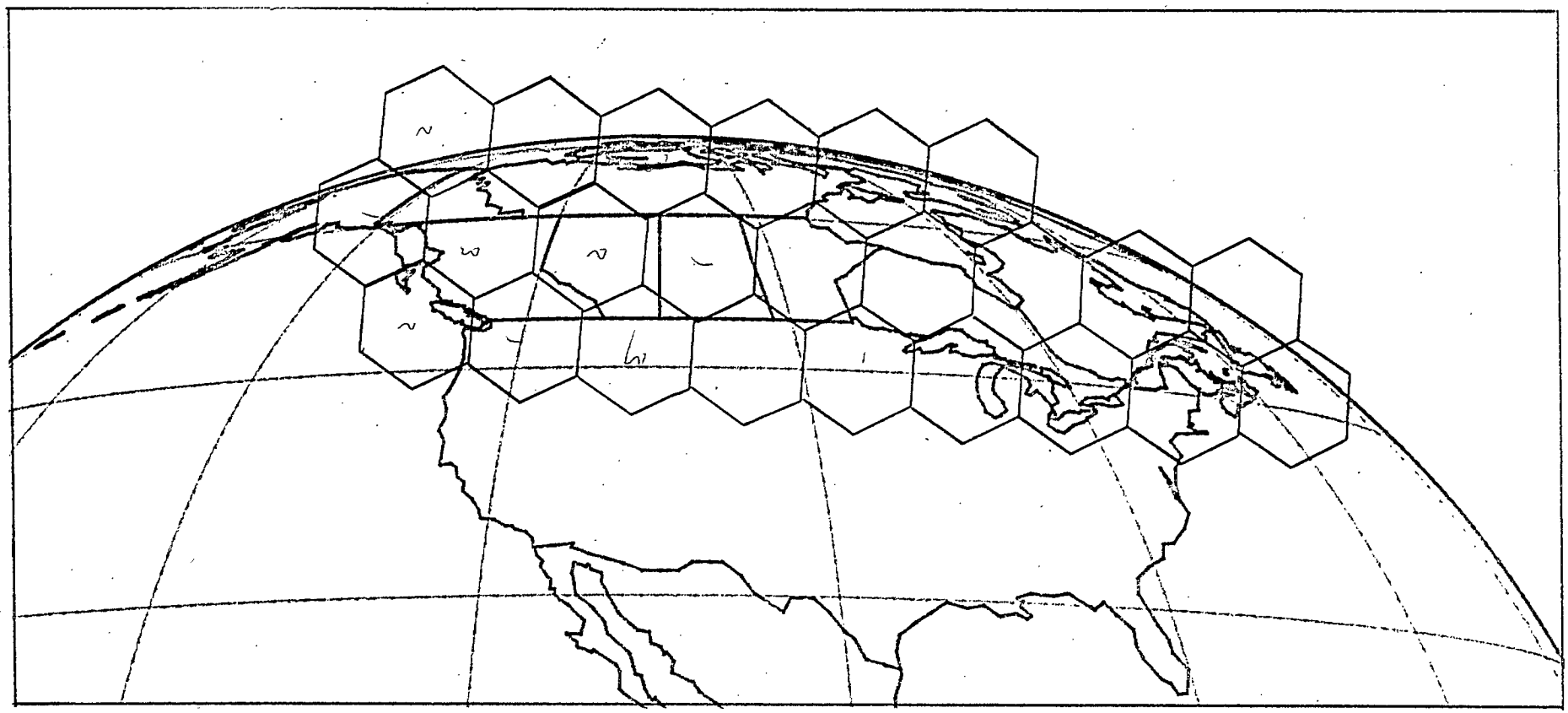

BEAM PATTERN FOR CANADIAN COVERAGE

FIGURE 3.2

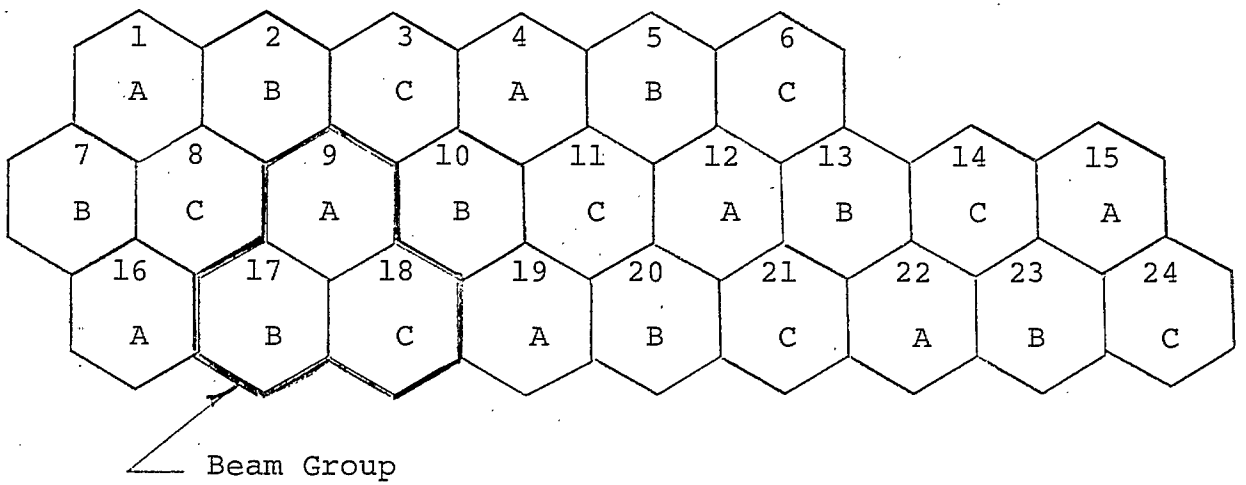

FIGURE 3.3 Frequency Reuse Plan

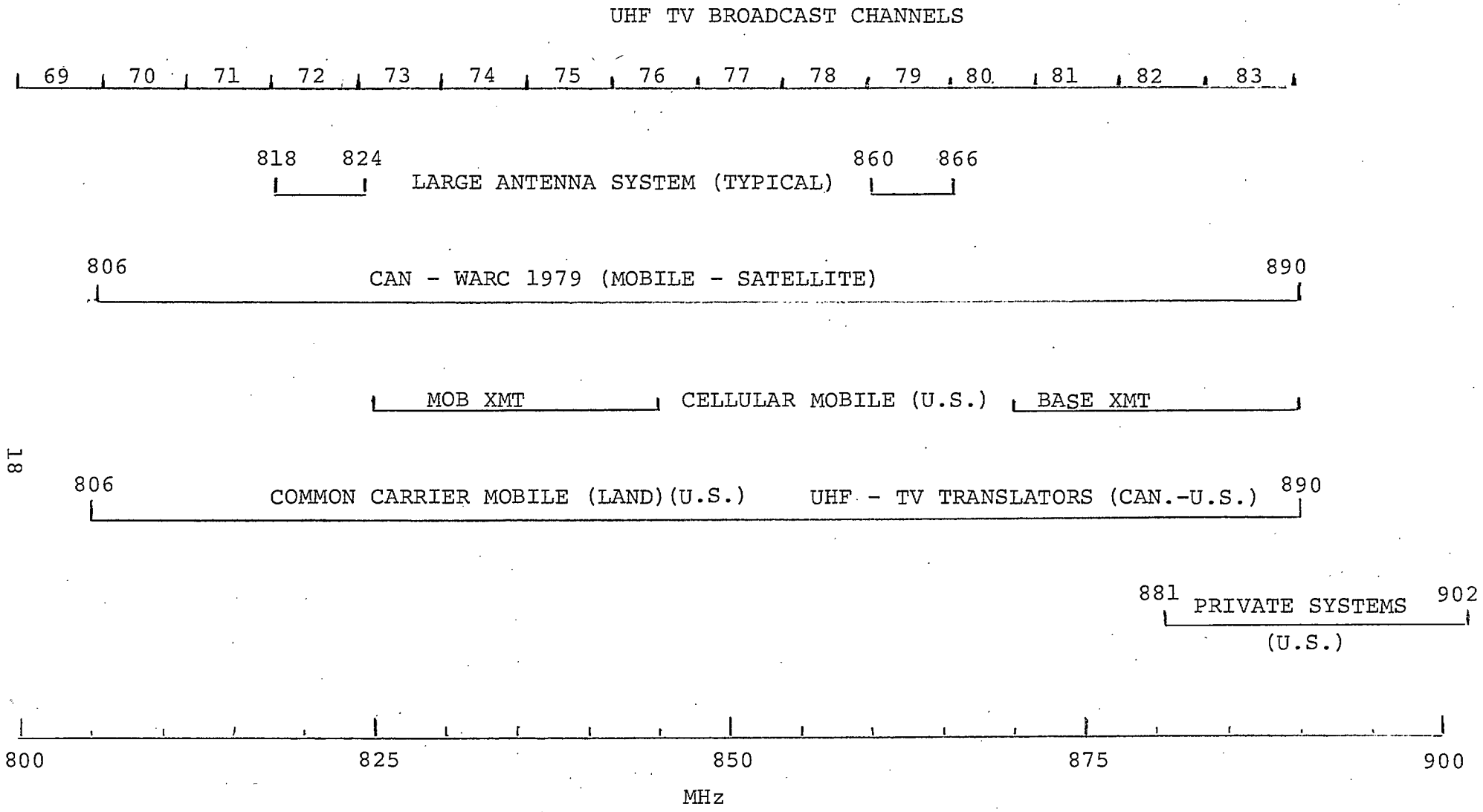

FIGURE 3.4 USE OF FREQUENCY SPECTRUM 800 - 900 MHz

3.1 System Design (Cont'd.)

The UHF uplink signals are frequency - translated to form a composite IF on board the spacecraft and this is frequency modulated on an SHF downlink. The return signals are transmitted on an SHF uplink to the spacecraft where they are demodulated to a similar IF and separated on the basis of frequency into the proper beam and band channel prior to frequency translation to the UHF downlink frequency.

3.1.1 Co-channel Interference Analysis

Using the interference criteria and the analysis technique presented in Section 5 of this report, it is possible to calculate the effect of transmissions in the same channel from sources located in other beams in the system. The results are presented in this section.

Co-channel interference is computed assuming the worst-case conditions with respect to the number and positions of interfering stations located in other beams sharing the same frequency bands. The signals from stations in other beams will combine with the existing system noise in an assumed additive manner, resulting in an effective noise level. The total signal level from other beams is directly dependent on the satellite antenna pattern, where sidelobes will be present in the direction of the interfering stations. Interference will occur on both the uplink and downlink. On the uplink, ground station transmitters in other beams will cause interference in the desired beam. On the downlink, sidelobes from other beams will cause interference to the desired ground station receiver. The uplink and downlink interference levels, considered separately, are identical due to the reciprocity condition. The assumption is made that the satellite transmit and receive beams are identical in beam width.

3.1.1 Co-channel Interference Analysis (Cont'd.)

Figure 3-5 shows the antenna pattern cross-sections for an unoptimized antenna. Similarity between the cross-section patterns at different cut angles indicated that the antenna pattern is circularly symmetric. Hence the level of interference is only dependent on the angular distance of the interferer from the main lobe, which is another simplifying factor.

For instance, if beam 9 of Figure 3.3 is considered, co-channel interference will result from stations in beams 1, 4, 12, 15, 16, 19 and 22, which all share frequency band A. Each of the frequency bands is shared by 8 beams.

Since the antenna pattern generally falls-off with increasing distance from the main beam, maximum interference will occur in a situation where a desired beam has the most adjacent or neighbouring beams. For example, beam 9 has 4 adjacent beams (1, 4, 16 and 19) in contrast to beam 14 which has only 2 adjacent beams. Beam 9 has the minimum total distance to all interfering beams since it is in the centre of the system. Hence beam 9 will be considered for the purposes of worst-case co-channel interference analysis.

Due to the hexagonal beam structure, interfering beams will occur at a fixed set of distances, which will be called levels of neighbours. For beam 9, interfering beams are loacted at distances of 1.5, 2.60 and 3.97 degrees, measured centre-to-centre. Beams at these distances will be called level 1, 2 and 3 neighbours respectively. In addition to 4 level -1 neighbouring beams, another beam will be placed 1.5 degrees below beam 13. This represents potential interference from the United States.

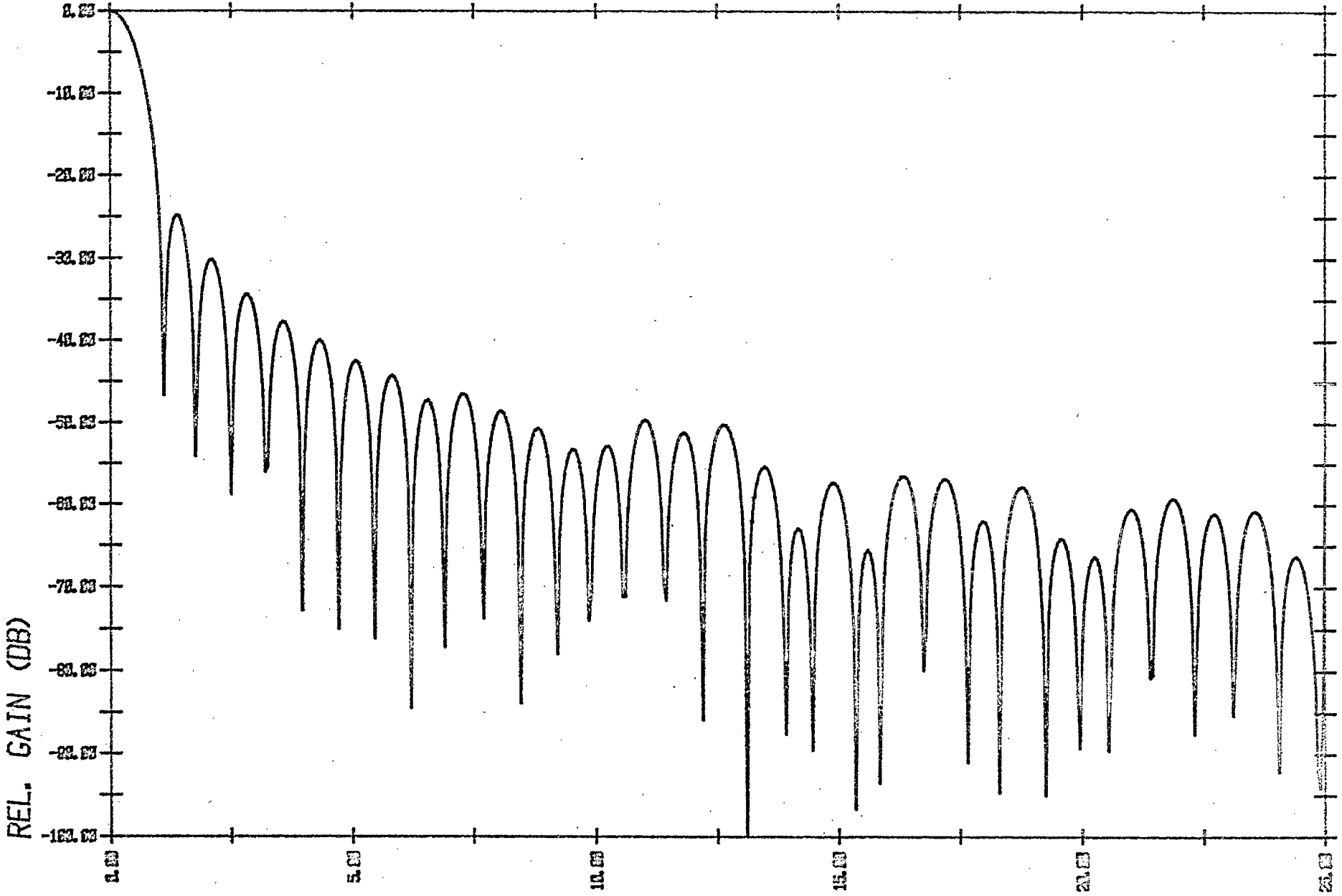

ANTENNA PATTERN WITH FINER GRID

FIGURE 3-5

3.1.1 Co-channel Interference Analysis (Cont'd.)

Shown in Figure 3.6 are the distance limits for each level of neighbouring beams. For a level -1 neighbour, the antenna rejection can range between 25 dB and 55 dB, depending on the location of the ground station within that beam. To maximize the co-channel interference, all interfering stations will be considered to be located at points B, C and D, which are at the points of highest antenna response within the distance limits. In addition, the desired station will be located at point A, which is at the edge of the main beam.

Table 3-2 contains the results of the interference calculations based on the antenna pattern in Figure 3.6. The details of the co-channel interference calculations are given in Appendix D.

The results of this analysis may be summarized:

- The nearest-neighbour beams contribute almost all of the interference to the system.
- The assumed antenna pattern results in an interference contribution 3.1 dB lower than the input receiver noise level.
- With regeneration the two-way link performance results in a SNR of 23.6 dB (unprocessed). The one-way link performance is 23.7 dB.
- Without regeneration, (i.e., with a linear transponder in the ground station) the SNR at IF frequency over the two links would be 5.6 dB, which is below FM Threshold.

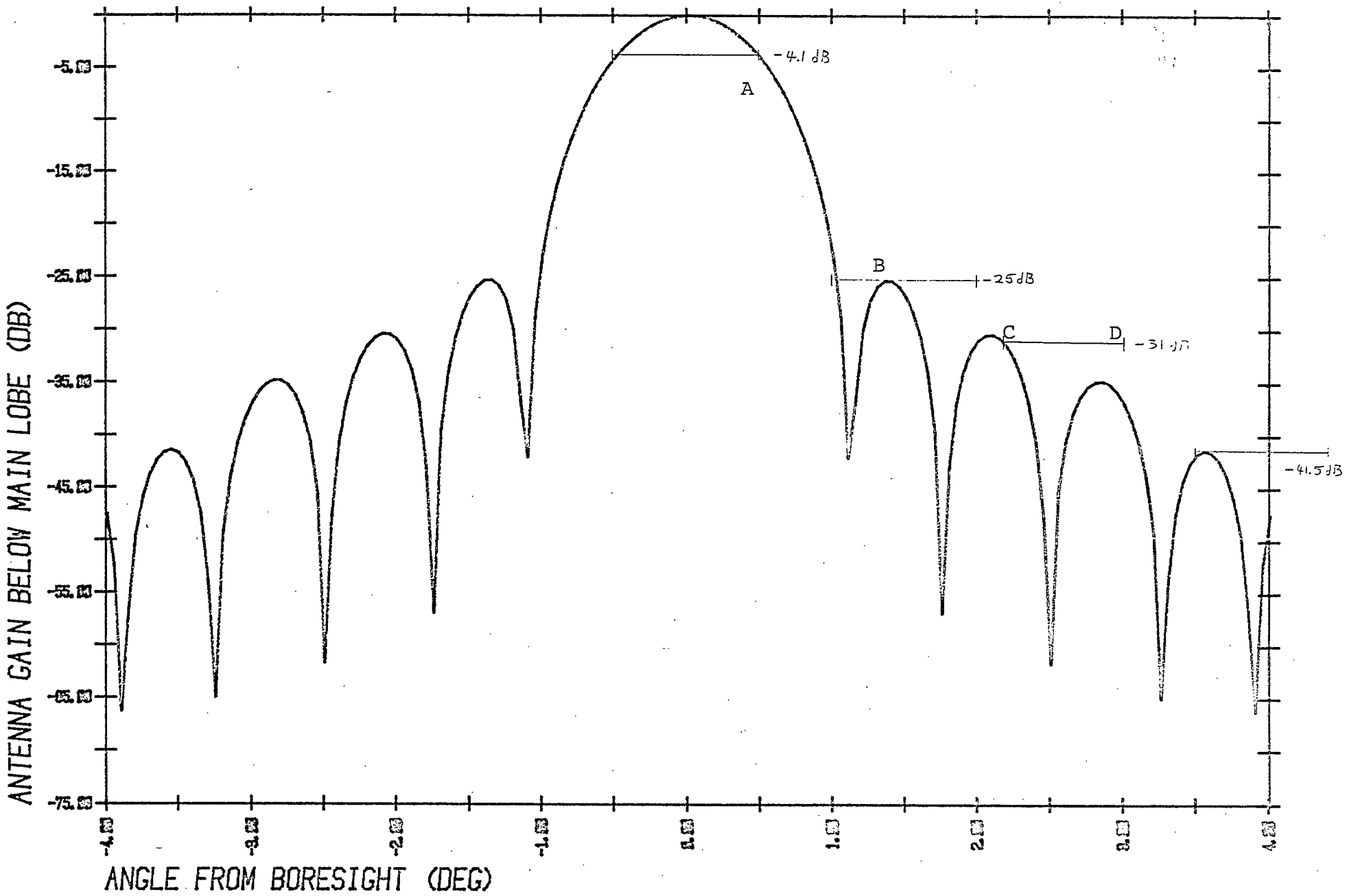

CROSS-SECTION PATTERN FOR AZ=Ø DEG. -MOD

FIGURE 3-6

3.1.1 Co-channel Interference Analysis (Cont'd.)

- Sensitivity analysis of SNR for the system shows that remodulation (regeneration) is necessary at the central control station, in order that the system can operate using only three frequencies.

Level of Neighbouring Beam 'i'	Distance Min	Max	Number of Interferer Beams n_i	Max Gain in level rel to pk G_i	n_i G_i
1	1^o	2^o	5	-25 dB	-18.0 dB
2	2.17^o	3.03^o	2	-31 dB	-28.0 dB
3	3.5^o	4.44^o	2	-41.5 dB	-38.5 dB

One-way Co-channel Interference = I_o = -17.6 dB

INTERFERENCE PRODUCED BY NEIGHBOURING BEAMS

Table 3-2.

3.2 Space Segment

3.2.1 General

The space segment of the system is composed of one active and at least one spare spacecraft. The distinctive feature of this spacecraft is, of course, the antenna. The remainder of the subsystems are based on existing hardware designs. Details of these subsystems are described in a later section.

The spacecraft are positioned in geostationary orbit and stabilized so that the antennas can be pointed at the proper parts of Canada. The communications subsystem is served not only by these large aperture antennas, but by an SHF dish antenna for the link to the control station.

3.2.2 Spacecraft Antenna Design Concept

The dominant feature of this spacecraft design is the large aperture antenna. The baseline design consists of an offset-fed parabolic reflector with a diameter of 26 meters (85.3 ft). The offset feed approach is preferred because the proposed phased-array feed would introduce excessive blockage when used with a symmetrical reflector.

3.2.2.1 R. F. Design

The antenna is equipped with an adjustable phased-array feed for each of the required 24 beams. Each beam is produced by illuminating the reflector from a sub-array of seven radiating elements. The phase and amplitude of each element is independently controlled under computer command, both for transmit and receive. A sketch of the concept is shown in Figure 3-10.

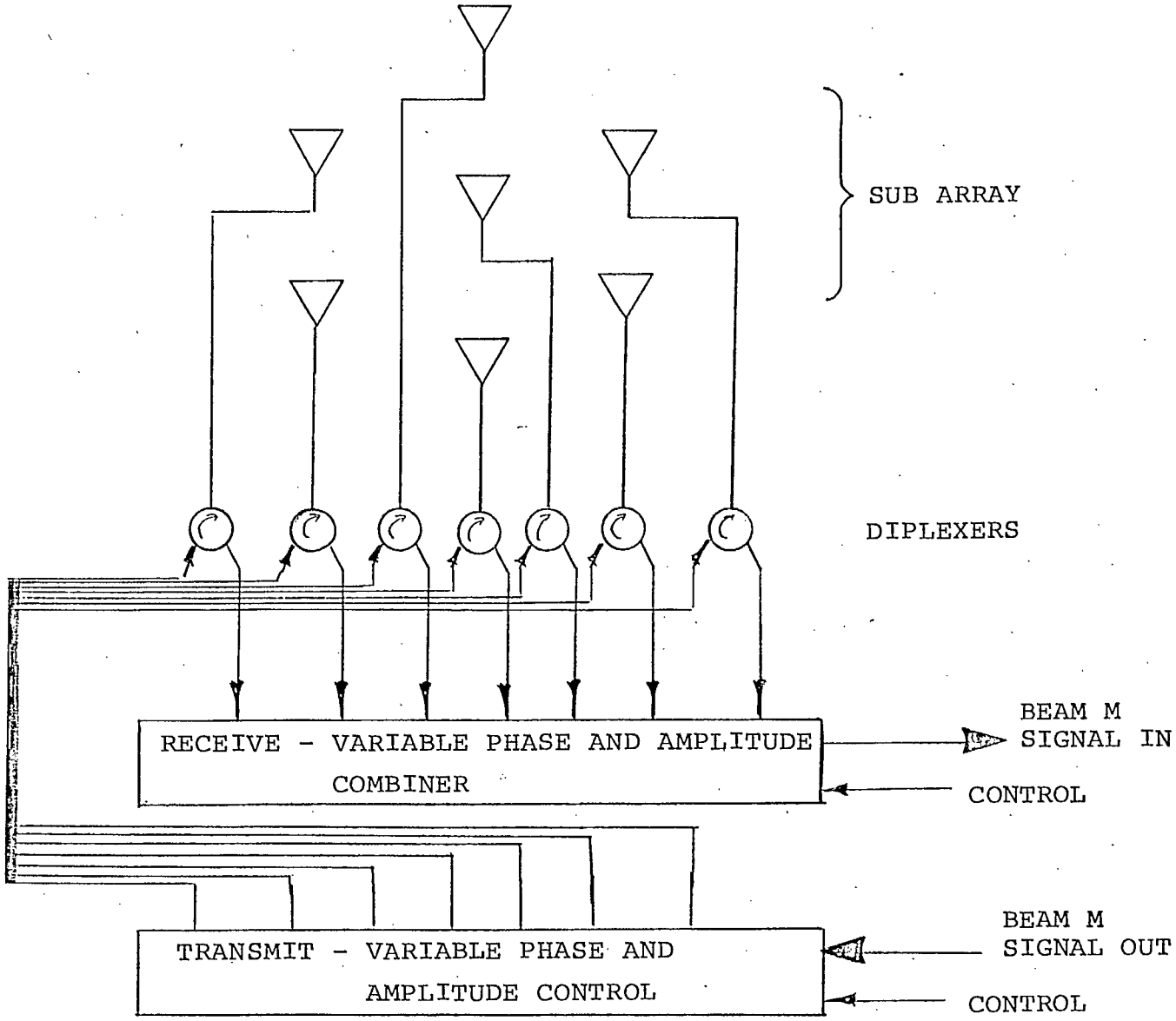

ADAPTIVE ANTENNA SUBSYSTEM FEED

FIGURE 3-10

3.2.2.1 R. F. Design (Cont'd.)

For the purposes of interference analysis, a standard 7 element sub-array configuration was established and the resulting feed field distribution used to calculate the far-field pattern. The pattern is shown in Figure 3-6.

Feed-back control is placed on the phase and amplitude of each sub-array element which combines to form an individual beam. This is done by optimizing the phase and amplitude distribution in an iterative way in order to maximize the ratio of pilot signal power to total noise power received in each beam. This is done by transmitting a broad-band pseudo-random code signal from the location of the desired center of each beam. (Each beam pilot transmits a different code.) A correlation detector is used to extract the pilot signal and this is compared to the signal detected by an un-correlated detector in that band. These signals are ratioed, and this ratio is maximized for each beam by adjusting the phase and amplitude of the sub-array elements. The phase and amplitude matrix for transmitting is calculated from the receive matrix values.

This approach permits the antenna system to compensate for thermally induced distortion, as well as to compensate for offset feed and non-parabolic surface effects. Unwanted noise signals are selectively rejected. In addition, the requirements on spacecraft attitude control are relaxed, as the system will compensate for changes in spacecraft pointing. The system can be entirely contained on the spacecraft, however, the baseline design places the detectors and computing system in the central control station.

3.2.2.2 Structural Design of Candidate Reflectors

The baseline 26 meter diameter, 24 beam, antenna can be designed by approaches. Some of the more developed designs today are:

a) The LMSC wrap-rib approach using either aluminum or graphite epoxy ribs (Figure 3-11)

b) The Harris Corporation TDRS type radial rib deployable antenna (Figures 3-12, 13, 14)

c) The Harris Corporation Maypole type Hoop and Column Mesh deployable antenna (Figure 3-15)

Other potential designs which are not yet at the above level of development are:

d) The Martin Marietta Orbital Assembly Antenna (Figure 3-16)

e) The General Dynamics Erectable Truss Antenna (PETA) (Figure 3-17)

f) The Grumman Space Fed Phased Array (Figure 3-18)

g) The Astro Research Antenna (Figures 3-19, 20)

and several others.

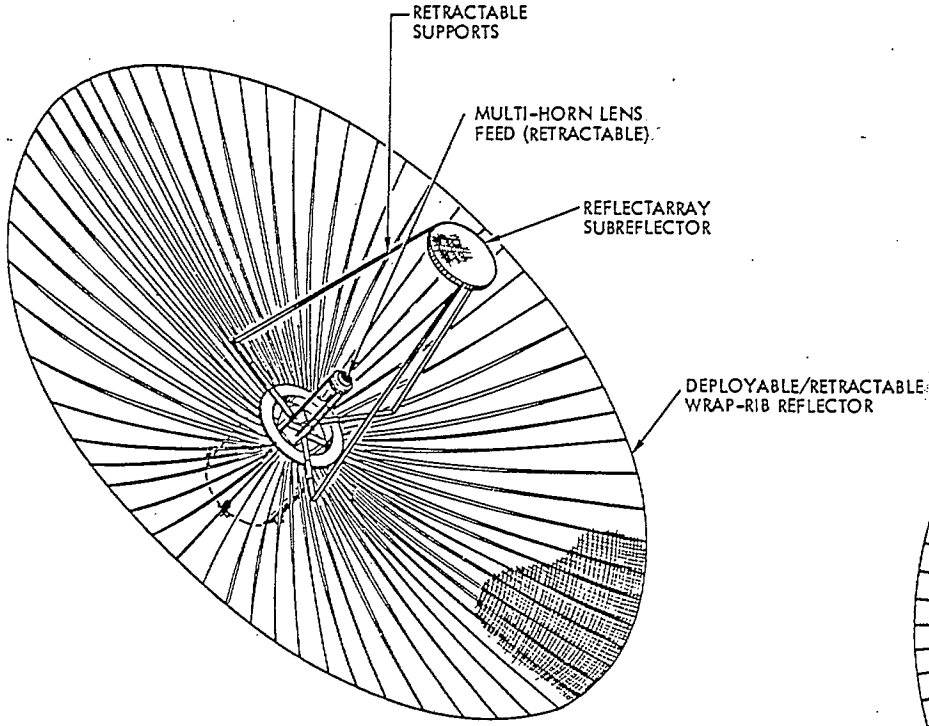

a. DEPLOYED ANTENNA

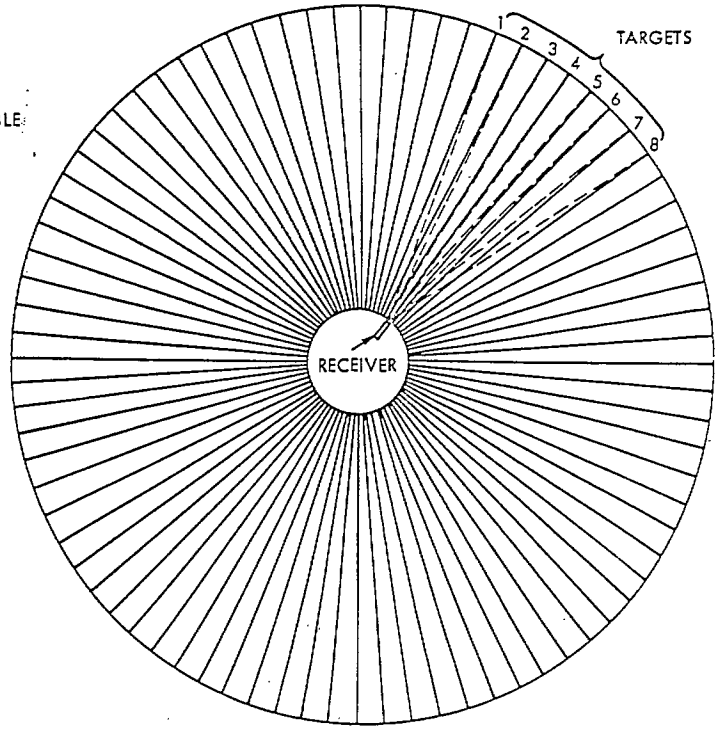

c. EIGHTY RIB ANTENNA, RECEIVER COVERAGE

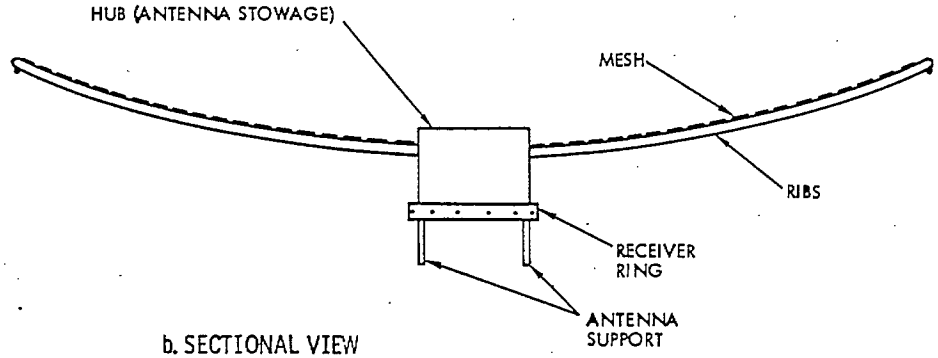

b. SECTIONAL VIEW

FIGURE 3-11 Lockheed Wrap-Rib Mesh Deployable Antenna

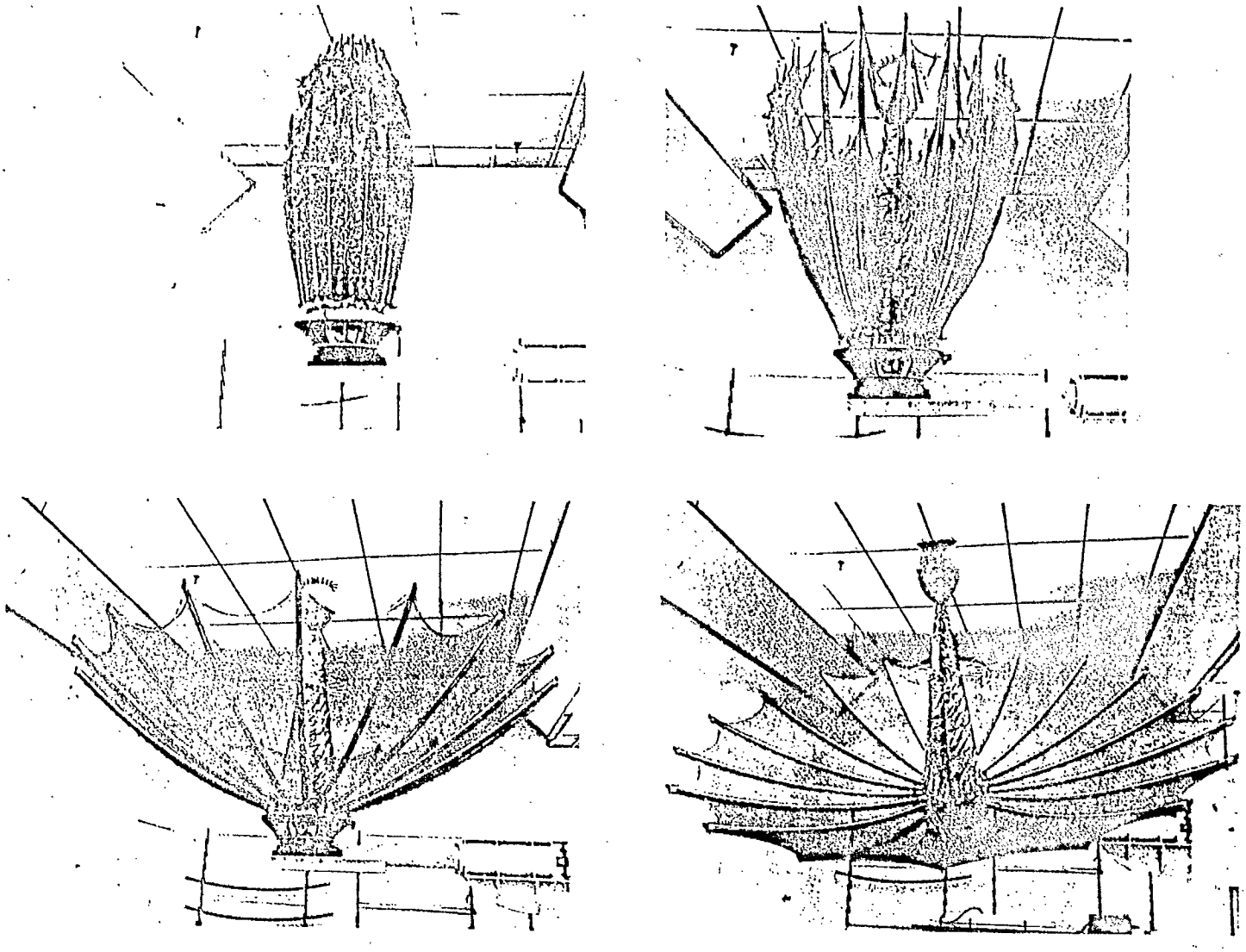

Harris Radial-Rib Antenna: Deployment Sequence

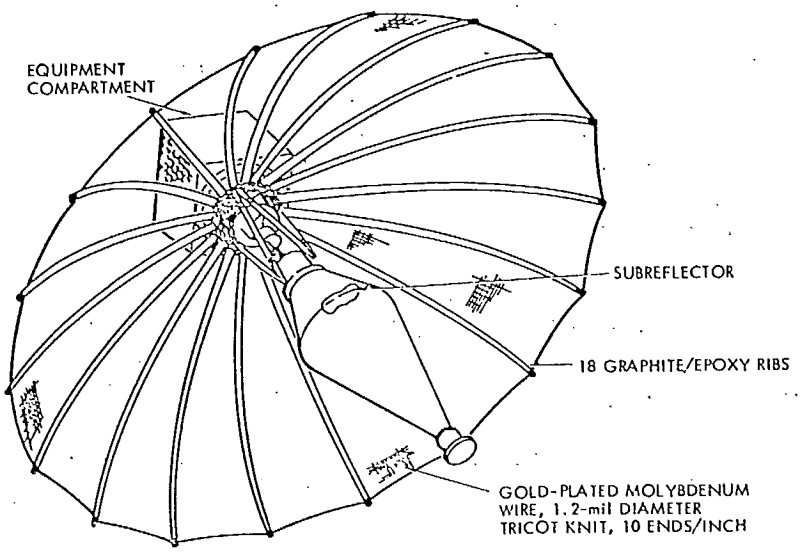

Design Elements of Harris Radial-Rib Antenna

FIGURE 3-12

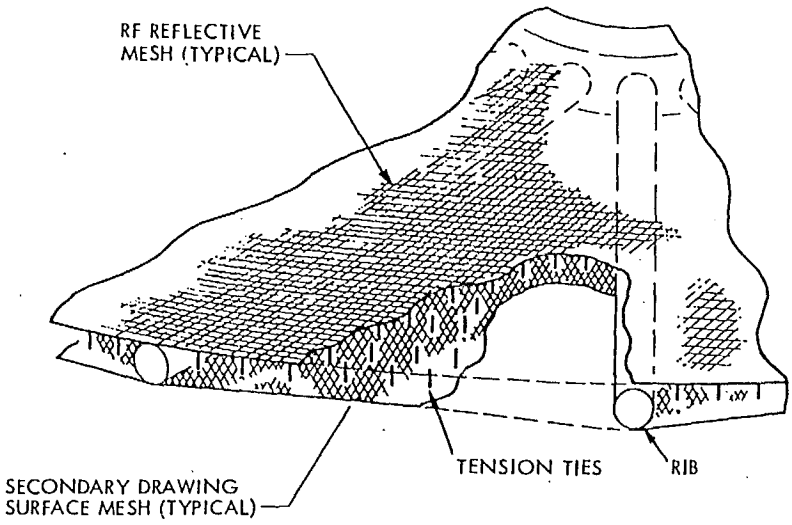

FIGURE 3-13 Harris Corporation Dual-Mesh Configuration

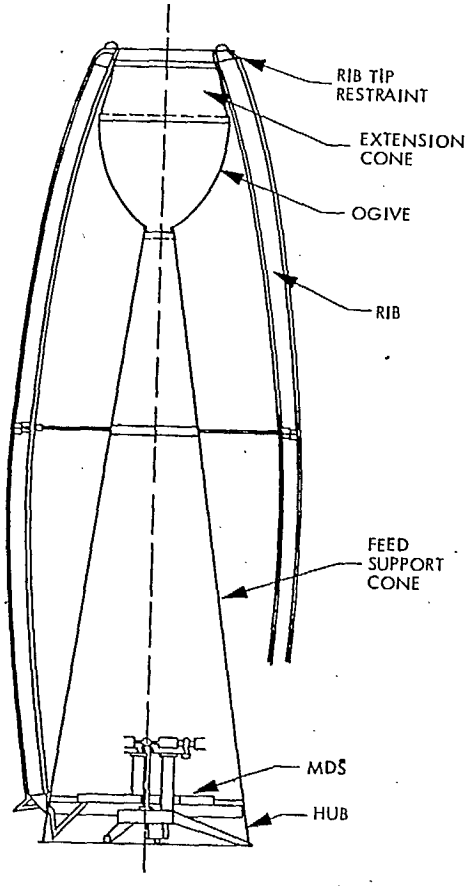

FIGURE 3-14 Feed Support Structure of Harris Corporation Radial-Rib Antenna

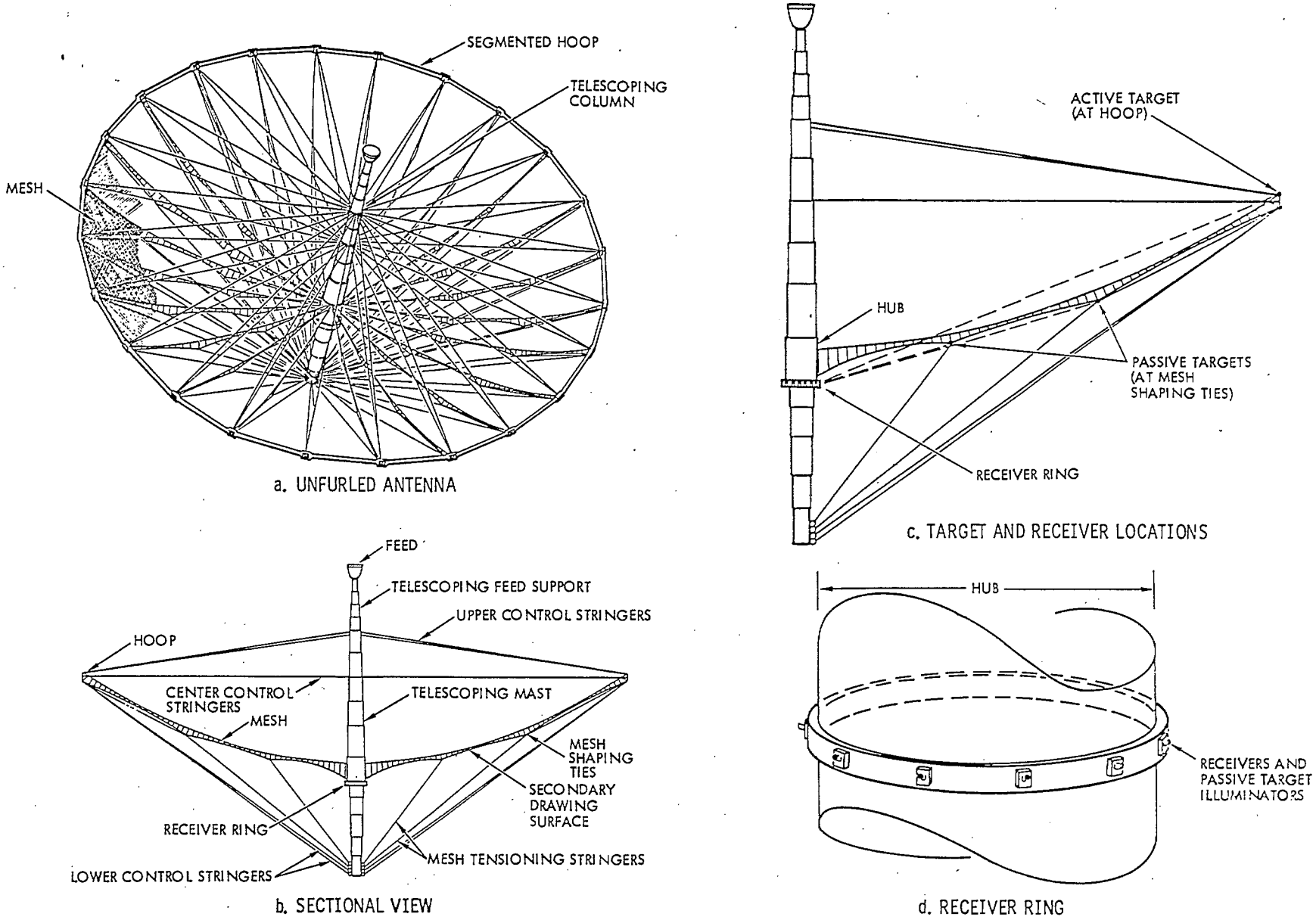

Harris Corp. Hoop-and-Column Mesh Deployable Antenna

Figure 3-15

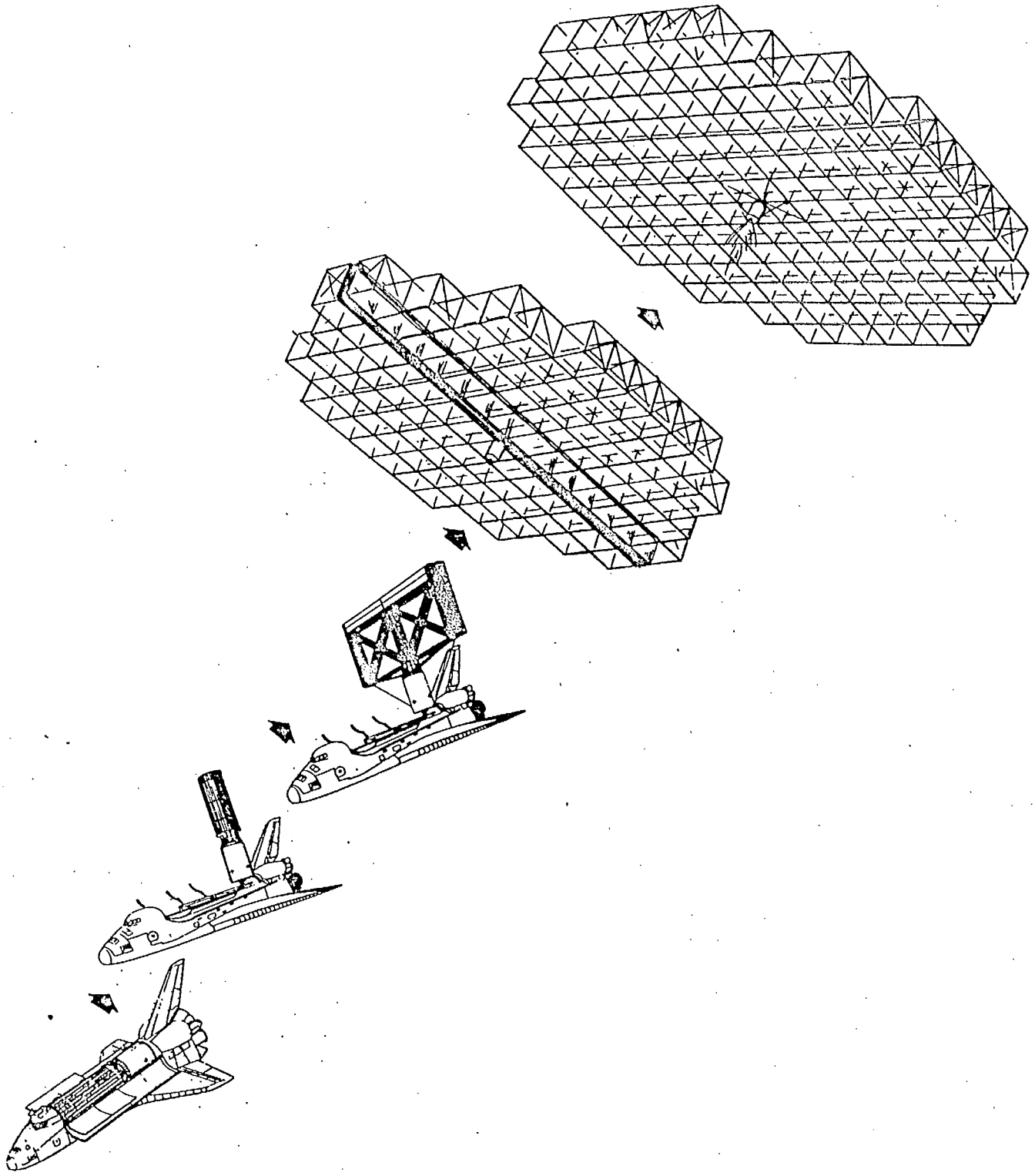

FIGURE 3-16

MARTIN MARIETTE DEPLOYABLE
BOX TRUSS - DEPLOYMENT SEQUENCE

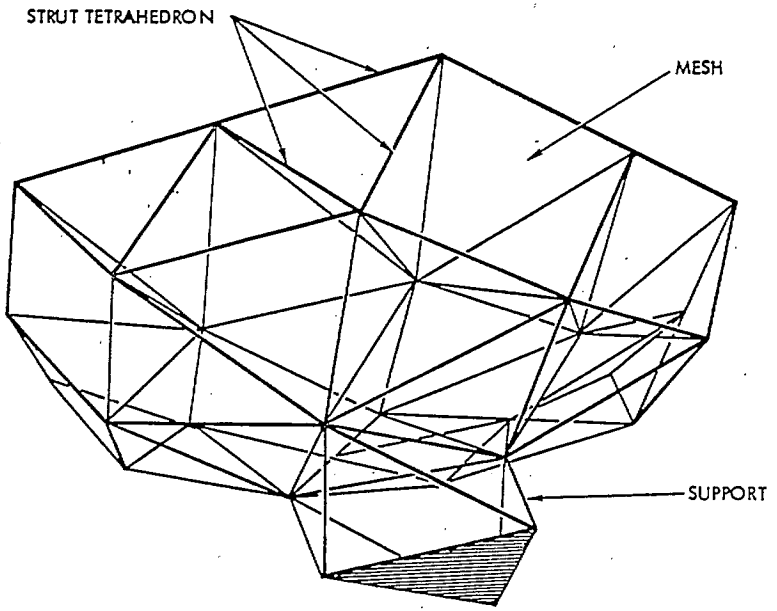

a. DEPLOYED ANTENNA

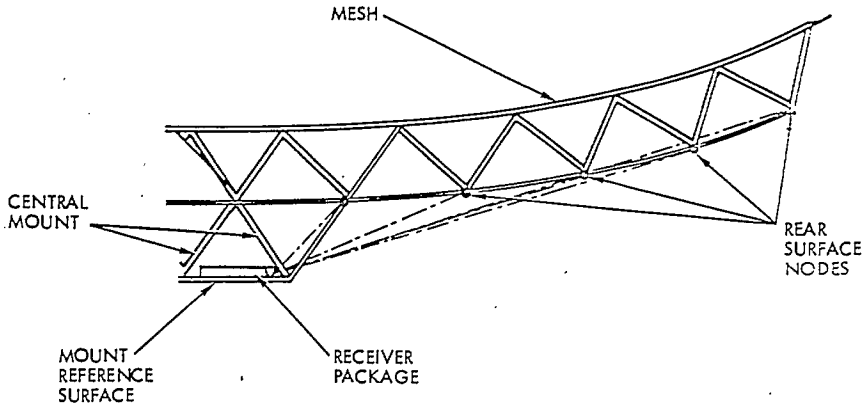

c. RECEIVER COVERAGE

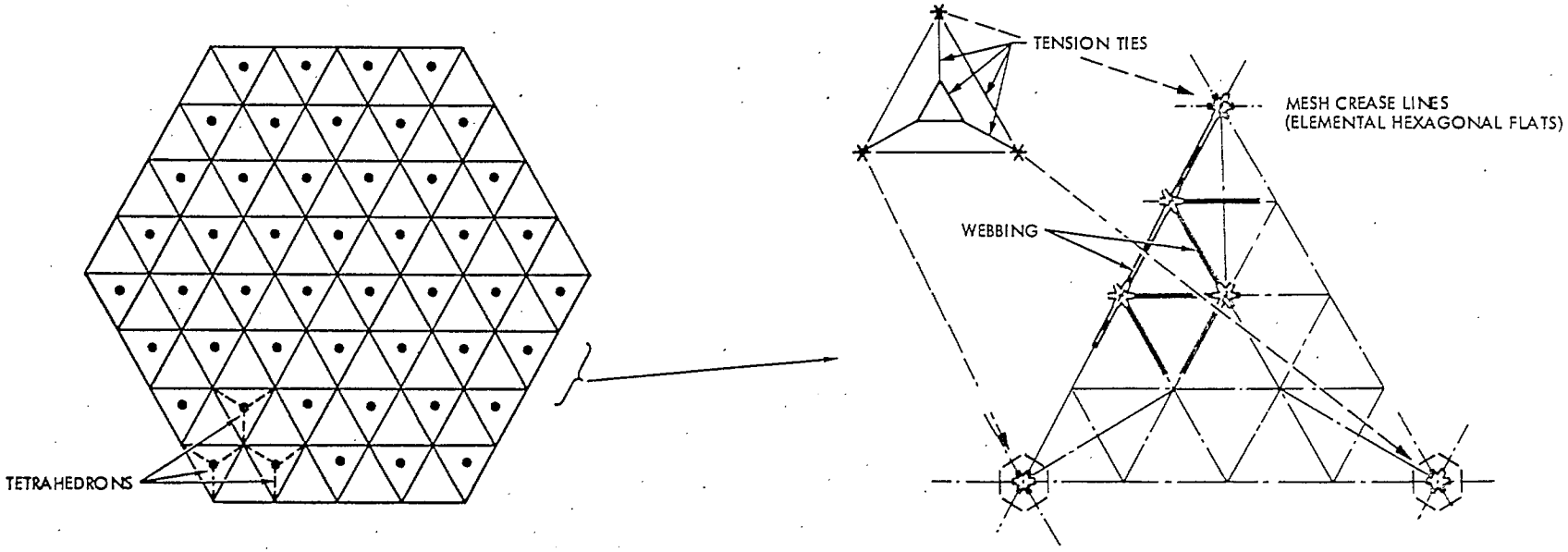

b. EIGHT-BAY PETA STRUCTURE, FRONT SURFACE

General Dynamics PETA Mesh Deployable Antenna

Figure 3-17

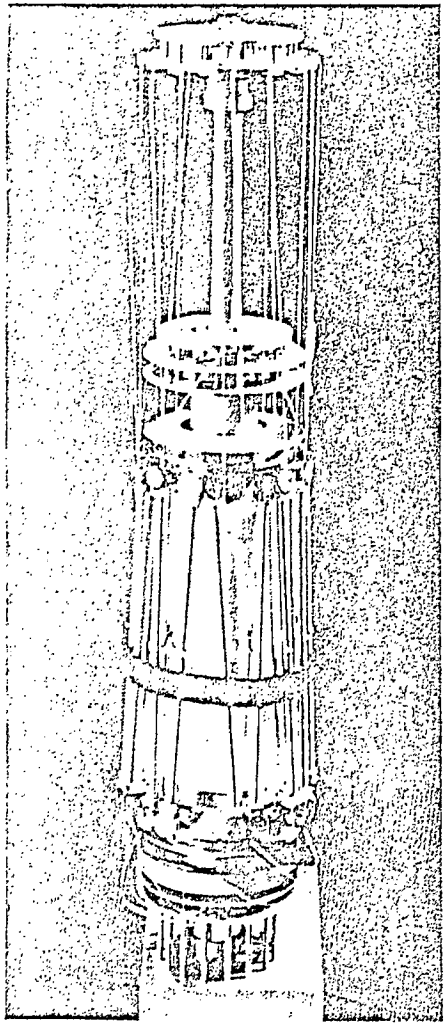

Grumman Mechanical Model: Furled Configuration

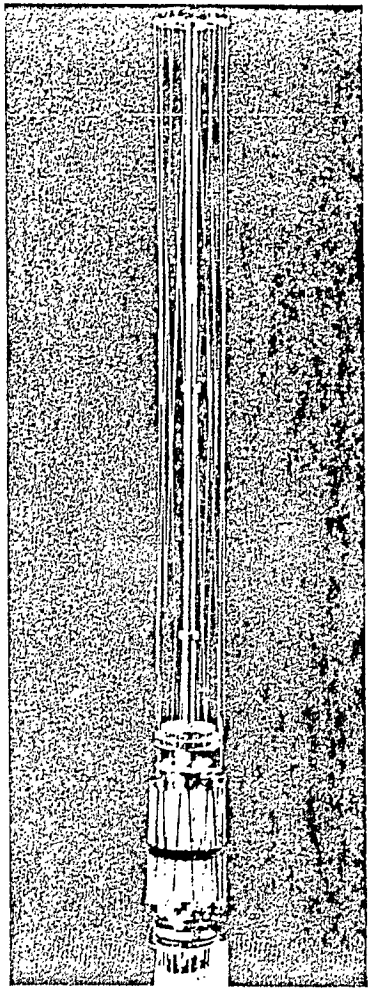

Grumman Mechanical Model: Furled Lens and Deployed Mast

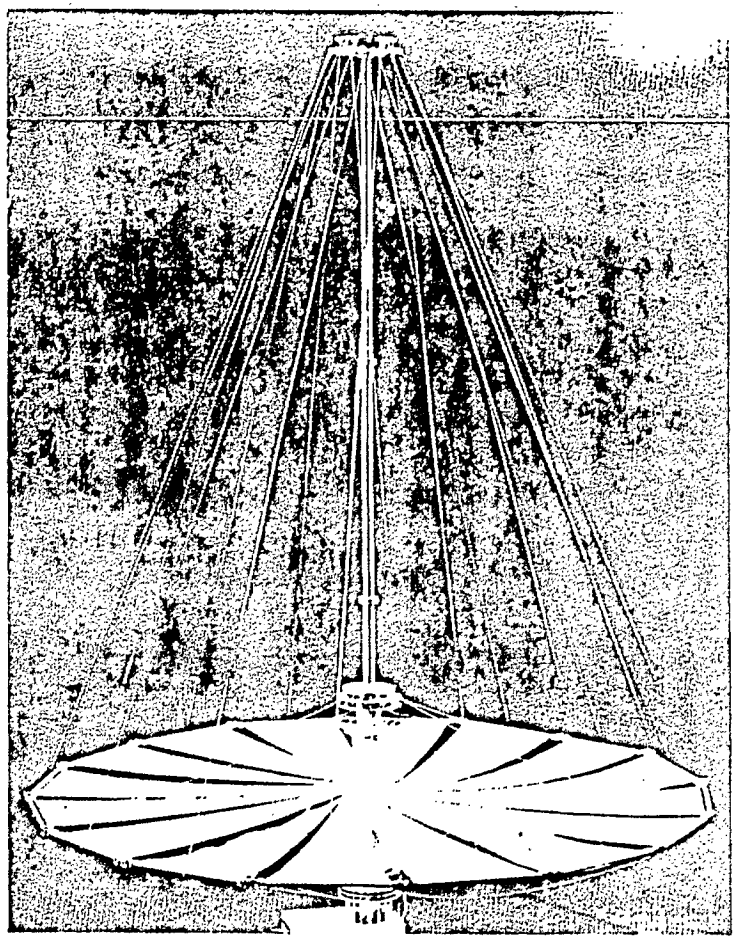

Grumman Mechanical Model: Deployed Configuration

Figure 3-18

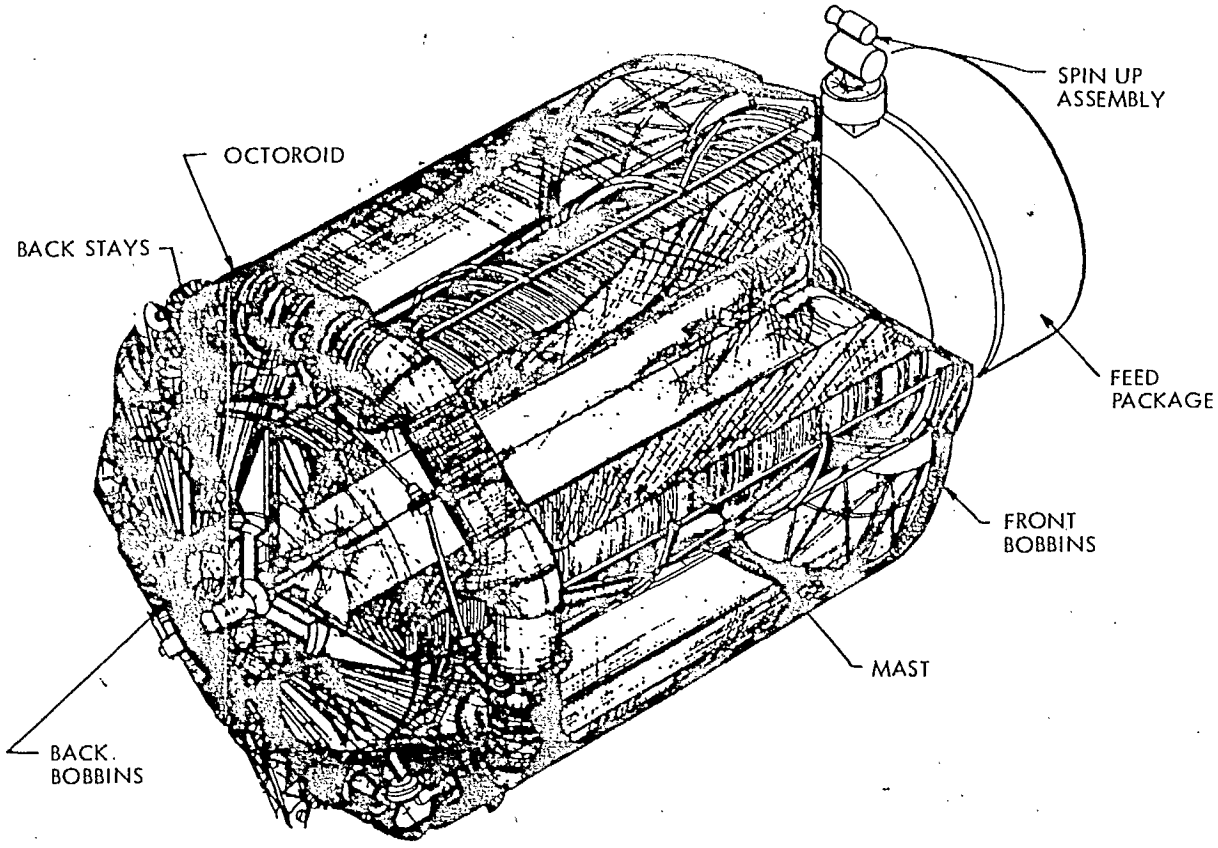

FIGURE 3-19 Astro Research Antenna: Launch Configuration

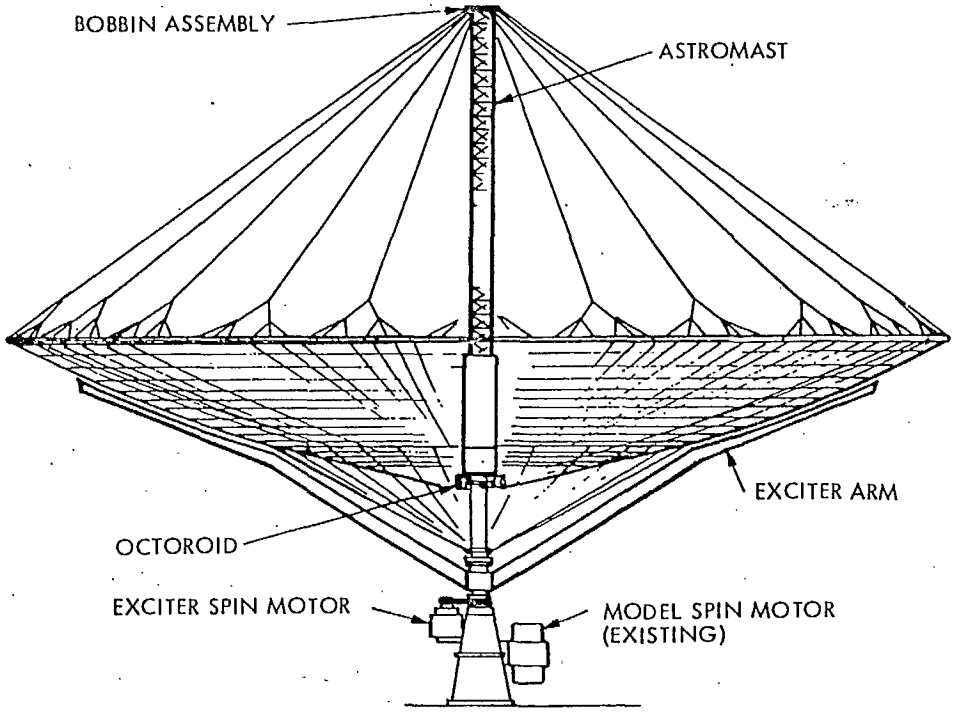

FIGURE 3-20 Astro Research Antenna: 5-m Mechanical Model

3.2.2.2 Structural Design of Candidate Reflectors (Cont'd.)

References 3-1 and 3-2 give a good overview of the state of the technology today. Reference 3-3 is also useful - particularly because the antennas described by SPAR for possible DOC missions still appear to be the most attractive approaches, 4 years later. References 3-5 through 3-11 are useful descriptions of the various antenna approaches as presented by their respective manufacturers.

A 26 m diameter aperture antenna operating at UHF to L band does not present overly severe mechanical design problems, in view of the current state of technology. Categorizing antennas as either a) deployable, b) erectable or c) space (fabricatable); only category a) is of interest for this study. This is consistent with DOC needs as well as the NASA Large Space Systems Technology (LSST) program implementation schedule. Consequently, in view of the flight proven success of the LMSC wrap rib and the successful TDRS development program of the Harris radial rib antenna, these two will be further considered. To give a more complete description of these antennas, we are reprinting as Appendix E, two recent technical papers, one by A. A. Woods and W. D. Wade from LMSC describing wrap rib technology; followed by a paper by B. C. Tankersley and H. E. Bartlett from Harris describing TDRS type radial rib technology.

Figure 3-21 is a conceptual design of a mobile communications spacecraft using an LMSC type wrap rib reflector and an offset feed assembly. It is configured to be launched on STS, using IUS to achieve geostationary orbit. A specific spacecraft configuration is discussed more fully in Section 3.2.4.4.

3.2.2.2 Structural Design of Candidate Reflectors (Cont'd.)

The wrap-rib reflector shown, according to LMSC data (Reference 3-10 and 3-11) would have a mass of 300 to 500 kg and would stow into a toroidal volume with an outer diameter of 2 to 2.5 m, an inner diameter of 1.5 to 2.0 m and a height of 0.25 to 0.5 m. The heavier mass would result if aluminum ribs were used (as they were for the ATS.6 antenna); if carbon composite ribs are used then the mass would be significantly decreased (Reference 3-10). Carbon composite ribs provide better thermal distortion characteristics than aluminum ribs however for the mission which is baselined, this increased performance capability does not appear to be required, and the aluminum ribs are cheaper. Considering an L band system and a 26 m aperture, a total of 40 ribs would produce a gain degradation of 0.1 dB due to surface irregularity and 25 ribs would produce a degradation of 0.5 dB. For a UHF band system the corresponding numbers of ribs are 22 to degrade by 0.1 dB and 15 to degrade by 0.5 dB (Reference 3-11).

Alternate reflector designs are discussed in the following paragraphs.

The Harris Corporation radial rib antenna configuration appears to be better suited to a Cassegrain or center focussed design than an offset feed design because the stowed reflector utilizes the center structure for rib support as shown in Figures 3-12 through 3-14). If a 26 m diameter antenna of this type were used the overall stowed length of the antenna would be approximately 14 m (46 feet). Considering a two stage IUS length of 4.5 m (14.8 ft) and the 19.8 m (65 ft) STS cargo bay limit; this allows only 1.3 m (4.2 ft) for the spacecraft body. If an alternate propulsion system to IUS were used, such as a Leasat class PAM and an optimized AKM or a liquid propellant orbital

transfer vehicle (OTV) then it is reasonable that more STS length could be allotted for the spacecraft body. But it is clear that a 26 meter aperture is close to the practical upper limit for this type of design, considering STS restraints.

The Harris Corporation Hoop and Column (Maypole) antenna (Figure 3-15) stows into a much more compact volume than the TDRS type antenna. Again, it appears better adapted to a center feed system than offset feed because of the presence of the axial telescoping mast. The stowed length in STS is roughly that of the length of each segment of the hoop. Using the upper LH illustration of Figure 3-15 as a representative design for the model, a 26m diameter aperature antenna will stow in roughly 4 m (13 ft.) of the cargo bay.

The hoop and column reflector's design development status is not as advanced as the TDRS type antenna. As far as we can determine it is not being developed for a particular program - although there is a possibility of its use on military missions. A 1.8 m diameter proof of concept model was successfully demonstrated (Reference 3-2) and a 15.2 m (50 ft) is currently being developed. Summarizing, the hoop and column antenna may be a proven operational design at the time the mobile communication satellite project begins but at this time it does not appear to be at the same stage of proven development as either the radial rib (TDRS) antenna or the LMSC wrap rib reflector.

3.2.3 Spacecraft Transponder

Figure 3.22 shows a block diagram of the remodulation type transponder chosen as the baseline for this study. For this application, it is an advantage to translate each beam-channel group to a different IF center frequency and then transmit the composite IF signal at an SHF frequency to the central control station or regional port. The SHF return link from the control station or regional port is handled in a complementary manner, whereby the uplink is demodulated on the spacecraft to a composite IF, then each beam-channel group selected on the basis of frequency and channeled to the appropriate amplifier-mixer for transmission at UHF to the mobile units in the desired beam.

Referring again to Figure 3.22, the uplink signals from the individual channels in each beam are received by the beam-forming sub-array and amplified by a LNA with integral automatic gain control. The signal is then multiplexed with signals from two adjacent beams which operate in different bands. For a twenty-four beam system using three frequency bands there are thus 8 beam-groups. Each beam-group is translated in frequency to an IF offset by 6 MHz from the previous one, and the composite IF of 48 MHz bandwidth is amplified and modulated on an SHF carrier for transmission to the central control station and the regional ports. The frequencies used for the local oscillators and IF are shown in Table 3.3.

The uplink signals from the central control station and the regional ports are received by an SHF LNA then demodulated resulting in an IF signal. The signal for each UHF downlink beam group is selected on the basis of frequency from this IF and multiplied by an appropriate LO signal to produce a downlink carrier for each beam. This signal drives an output amlifier which is connected via the

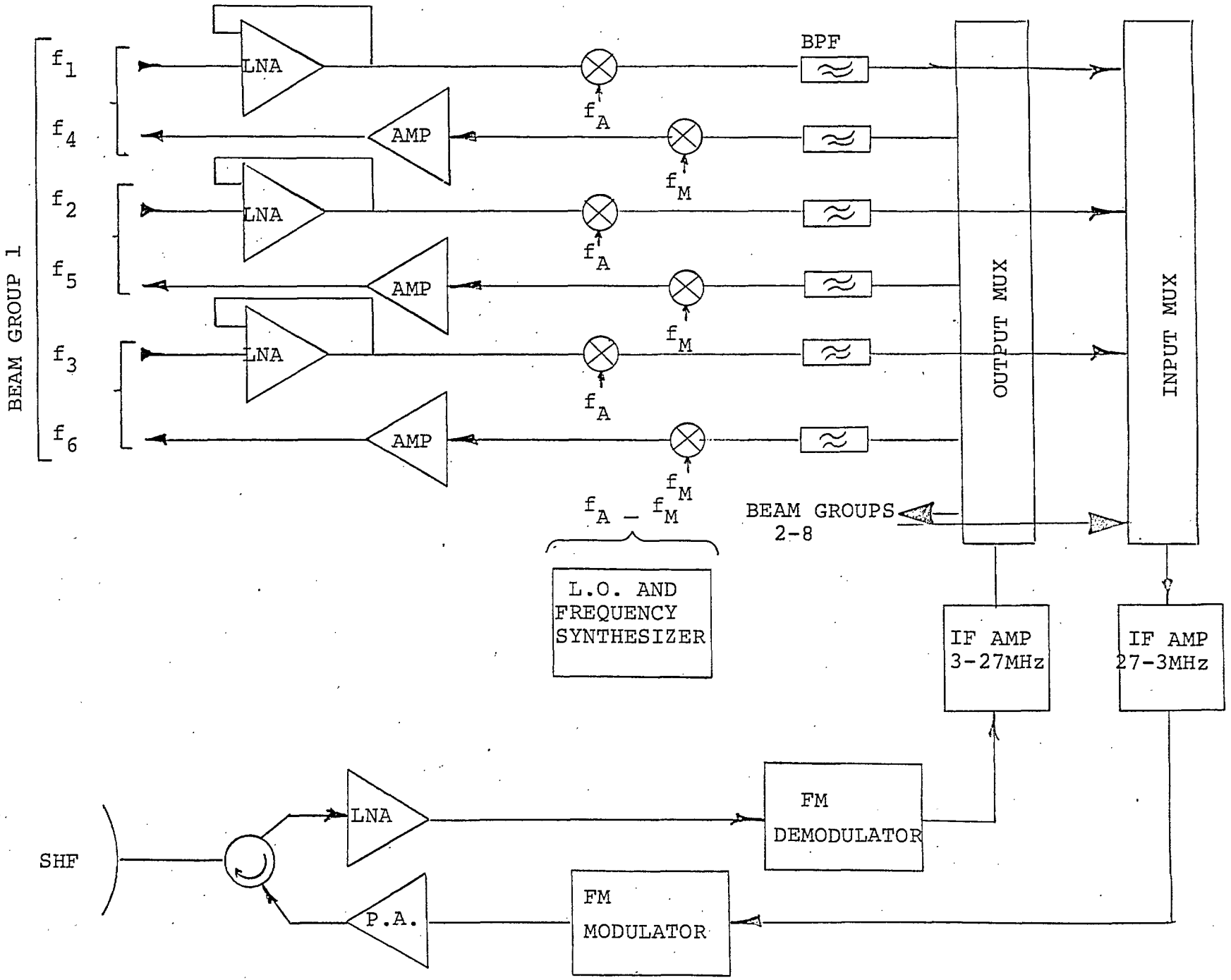

FIGURE 3-22 TRANSPONDER BLOCK DIAGRAM

BEAM GROUP	BEAM	UPLINK CF BAND	L.O. MHz	IF (INVERTED) MHz	L.O. MHz	DOWN LINK CF BAND
	1	f_1		2		f_4
1	2	f_2	$f_a = 825$	4	$f_m = 859$	f_5
	3	f_3		6		f_6
	4	f_1		8		f_4
2	5	f_2	$f_b = 831$	10	$f_n = 853$	f_5
	6	f_3		12		f_6
	7	f_1		14		f_4
3	8	f_2	$f_c = 837$	16	$f_o = 847$	f_5
	9	f_3		18		f_6
	10	f_1		20		f_4
4	11	f_2	$f_d = 843$	22	$f_p = 841$	f_5
	12	f_3		24		f_6

Cont'd.....

BEAM GROUP	BEAM	UPLINK CF BAND	L.O. MHz	IF (INVERTED) MHz	L.O. MHz	DOWN LINK CF BAND
	13	f_1		26		f_4
5	14	f_2	$f_e = 849$	28	$f_i = 835$	f_5
	15	f_3		30		f_6
	16	f_1		32		f_4
6	17	f_2	$f_f = 855$	34	$f_j = 829$	f_5
	18	f_3		36		f_6
	19	f_1		38		f_4
7	20	f_2	$f_g = 861$	40	$f_k = 823$	f_5
	21	f_3		42		f_6
	22	f_1		44		f_4
8	23	f_2	$f_h = 867$	46	$f_l = 817$	f_5
	24	f_3		48		f_6

TABLE 3-3 TRANSPONDER FREQUENCIES

1 = 823
2 = 821 MHz
3 = 819

4 = 861
5 = 863 MHz
6 = 865

diplexer to the appropriate beam-forming sub-array. The beam-group and local oscillator assignments are shown in Figure 3-23.

3.2.4 Impact on Other Spacecraft Elements

If a large reflector is used on a spacecraft there will necessarily be changes in some subsystems compared to their designs for present day spacecraft. In particular, the ACS, and RCS must meet more severe requirements because of the high pointing accuracy required, the large structural mass and the large inertia properties. This section discusses these impacts - in general - without reference to a specific spacecraft configuration, but considering the mission system requirements of Section 3.1 and the 26 meter antenna described in Section 3.2.2.

3.2.4.1 Power

The power subsystem will be configured in a very similar manner to existing systems. This is because the DC power requirements are relatively small. Advanced energy storage systems such as advanced Ni Cd or NiH_2 couples will be employed.

The only new development item for the power system will be the design and test of the solar array. This part of the system must be designed so that it is not shadowed to any significant extent by the large reflector. It may be necessary to mount the array on an extendable boom, or to mount extra array subpanels on the perimeter of the disk in order to compensate for shadowing.

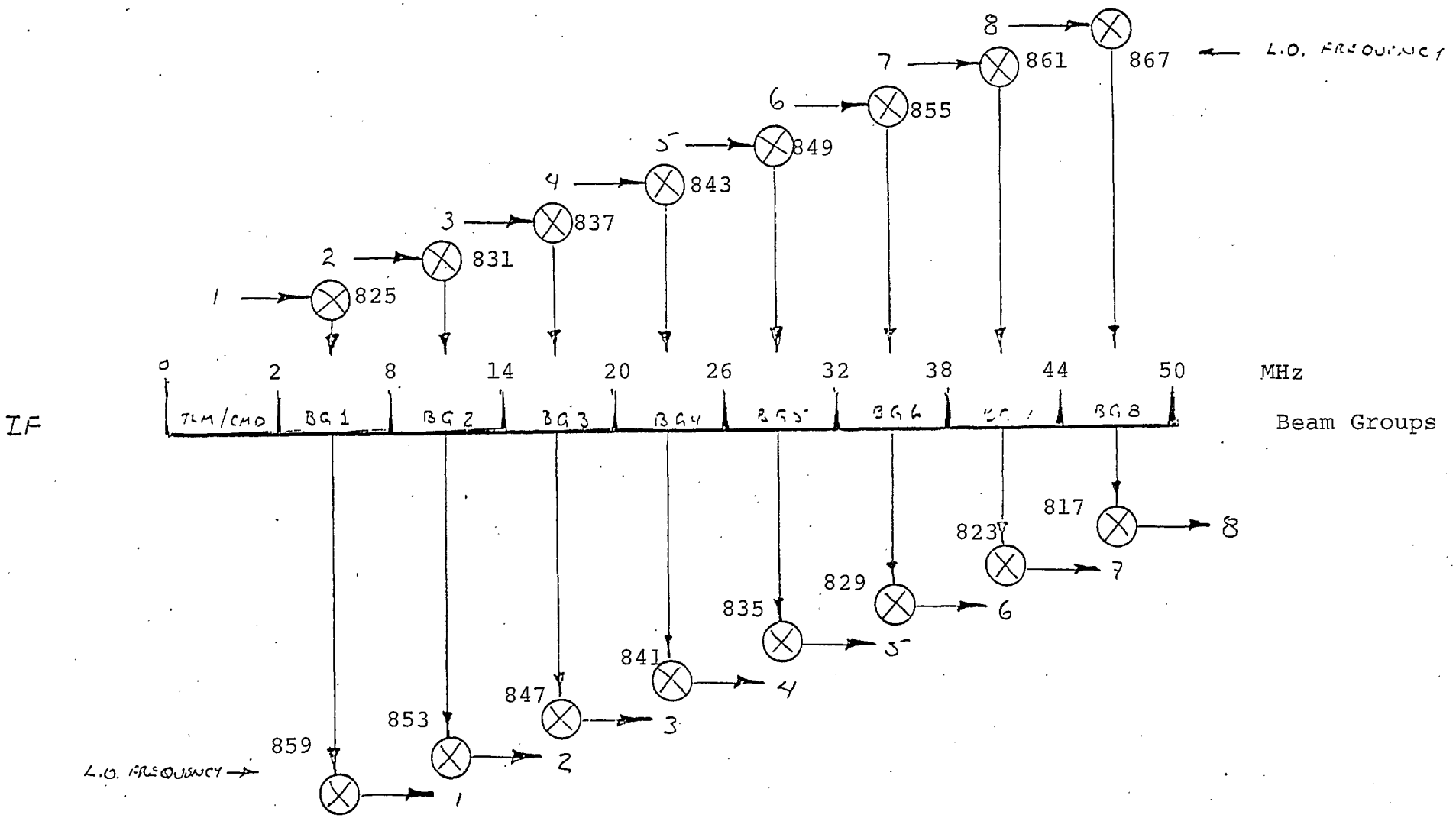

FIGURE 3-23 BEAM GROUP AND LOCAL OSCILLATOR ASSIGNMENTS

3.2.4.2 TT & C

No new development is needed for the telemetry and command system. It is anticipated that a small part of the SHF backhaul link spectrum will be allocated for T & C purposes. The encoder and decoder will be very similar to existing designs.

It is envisioned that a greater amount of autonomous control will be incorporated in future spacecraft. This implies significantly greater computational power on the spacecraft, as well as a considerable amount of system-specific software. The on-board controllers will be used for attitude control, antenna pointing and power subsystem management functions.

3.2.4.3 Attitude Control and Station Keeping

A large flexible antenna will have a significant impact on the design of a 3 axis ACS system, in that, (similar to CTS) the flexibility and damping of the antenna must be considered. This is an important field of research in the US at present, and it is noteworthy that Canada has a record of significant achievement in this area from Alouette and ISIS through CTS.

Figures 3-24 and 3-25 are taken from a presentation by Lee Farnham (GE) at the AIAA/NASA Conference on Advanced Technology for future Space Systems and summarize the technology development foreseen for large antenna system equipped spacecraft.

Comparing the 26 meter antenna aperture dimension to the tip-to-tip solar array dimension of CTS - which is approximately 17 m - it is obvious that the large antenna will present a more severe problem because of its greater size and significantly larger mass. Considering an

FUTURE STRUCTURES MEAN MORE COMPLEX CONTROLS

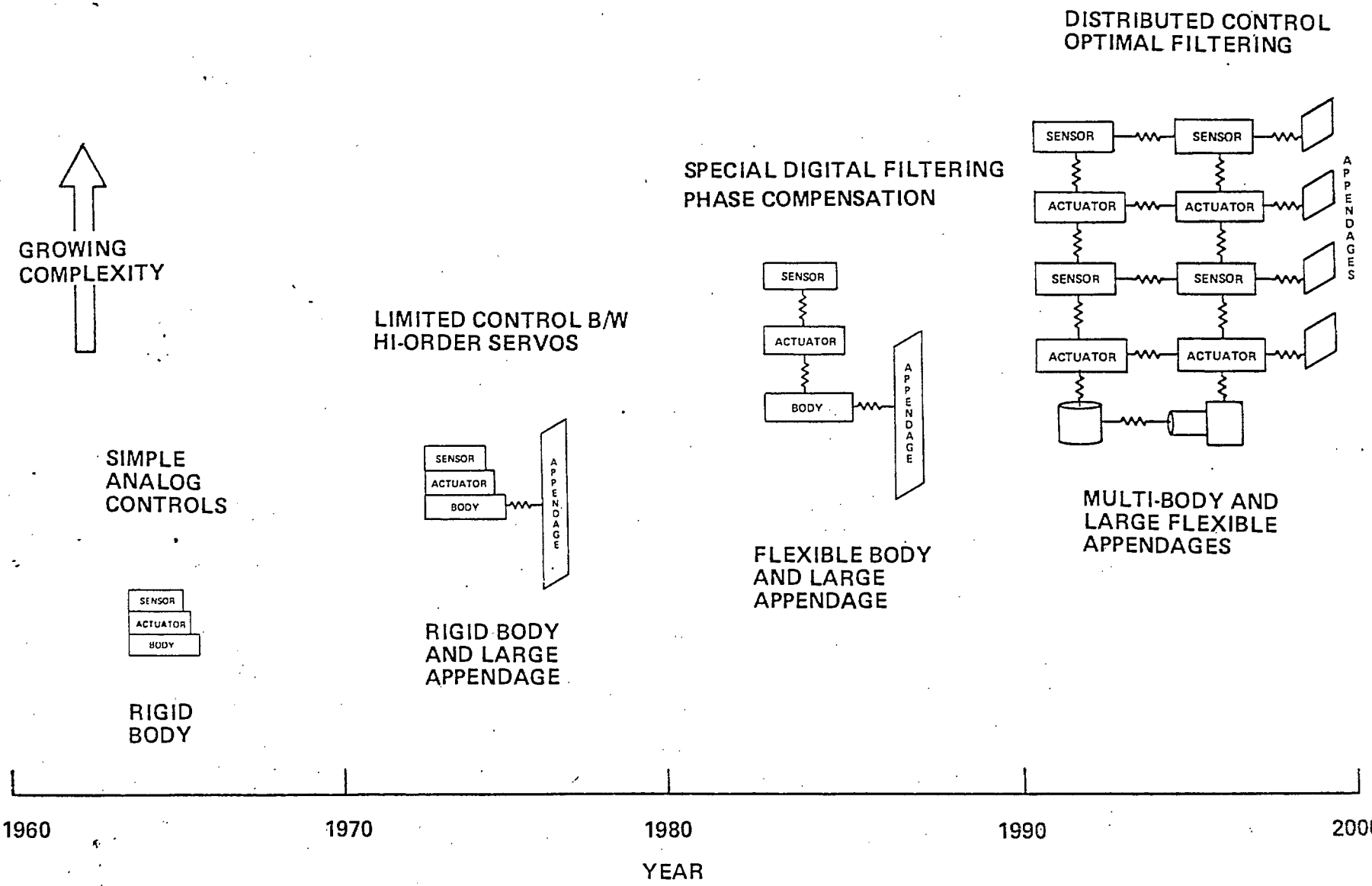

FIGURE 3-24

FUTURE COMPLEX CONTROLS WILL USE COMPLEX SYSTEM LOGIC

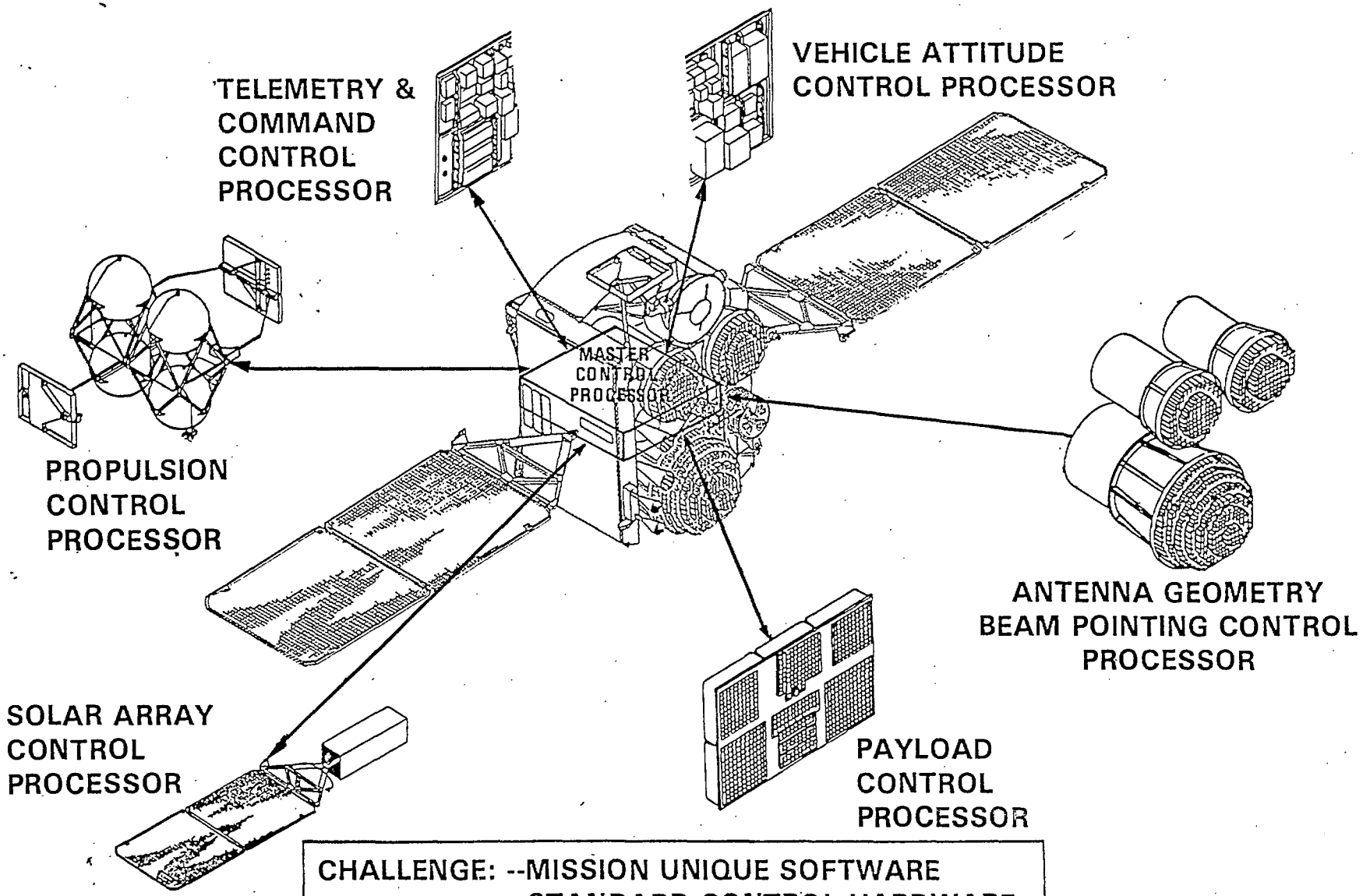

CHALLENGE: --MISSION UNIQUE SOFTWARE
--STANDARD CONTROL HARDWARE

FIGURE 3-25

3.2.4.3 Altitude Control and Station Keeping (Cont'd.)

LMSC wrap rib reflector, its own primary modes will be approximately: (Reference 3-1 and Appendix A)

f_1 (rocking)	1.5 Hz
f (torsion)	0.3 Hz

and as mentioned, the mass of the reflector and its container hub will be in the range of 300 to 500 kg. For a particular spacecraft design (e.g. the one presented in Section 3.2.5), the spacecraft structural dynamics are accounted for by considering the reflector, the deployment booms, the solar array and any other significant masses. It is reasonable that the primary modes can be in the range of .001 to .05 Hz, whereas the CTS primary modes were in the 0.1 Hz range. This presents more severe requirements to the ACS than imposed by CTS, but they are believed to be within the current technology capability. CTS has performed very well throughout its 3½ years of operation. (Reference 3-13).

Another data point is that ATS-F behaved well with a 9.1 m diameter LMSC wrap rib antenna. Some early ATS information, taken from Reference 3-12, is reproduced on the following pages. The conclusion from CTS and ATS-F flight results is that the technology exists for the development of a control system for a communications satellite with a 26 m antenna.

Excerpts from Reference 3-12' "ATS-6 Experimental Communications Satellite Report on Early Orbital Results"

"ATS-6 is a three-axis body stabilized vehicle with the capability of providing precision offset pointing. It is designed to usher in a new era in communication satellite technology where the traditional roles of small satellites and large earth terminals are reversed. A high gain 9.1 m (30 ft) diameter parabolic antenna is deployed on the spacecraft so that communications can be established with correspondingly small, austere, ground terminals. With rf gains of from 34 dB up to more than 50 dB over the range of uhf to C-band, relatively conventional satellite transponder performance parameters are able to achieve highly unconventional results."

"The objectives of ATS-6 are:

- To demonstrate deployment of a 9.1 m diameter parabolic reflector in space.
- To provide 0.1 deg. fine pointing at any offset angle within ±10 deg. of the local vertical.
- To provide tracking of fixed and moving targets to less than 0.5 deg. accuracy.
- To provide an integrated transponder and feed system for the experiments."

Spacecraft Description

"It is designed to be launched atop an Air Force Titan IIIC booster. The 9.1 m reflector is a furlable, 48 rib design with a copper-coated dacron mesh that can be coiled into a compact, torus-shaped package for launch. The truss to support the antenna elements at the focal plane of the reflector is an eight-element, A-frame design made of graphite-reinforced plastic. This material was chosen because of its excellent dimensional stability over wide temperature variations. The reflector is designed for

an F/D = 0.44."

"The deployed spacecraft measures 15.8 m (51.7 ft) from tip to tip of the solar arrays and 8.2 m (26.9 ft) from the bottom (earth viewing face) of the EVM to the top of the magnetometer boom. The gross launch weight of 1397.5 kg (3078.3 lb) includes a 48.2 kg (106.1 lb) adapter structure which remains with the Transtage."

"The basic elements of the ACS are depicted. The control reference signals are obtained from the following sensors:

- Two (redundant) three axis rate gyro assemblies provide angular rate data for rate damping and rate compensation during the acquisition modes.
- Analog and digital sun sensors provide all-attitude pitch/yaw sun angle data for use during the initial sun and earth acquisition modes.
- The earth sensor assembly is used for measuring roll/pitch angles of the spacecraft Z-axis off the local vertical (up to $\pm 14^{\circ}$) during the initial earth acquisition mode and subsequent operational modes.
- The yaw inertial reference unit and the Polaris sensor are used for measuring angular motions around the spacecraft Z-(yaw) axis.
- A C-band interferometer, when illuminated by rf energy from a ground transmitter, measures the spacecraft roll and pitch angles (over a primary angle range of $\pm 17.5^{\circ}$) relative to a line-of-sight vector from the spacecraft to the transmitter.

- A monopulse mode in the communication subsystem also provides roll/pitch error signals which enable the ACS to boresight the 9.1 m reflector to a ground station emanating a vhf, S-band or C-band signal. The S-band monopulse mode can also be used for a closed-loop satellite track mode based on S-band transmissions from the target satellite.

The ACS features two redundant digital operational controllers (DOC's). The basic control laws for the various acquisition and operational modes are programmed into the DOC memory, which can be reprogrammed by ground command. The DOC accepts mode/pointing commands from the ground, as well as orbit ephemeris data for the purposes of holding a fixed ground aim point (by compensating for nongeostationary orbit effects) or of tracking a low-orbiting satellite in an open-loop programmed track mode. The analog backup controller (ABC) serves as a backup to the DOC's for the acquisition modes and for the local vertical and station point (monopulse) operational modes.

The actuator control electronics (ACE) include the wheel drive electronics, the wheel unload logic and the spacecraft propulsion subsystem (SPS) control electronics and associated power supplies. The ACE drives the inertia wheels or the SPS thruster valves in response to attitude error signals from either one of the DOC's the ABC, or by ground command. The three inertia wheels serve as the prime torquers for all modes of operation except acquisition, orbit control, and jet-only control.

The spacecraft propulsion subsystem provides fully redundant thrusters for orbit control and three-axis attitude control, including inertia wheel momentum unloading. It utilizes 16 catalytic hydrazine thrusters fed from two propellant tanks with positive expulsion bladder control operating in a single blowdown mode. Thrust levels for all

thrusters average about 0.46 N (0.10 lbf). The total propellent load is 49.9 kg (110.6 lb) plus 0.82 kg (1.8 lb) of pressurant."

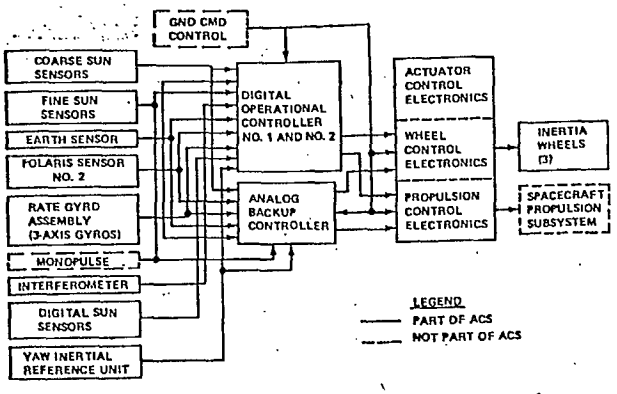

Simplified block diagram of attitude control subsystem.

ACS in-orbit performance

Mode	Parameter[a]	Spec	Actual
ABC sun acquisition	Time to acquire (min)	30	10
	Pointing accuracy (deg)	4.5	2
ABC Earth acquisition	Time to acquire (min)	80	50
	Pointing accuracy (deg)	1.0	0.35
ABC local vertical	Pointing accuracy (deg)	1.0	0.35
DOC vhf monopulse	Pointing stability (deg)	1.0	0.5
DOC S-band monopulse	Pointing stability (deg)	0.3	0.01
DOC C-band monopulse	Pointing stability (deg)	0.1	0.002
DOC offset point ground[b]	Pointing accuracy (deg)	0.1	0.049
	Pointing stability (deg)	0.1	0.01
DOC low jitter[b]	Pointing accuracy (deg)	0.5	<0.1
	Pointing stability (deg)	0.01	0.005
	Rate stability (low frequency) (deg/sec)	0.001	0.0003
DOC satellite track	Tracking accuracy (deg)	0.5	<0.2
DOC offset point slew	Rate (deg/min)	≥0.5	1.2
	Settling time (min)	≤10	<3
DOC operational modes (above)	Yaw accuracy using PSA (deg)	0.15	<0.1

[a] Indicated parameters pertain to roll and pitch, except for the first mode, which pertains to pitch and yaw and the last mode, which pertains to yaw. [b] Using either the Earth sensor or the interferometer.

3.2.4.3 Attitude Control and Station Keeping (Cont'd.)

It is anticipated that the ACS system chosen for the baseline mission will utilize either an inertia wheel approach (like ATS-F) or a momentum wheel approach (like CTS) and a current technology hydrazine reaction control subsystem. Attitude sensing can be accomplished in numerous ways. It is likely that RF sensing (as done for ATS.F and Anik C/D) will be incorporated in the ACS design.

One area which will require further development is the thruster subsystem for long term missions. ATS-F has experienced a number of RCS malfunctions and the causes are currently under investigation. Similarly OTS and to some extent CTS have experienced problems. All of the above are hydrazine subsystems. If hydrazine is not used, alternate technologies might include electric propulsion.

3.2.4.4 Structure and Thermal Design

The large reflector and its supporting structure dominates the spacecraft structural design. Because of the relatively low power requirements (400 W DC input range) and the conventional RF equipment required for the transponder and feed horn assembly - the design of the remainder of the communications payload does not present a significant problem. Similarly, the housekeeping units consist of conventional types of units and should impose no unusual structural/thermal problems.

The challenging design areas are:

a) configuring the stowed antenna and its deploying elements (booms etc.) to withstand STS launch and subsequently deploy reliably.

3.2.4.4 Structure and Thermal Design (Cont'd.)

b) Developing a structural configuration compatible with the secondary propulsion stage used to go from LEO to GEO. This could be:

- IUS
- an OTV
- a mission specific solid/solid, solid/bipropellant or complete bipropellant system.

c) Developing a deployed configuration which:

- minimizes thermal distortion of the reflector and the relative orientation of the feed horn assembly to the reflector.
- minimizes solar torque.
- prevents shadowing of the solar array by any part of the spacecraft during all seasons.
- provides mounting locations so that thrusters can fire through the C of M for N/S and E/W stationkeeping.
- allows the housekeeping and payload units to have adequate thermal control radiative control surfaces.

Section 3.2.5 discusses a specific configuration concept in more detail.

3.2.5 A Specific Spacecraft Configuration

Figure 3-21 shows a spacecraft which meets the mission requirements and utilizes a 26 m LMSC type wrap rib offset feed antenna. The spacecraft consists of three modules, connected by two Astromast type booms. In the stowed configuration it can be accomodated as a cantilevered mass interfaced to an IUS and as such it needs no cradle mounting system to the orbiter itself. The total length of orbiter required is:

IUS	4.5 m	(14.6 ft)
S/C	≈2.5 m	(8.2 ft)
	7.0 m	(22.8 ft)

However, due to the large mass of the IUS, approximately 45,000 lb, the launch cost will be based on mass rather than length criteria. Considering a 5000 lb spacecraft, this cost would essentially be that of a dedicated STS launch.

At present the IUS has a planned 5000 lb payload capability from LEO to GEO but work is underway now to increase this capability to ≈6000 lb. It is reasonable that by the time of the baseline mission, this capability will be available.

A rough cut mass estimate of the conceptual design spacecraft is shown on following page. (Table 3-4).

Payload	
26 m reflector and hub	350 kg
14 m Astromast and cannister	135
17 m Astromast and cannister	150
Feed horn assembly and diplexors	75
Transponder	230
	940 kg
Housekeeping	
TT&C	30 kg
ACS	60
RCS (dry)	50
Structure/thermal for the 3 modules	250
Power:	
batteries	23
solar array	25
other	25
	463 kg
Interface	
Interface hardware for attachment to IUS	100 kg
Total dryweight of spacecraft (considering 50% of interface hardware)	1,503 kg
Hydrazine for 10 year mission	400 kg
Total mass required to be placed in GEO by IUS	1,903 kg

This leaves a contingency of 370 kg for a 2,273 kg (5,000 lb) capability IUS.

TABLE 3.4 MASS ESTIMATE OF SPACECRAFT LARGE ANTENNA

3.2.5 A Specific Spacecraft Configuration (Cont'd.)

Astromasts of this size are feasible. Reference 3-14 reports Astro's hardware development of a 25.6 m long (84 ft), 0.5 m diameter (20 inches), 97 kg (214 lb) articulated Astromast which has 3000 ft. lb bending moment strength and 2.8×10^8 lb . in^2 cross sectional (effective EI) bending stiffness. It is believed that a stiffer (larger diameter) Astromast may be necessary for the baseline mission.

The solar array can be either a CTS type flexible array, or more likely a semi-rigid deployable panel array, since the DC power demand level is in the 400 W range. One array is shown, deployed from the North face of the payload module. The other two modules are electrically connected to this module by deployable wire bundles (or FCC's). Auxiliary body-mounted solar arrays may be required on the other modules to supply keep-alive power for the mission period between IUS separation and attitude acquisition.

The middle module can be used for ACS and other housekeeping units. All three modules can be constructed using standard honeycomb construction, or, they can be constructed as box-like space frames with honeycomb or integral panels added where required for equipment mounting.

Some on-orbit adjustment capability may be required to precisely position the feed horn system with the reflector. This can be done in a number of ways. It is desirable to have a design which does not require this added complexity however.

3.2.5 A Specific Spacecraft Configuration (Cont'd.)

The RCS system consists of thrusters which will likely be mounted on each of the three modules. The design does not allow for East - West thrusting directly through the center of mass therefore East West control will have to be done by firing module thrusters in a torque cancelling mode. The hydrazine tanks would be located at each module, so that the RCS would consist essentially of three mechanically independant assemblies. Electric propulsion may also be considered for stationkeeping.

The ACS can be a CTS momentum bias system with a relatively large wheel. An on-board microprocessor controller would likely be utilized.

3.3 Ground Segment

The four elements of the ground-based equipment are the central control station, the pilot beam transmitters, the regional ports and the user terminals. Each of these elements will be described in turn.

3.3.1 The Regional Port

The system is established with a number of regional ports. These ground stations operate at SHF and have the capability to receive signals from any channel in the entire coverage area and in turn to transmit on any channel in the Canadian coverage area. The purpose of these ports is to provide interconnection between the existing land-based telephone services in a given area. Typically, regional ports would be required to connect with:

- BC Telephone
- Alberta Telephone
- Saskatchewan Telephone
- Manitoba Telephone
- CN/CP (Northwest Territories)
- Bell (Perhaps 2 ports)
- Maritimes
- Newfoundland

Each agency will thus have control over the charges levied on its own subscribers for use of the mobile-satellite system.

3.3.2 The Central Control Station

The central control station provides control of the mission as well as for control of the communications system. The station is equipped with the same SHF communication capability as the Regional Ports. However, instead of inter-connection to existing systems, the central station completes calls between two mobile stations anywhere in the system. The CSS establishes channel assignments for each beam and governs the protocall of the signals such as dialling, ringing, busy and hang up signals. Charges incurred by each mobile-satellite user are logged in the CCS.

In addition to these communication-related tasks, the CCS will have the capability of orbit determination, telemetry decoding and display, S/C command generation, state-of-health monitoring of the spacecraft and station-keeping control. Typical parameters for the CCS are given in Table 3-3.

The adaptive control algorithms for the antenna-feed phase shifters are controlled from the CCS.

3.3.3 Pilot Beam Transmitters

Each beam is directed to the appropriate coverage area by means of a pilot transmitter which is located at the approximate center of its beam. These transmitters will normally be located at a permanent townsight for ease of servicing. The uplink signal contains information on the status of the transmitter and its environs as well as a unique identifying code. The system will maximize the signal strength of the pilot carrier with respect to all other transmissions in the same bands. The transmit parameters are listed in Table 3-3.

3.3.3 Pilot Beam Transmitters (Cont'd.)

The pilot beam transmitter is similar in many ways to a data collection platform for LANDSAT.

3.3.4 User Terminals

The user terminals for the system are similar to those presently used for mobile telephone service. The intent of the design is to make the operation identical with the use of a conventional telephone. Thus channel allocation and call termination will be done automatically. The transmit and receive parameters are given in Table 3-3.

	Receive G/T	Transmit EIRP	Antenna Gain	Power dBW	Watts
Central Control Station, Regional Port	19 dB/^{o}K	60.5 dBW	47.5 dB	13 dBW	20 W
Pilot Beam Transmitter	---	0 dBW	3 dB	-3 dBW	500 mW
Mobile Transceiver (User Terminal)	-23 dB/^{o}K	-2.7 dBW	3 dB	-5.7 dBW	270 mW

GROUND SEGMENT PARAMETERS

TABLE 3-3

4.0 INTERFERENCE CALCULATIONS

4.1 Calculation Method

The interference calculations follow the same general method described in previous work performed for DOC (Ref. 5-1). In this approach, the mutual coupling between the transmit and receive antenna is calculated from the relative location and orientation of the patterns. This data is used in conjunction with the power spectral density of the transmitter signal which falls in the bandwidth of the receiver in order to calculate the carrier-to-interference signal ratio. The details of these calculations are described below.

In this calculation, the interference level in the mobile-satellite system channel bandwidth (BW) is determined. Since this calculation includes both co-channel and adjacent channel interference contributions, the interferer TX and satellite uplink frequencies are not necessarily the same. Interference from other satellite transmitters is considered to be negligible.

4.1.1 Description of Calculation Steps

The calculation of interference to a mobile satellite service from fixed and mobile services in the same band is accomplished according to the steps outlined in this section:

4.1.1 Description of Calculation Steps (Cont'd.)

STEP	CALCULATION
(1)	Determine the interferer transmitter (TX) effective radiated power in the direction of the intended receiver for the specified emission bandwidth

$$ERP = P + G$$

ERP = Interferer TX effective Radiated Power
P = Interferer TX transmitted power for emission bandwidth B
G = Gain of interferer TX antenna

(2) Determine the interferer emission spectrum for the licensed interferer emission bandwidth and calculate the portion of the Interferer TX effective radiated power falling in the satellite channel bandwidth centered at the uplink frequency. For these calculations two types of emission spectra are considered, narrowband FM and UHF TV emissions. The details of the spectra assumed are described in Section 4.1.2.

(3) Determine the interferer TX antenna pattern isolation in the direction of the satellite. This isolation is the amount of antenna gain reduction at the difference angle α between the interferer intended direction of transmission and the angle to the satellite. (See Figure 4.1.)

For the narrow band FM emitters, this angle includes both the elevation and

azimuth components. The patterns used are typical for each type of antenna as shown in Figure 4-2 (Ref. 5-2).

$$ITX = G - G(\alpha)$$

ITX = Interferer TX antenna pattern isolation.

G = On-axis interferer TX antenna gain

$G(\alpha)$ = Interferer TX antenna gain at angle α from main beam.

α = Satellite - intended RX difference angle.

For UHF TV stations, the transmit antenna elevation pattern is considered to be approximated by a dipole field, and the gain reduction from the peak is calculated as the sum of a symmetrical azimuthal pattern and the assumed elevation pattern of that of a vertical dipole. This also applies to omni-directional FM interferers.

(4) Determine the satellite receive antenna pattern isolation in the direction of the interferer TX. This isolation is the amount of antenna gain reduction at the difference angle β between the satellite beam pointing direction and the direction to the interferer TX, since the satellite antenna pattern is assumed to be circularly symmetric.

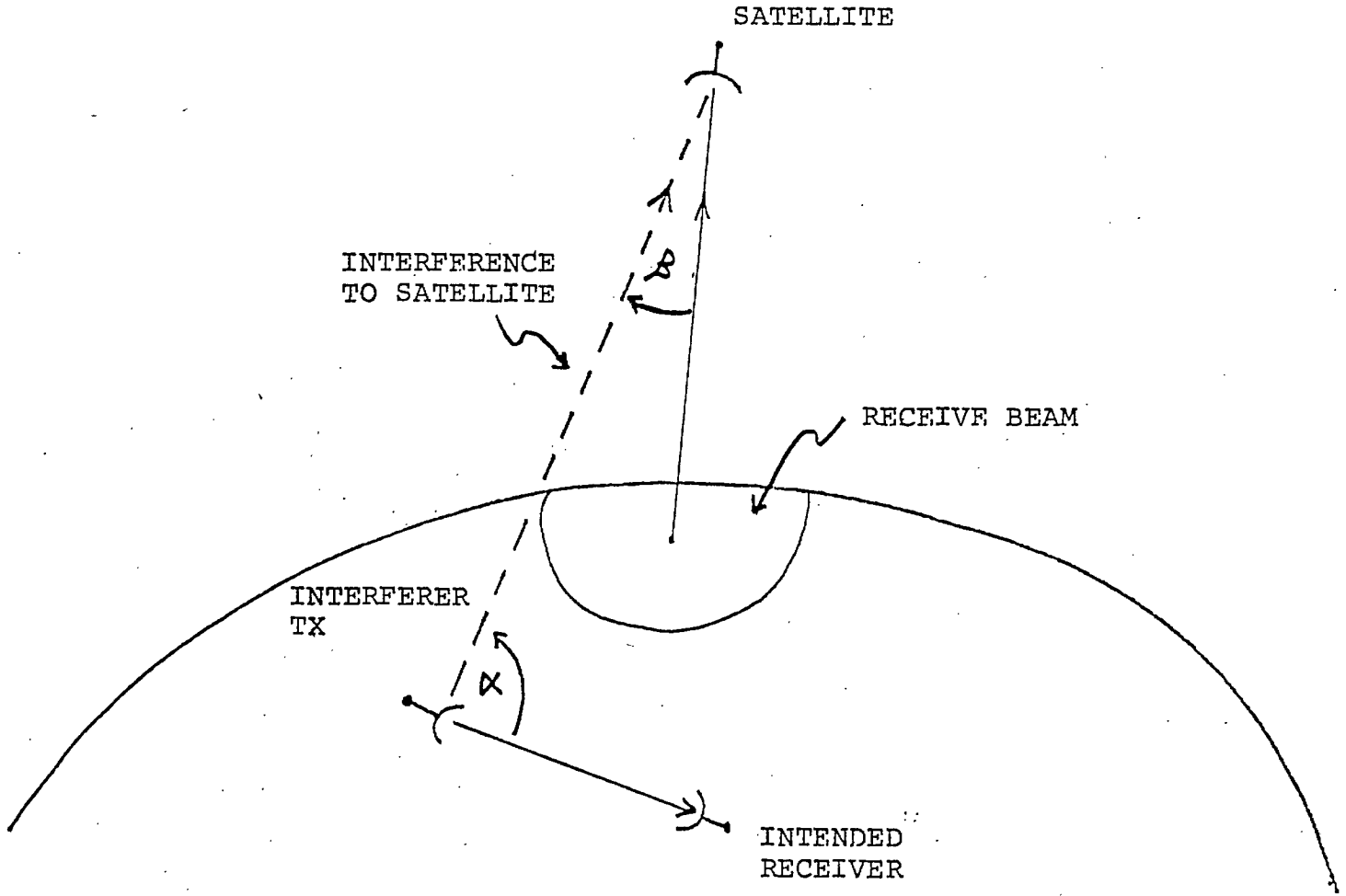

INTERFERENCE GEOMETRY

FIGURE 4 -1

307 = Yagi
360 = Parabolic Cylinder Reflector
227 = Corner Reflector
224 = Dipole

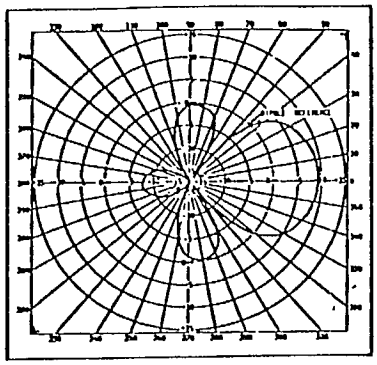

206 and 307

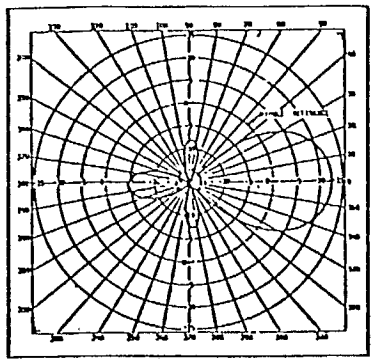

206-2 and 307-2

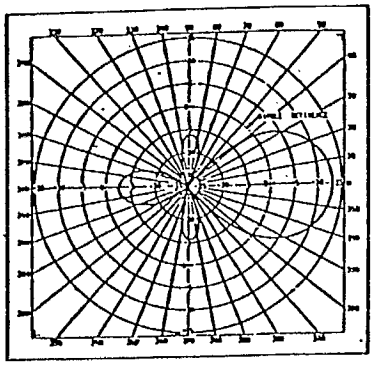

206-4 and 307-4

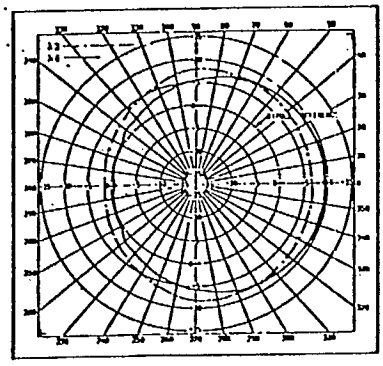

210-4 and 310-4

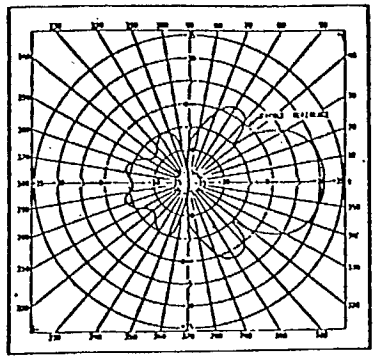

215

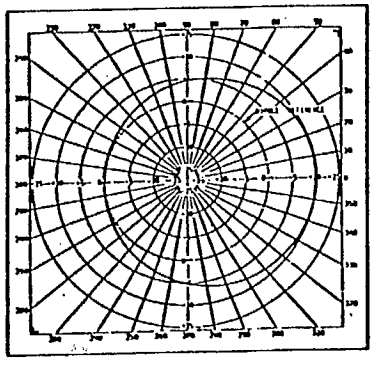

224

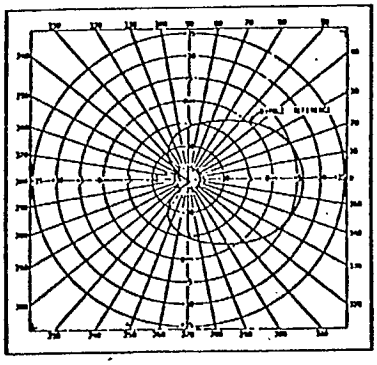

227

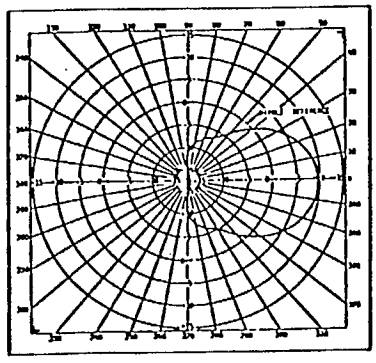

228

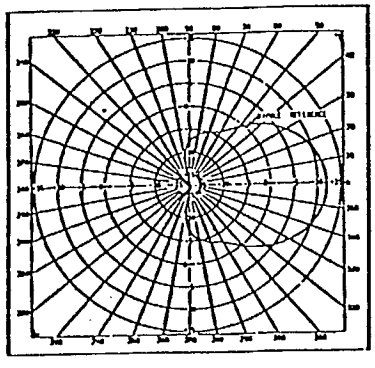

228-2

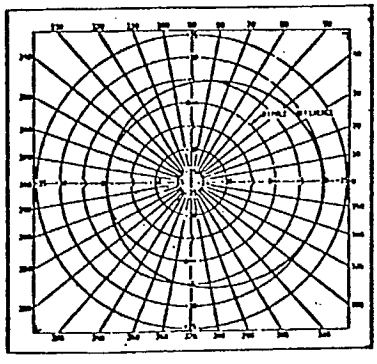

237

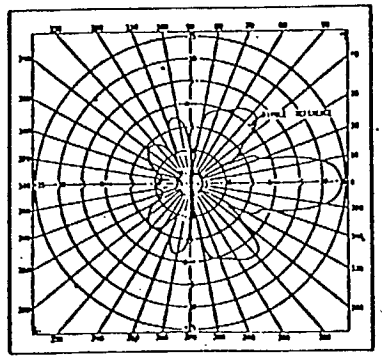

260 and 360

ANTENNA PATTERNS FIGURE 4 -2

4.1.1 Description of Calculation Steps (Cont'd.)

$$ISAT = GS - GS(\beta)$$

ISAT = Satellite receive antenna pattern isolation

GS = on-axis gain of satellite receive antenna

GS(β) = Satellite receive antenna gain at angle β from main beam.

β = Interferer TX - beam pointing difference angle

(5) Determine the effective interfering power by including the antenna isolation between the satellite and interferer TX in the calculation of Step 2.

$$EIP = IP - (ITX \pm ISAT)$$

EIP = Effective interfering power

IP = Interfering power (Step 2 and Section 4.1.2).

ITX = Interferer TX antenna isolation (Step 3).

ISAT = Satellite receive antenna isolation (Step 4).

4.1.1 Description of Calculation Steps (Cont'd.)

(6) Determine the earth-station effective radiated power in the satellite channel bandwidth BW for the wanted signal.

$$CM = PM \pm GM$$

CM = Earth-station effective radiated power

PM = Earth-station transmitter power in the system channel bandwidth BW

GM = Mobile antenna gain.

(7) Calculate the ratio of the earth-station effective radiated power to the effective interfering power.

$$C/I = \frac{CM}{EIP}$$

C/I = Carrier to interference ratio in the satellite channel bandwidth BW

CM = Mobile-satellite effective radiated power (Step 6)

EIP = Effective interfering power (Step 5)

4.1.1 Description of Calculation Steps (Cont'd.)

(8) Determine the mobile-satellite system degraded overall carrier to noise ratio taking the minimum overall design carrier to noise ratio of the satellite system and including the interference

$$C/(N+I) \quad \frac{1}{\frac{1}{C/N} + \frac{1}{C/I}}$$

$C/(N+I)$ = Degraded C/N ratio

C/I = Carrier to interference ratio (Step 7)

C/N = Satellite system overall carrier to noise ratio in channel bandwidth BW

(9) The degradation of the minimum overall C/N ratio due to the interference I is thus

$$DEG = C/N - C/(N+I)$$

DEG = Degradation level

C/N = Satellite System overall carrier to noise ratio in channel bandwidth BW

$C/(N+I)$ = Degraded C/N ratio.

4.1.1 Description of Calculation Steps (Cont'd.)

The degradation level calculated above is applicable for signal to noise ratios in the receiver I.F. The degradation level at the receiver output is a function of the input degradation and the actual SNR.

The total interference energy at the mobile-satellite uplink frequency is computed by repeating Steps 1 to 5 for all potential interferers and summing the individual interference energies. The degradation to the mobile-satellite overall C/N_o caused by the total interference energy is computed in Steps 6 to 9.

In this calculation, the interferer RF emission spectrum was determined theoretically given the RF emission bandwidth. This represents a worst case since inclusion of transmitter filtering may provide a faster spectrum roll-off outside the emission bandwidth. Filtering at the transmit output port is normally included to suppress carrier harmonics and spurious, and thus may be wider than the emission bandwidth.

4.1.2 Power Spectra of Interferers

Two types of interfering sources are considered in this study, an FM emission type (i.e. F1, F2, F3, F9) using the theoretical Gaussian spectrum distribution corresponding to the given emission bandwidth, and UHF television broadcast boosters and translators.

4.1.2.1 FM Emission Spectra

For the FM emission spectra, it is expected that all F3 and F9 emissions (voice and FDM) can be modelled as Gaussian random processes. Based on this assumption, and an interferer emission bandwidth defined for 98% power transmission, the power spectrum corresponding to a bandwidth B is shown in Figure 4.3. The Gaussian power spectral density function is expressed as (Ref. 5-3):

$$G(f) = \frac{ERP}{\Delta f_{rms}\sqrt{2\pi}} \exp(-(f-f_c)^2/2\Delta f_{rms}^2)$$

and $B = 4.6\ \Delta f_{rms}$

$G(f)$ = Power spectral density function

ERP = Interferer TX effective radiated power (Step 1)

Δf_{rms} = r.m.s. peak frequency deviation

f = frequency

f_c = interfering carrier frequency

B = interfering emission bandwidth

The power falling in the satellite channel bandwidth BW at the uplink frequency f_s is determined by integrating the power spectral density function as follows:

$$IP = \int_{f_s - \frac{BW}{2}}^{f_s + \frac{BW}{2}} G(f)\,df$$

IP = Portion of the interferer TX effective radiated power in bandwidth BW

BW = Satellite system channel bandwidth

f_s = Satellite uplink frequency

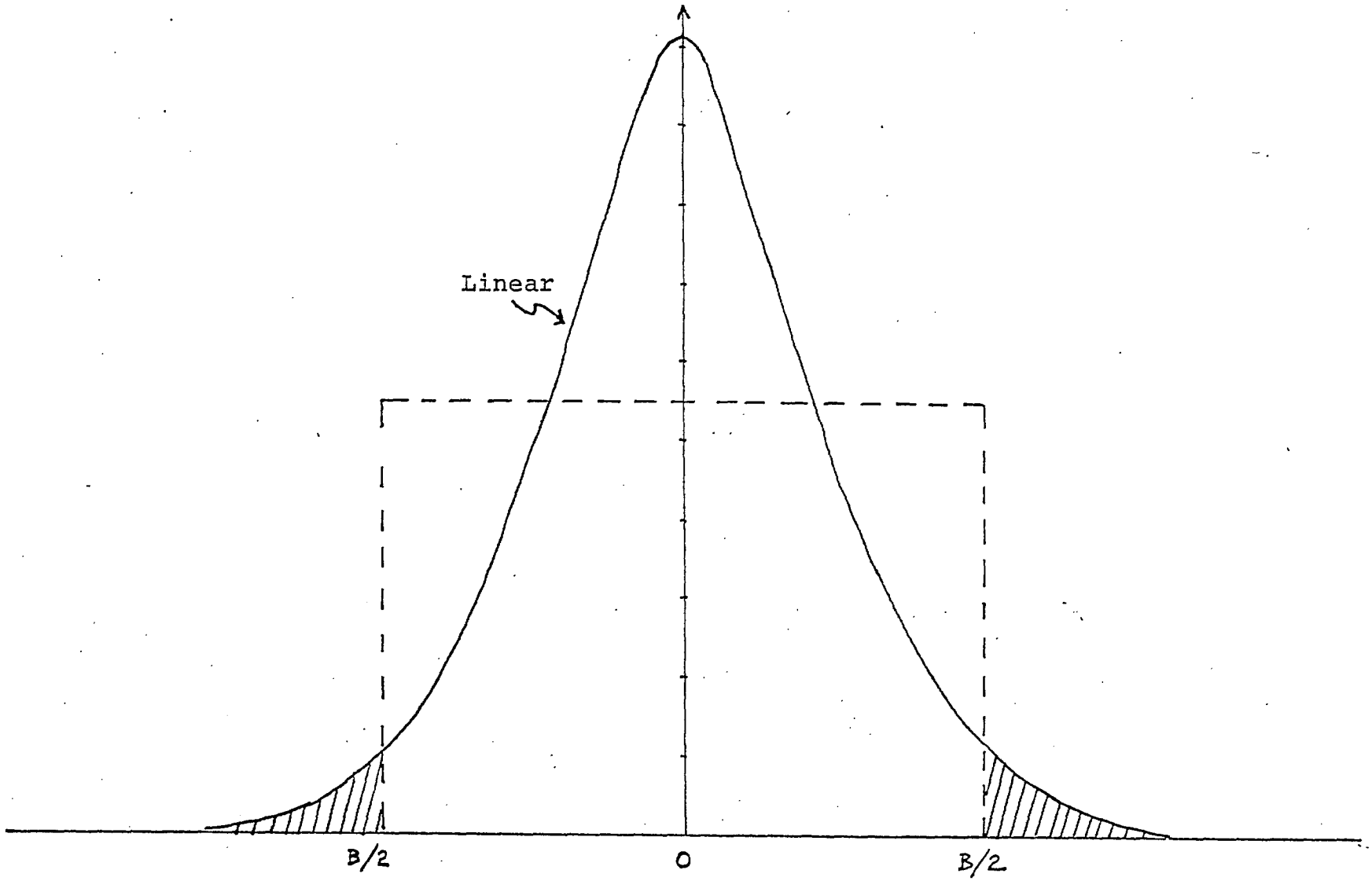

GAUSSIAN EMISSION SPECTRUM

FIGURE 4 -3

4.1.2.2 UHF TV Emissions

For UHF TV signals, the emission spectra of television boosters and translators must be considered. Reference 5-4 contains information regarding these types of television emissions. All these TV emissions use vestigial sideband amplitude modulation, AM/VSB. The bandwidth of this emission is 6 MHz as shown on the emission spectrum below.

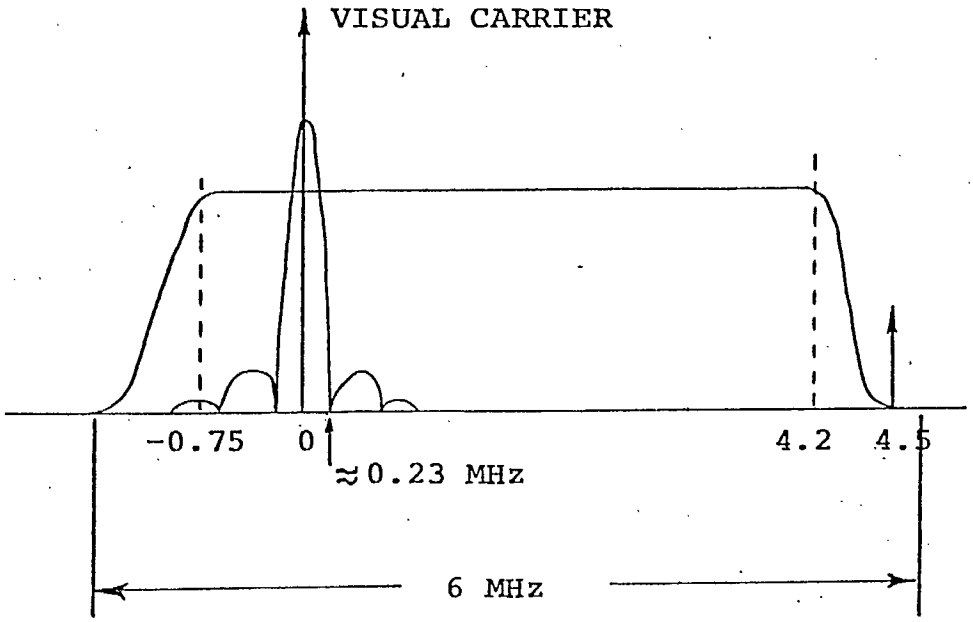

The spectrum energy distribution essentially consists of the wideband picture energy and the energy in the synchronization pulses (primarily the line synch pulse) which is concentrated at the visual carrier. Thus video transmission amplitude modulation with a non-suppressed carrier). Consider a rough video time waveform below:

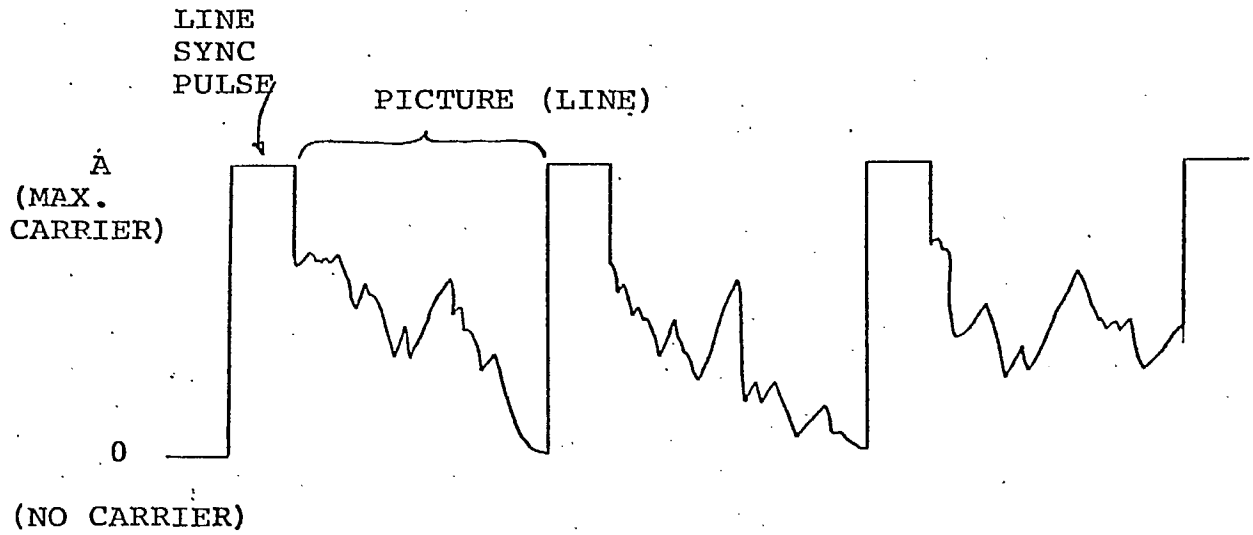

where A is the peak visual amplitude. For 525 line NTSC video the line synch pulse is about 5 μsec wide and the line period about 64 μsec. So for the synch pulse spectrum the repition frequency is 15.75 KHz line rate and the duty cycle is about 0.07. Thus its spectrum will be:

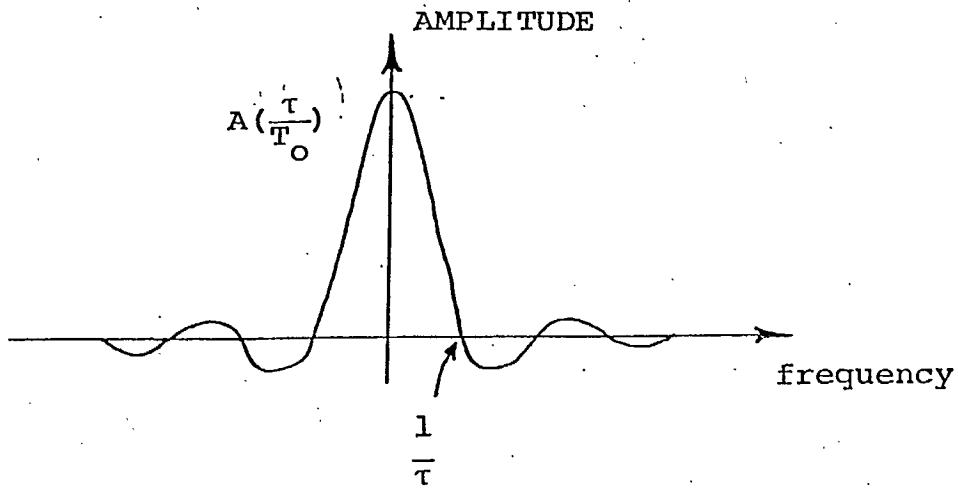

where τ = 5 μsec, T_o = 1/15.75 KHz = 64 μsec. So the power in the carrier itself is its amplitude squared:

$$A^2(\tau/T_o)^2 \text{ where } \tau/T_o = \text{Duty cycle}$$

but A^2 = peak visual power C

so $P_{carrier} = C\ (\text{Duty cycle})^2$

and since the total power in the synchronization pulse is:

$$P_{sync} = C\ (\text{Duty Cycle})$$

the remaining power in the synch modulation is

$$P_{sync-mod} = C(D)-C(D)^2$$
$$= CD(1-D)$$

where D = Duty cycle

For the picture modulation spectrum the content of the video signal has a duty cycle of about 58.9 μsec out of 64 μsec or a duty cycle of about 0.93. Now since the maximum picture amplitude is 0.68 (out of a maximum video amplitude of 1) corresponding to all black and the minimum picture amplitude is 0.125 for an all white image we can consider an average picture amplitude of about 0.5. So of the total visual power C in one line period, the picture power per line will be given by

$$\text{(Picture power level)(Duty cycle)}C$$

$$= (0.5)^2(0.93)C$$

$$\approx 0.23\ C$$

This enables the determination of the video (picture) spectral density given the peak radiated visual power and the emission bandwidth. As an example for a visual peak radiated power of 100 KW the power in the picture carrier itself should be about 500 watts. The power in the sync is 7 KW. The power in the picture modulation is 23 KW. So the radiated spectral density, shall be in a 4.95 MHz emission bandwidth.

$$23\ \text{KW} = 43.6\ \text{dBW}$$

$$4.95\ \text{MHz} = 67\ \text{dB}$$

$$\text{Spectral density} = -23.4\ \text{dBW/Hz}$$

Given the spectral density of the emission it remains to determine the power in the wanted channel bandwidth.

4.1.3 Calculation of Antenna Coupling

The off-boresight angles used for the calculation of the antenna coupling in Steps 1, 3 and 4 of Section 5.1.1 is included in this section.

4.1.3.1 Interferer-to-Satellite Pointing Angle

The interferer transmitter antenna isolation is determined from a knowledge of the antenna pattern and the pointing angle from interferer to satellite relative to the antenna on-axis direction. The calculation proceeds in two steps, given the satellite geostationary orbit position, interferer coordinates and transmission azimuth. The first step is the calculation of the satellite elevation angle at the interferer and the second involves the calculation of the bearing to the satellite from the interferer. From these two angles the net pointing angle can be obtained.

Pointing Angle in Elevation

Satellite slot position:

1) Latitude, $X = 0^{o}$
2) Longitude, $Y = 95^{o}$ to 115^{o}
3) Orbit altitude $h = 35,788$ km

Interferer Coordinates:

1) Latitude, S
2) Longitude, T

so let

$$\Delta L_a = (S-X) \text{ degrees}$$

$$\Delta L_o = (T-Y) \text{ degrees}$$

Now from spherical trigonometry it is determined that the angle ω substended by the interfer and satellite, at the centre of the earth is given by

$$\omega = \cos^{-1}\left[\cos\Delta L_a \cos\left|\Delta L_o\right|\right]$$

The corresponding distance from interferer to satellite is given by

$$r = \sqrt{R^2 + (R+h)^2 - 2(R)(R+h)\cos\omega}$$

where R is the radius of the earth
~ 6378 km
h is the geostationary orbit altitude
~ 35,788 km

The satellite elevation angle, θ, at the interferer can now be calculated using the following equations

$$\frac{\sin\omega}{r} = \frac{\sin\phi}{R}$$

$$\text{so} \quad \phi = \sin^{-1}\left[\frac{R}{r}\sin\omega\right]$$

and thus $\theta = (90-\omega)-\phi$

The relationship of these variables is shown in Figure 5.4. Note that this angle is used to calculate the dipole field of the UHF TV antenna.

Pointing Angle in Azimuth

The pointing angle in azimuth from interfer to satellite is the difference angle between the bearing to the satellite sub-orbital point and the interfer antenna on-axis direction. The satellite bearing is determined as follows:

$$\text{Let} \quad C = R\phi$$
$$b = R\Delta L_a$$
$$a = R\Delta L_o$$

From spherical trigonometry a right spherical triangle with sides a, b and C and angles γ and Ψ, as shown in Figure 5.5 can be described by the following equation for γ

$$\gamma = \sin^{-1}\left[\frac{\sin a}{\sin C}\right]$$

Now if ΔL_o is positive, the satellite bearing is

$$180^o + \gamma$$

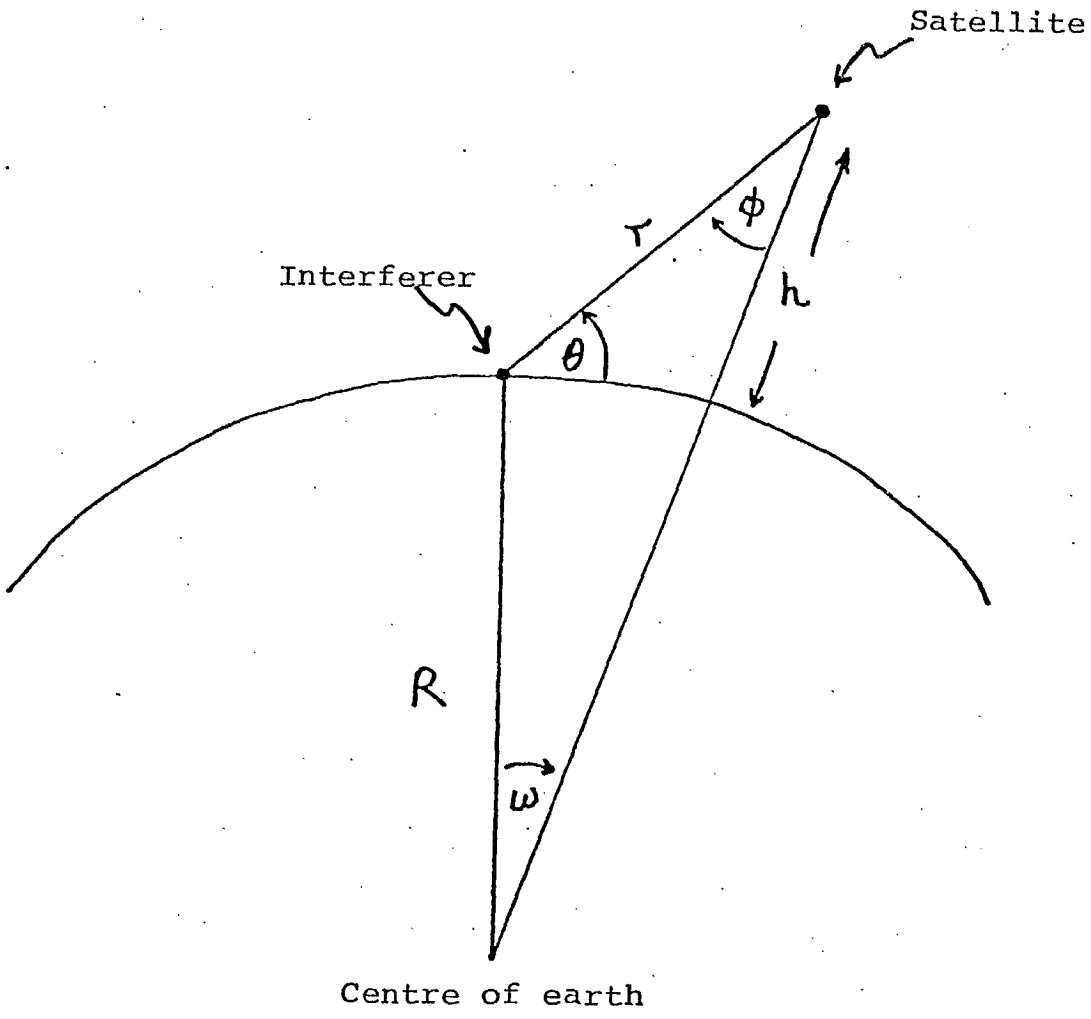

POINTING ANGLE IN ELEVATION

FIGURE 4.4

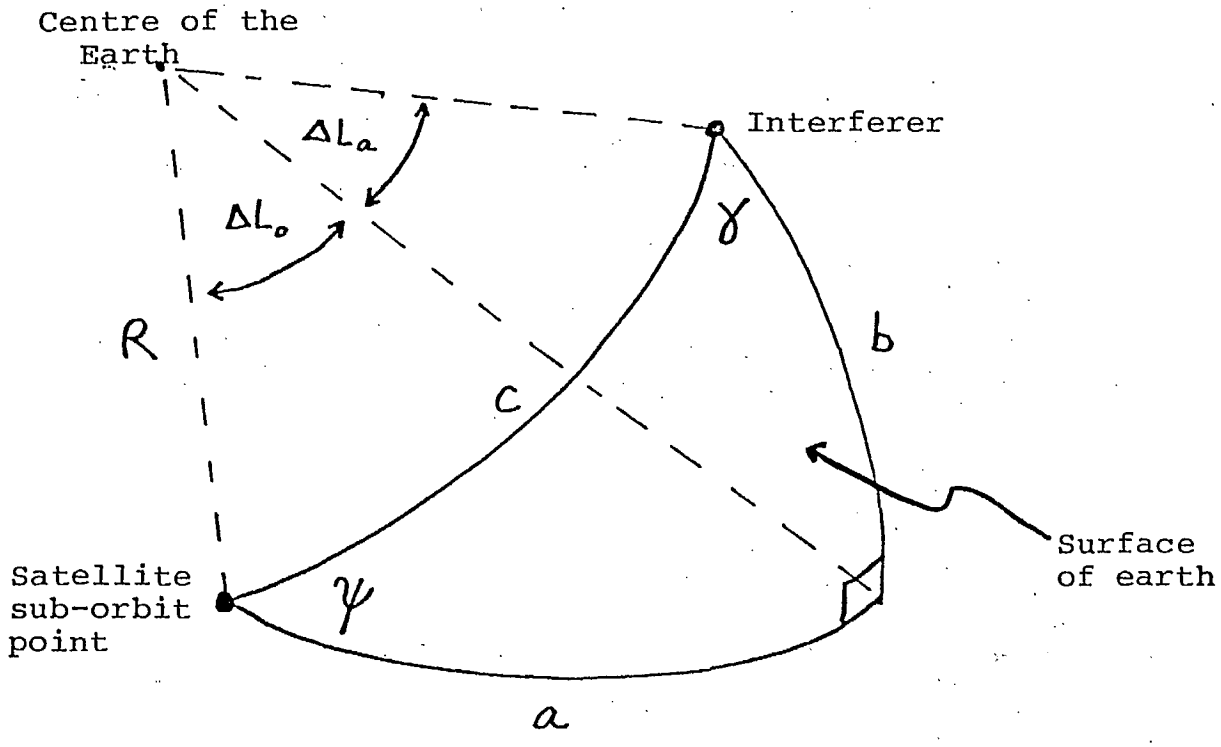

POINTING ANGLE IN AZIMUTH

FIGURE 4.5

and if ΔL_o is negative, the satellite bearing is

$$180^o - \gamma$$

Given the interferer transmission azimuth A, the azimuth pointing angle λ is thus

$$\lambda = \left| A - (180^o \pm \gamma) \right| \quad \text{degrees}$$

Net Pointing Angle

The net interferer to satellite pointing angle α is determined, using the following equation from spherical trigonometry.

$$\alpha = \cos^{-1} \left[\cos \theta \cos \lambda \right]$$

where θ Pointing angle in elevation
λ Pointing angle in azimuth
α Net Pointing angle, degree

4.1.3.2 Satellite to Interferer Pointing Angle (β)

The amount of discrimination to interferers provided by the satellite receive antenna is determined by the directivity of the satellite antenna and the difference angle between the satellite beam pointing direction and the direction to the interferer. This difference angle is computed using vectorial analysis. Given the interferer, beam pointing and satellite coordinates the corresponding Cartesian coordinates referenced to the centre of the earth are determined using the following transformation

$$X = R(\cos LAT)(\sin LONG)$$
$$Y = R(\cos LAT)(\cos LONG)$$
$$Z = R(\sin LAT)$$

where LAT Latitude
LONG Longitude
R Radial distance from centre of Earth

The vectors representing the satellite interferer and beam pointing locations in a Cartesian 3-D space are defined as follows

$$\overline{VS} = ix_1 + jy_1 + kz_1$$
$$\overline{VI} = ix_2 + jy_2 + kz_2$$
$$\overline{VB} = ix_3 + jy_3 + kz_3$$

where

$\overline{VS}$ Satellite vector
$\overline{VI}$ Interferer vector
$\overline{VB}$ Beam pointing vector

The vectors representing the satellite beam pointing direction and the satellite to interferer pointing

direction are determined as follows

$$\overline{VSI} = \overline{VS} - \overline{VI}$$
$$= i(x_1-x_2) + j(y_1-y_2) + k(z_1-z_2)$$

$$\overline{VSB} = \overline{VS} - \overline{VB}$$
$$= i(x_1-x_3) + j(y_1-y_3) + k(z_1-z_3)$$

where $\overline{VSI}$ Satellite to interferer vector

$\overline{VSB}$ Satellite beam pointing direction vector

By using the Scalar product relation for two vectors, the difference angle β between these two directions is given by

$$\beta = \cos^{-1}\left[\frac{\overline{VSI}\cdot\overline{VSB}}{|\overline{VSI}||\overline{VSB}|}\right]$$

and

$$\overline{VSI}\cdot\overline{VSB} = (x_1-x_2)(x_1-x_3) + (y_1-y_2)(y_1-y_3) + (z_1-z_2)(z_1-z_3)$$

4.1.4 Interference Criteria

There are two limits which establish the maximum level of interference that can be tolerated in a mobile system. These are: the minimum C/N in order to be above the threshold point required by the receiver demodulator and the minimum C/N_o required to provide adequate intelligibility of the desired signal. At high degradation levels, crosstalk and breakthrough may be more of a problem than noise-like degradation. The first factor, however, can be accurately estimated and may well limit the allowable interference before intelligibility becomes a problem. The later factor is more difficult to ascertain, and requires experimental analysis due to the somewhat subjective aspects involved.

4.1.4.1 Threshold Limitation

The demodulation threshold criterion of interference is dependent upon the type of demodulation used. For example, it is expected that an FM demodulator for voice (using a phase lock loop) will have an actual threshold of about 7 dB, including losses in the loop.

If the allowable interference is assumed to double the effective noise in the receiver, then a 3 dB margin must be added to this threshold, resulting in a required C/N of 10 dB. Thus for a 18 kHz channel (42.6 dB), the threshold becomes 52.6 dB - Hz.

4.1.4.1 Note that a decrease in channel bandwidth will lower the threshold C/N_o, and thus permit a higher level of interference. Generally the maximum allowable level of interference can be determined for other values of overall operating C/N_o, threshold C/N_o and transmitted ground station EIRP, by use of the following equation:

$$I = (C)(BW)\left[\frac{1}{\left(C/N_o\right)_{TH}} - \frac{1}{C/N_o}\right]$$

where C = Uplink EIRP

BW = Satellite channel bandwidth

$\left(C/N_o\right)_{TH}$ = Threshold overall C/N_o ratio

C/N_o = operating overall carrier to noise density ratio

4.1.4.2 Intelligibility Limitation

The intelligibility criteria for this type of voice communication has been assessed in Reference 5-5.

Table 4.1 and attached figures present the results of intelligibility tests performed to establish threshold C/N_o values for narrow band FM transmission. It can be seen that 90% intelligibility for satisfactory voice transmission in a 25 kHz bandwidth is approximately (44 dB-Hz ± 6 dB)= 50 dB-Hz. For interference noise equal to the front end noise, the threshold C/N_o is thus 53 dB-Hz.

NBFM (Reference: CCIR Report (509-2))

RF BANDWIDTH (KHz)	*THRESHOLD C/N_o	ARTICULATION INDEX	**INTELLIGIBILITY %
8	45	0.51	82
10	46	0.58	88
18	48.6	0.67	93

* Assumes a 6 dB C/N is required

** Assumes untrained user (modified rhyme tests)

Intelligibility of 90% is considered satisfactory for voice transmission.

It is noted that an increase of RF bandwidth lowers performance under marginal signal conditions but yields a higher level of articulation index when exceeding receiver threshold.

The transmission C/N_o must allow for worst-case fading losses occuring within say 95% of the time for a transmission reliability of 95%.

It is considered that for NBFM voice transmission an RF bandwidth between 10 KHz and 18 KHz is suitable for satisfactory (90% intelligibility) service.

D-1 Analogue Transmission for Voice

TABLE 4-1

(Doc. 8/1069-E)

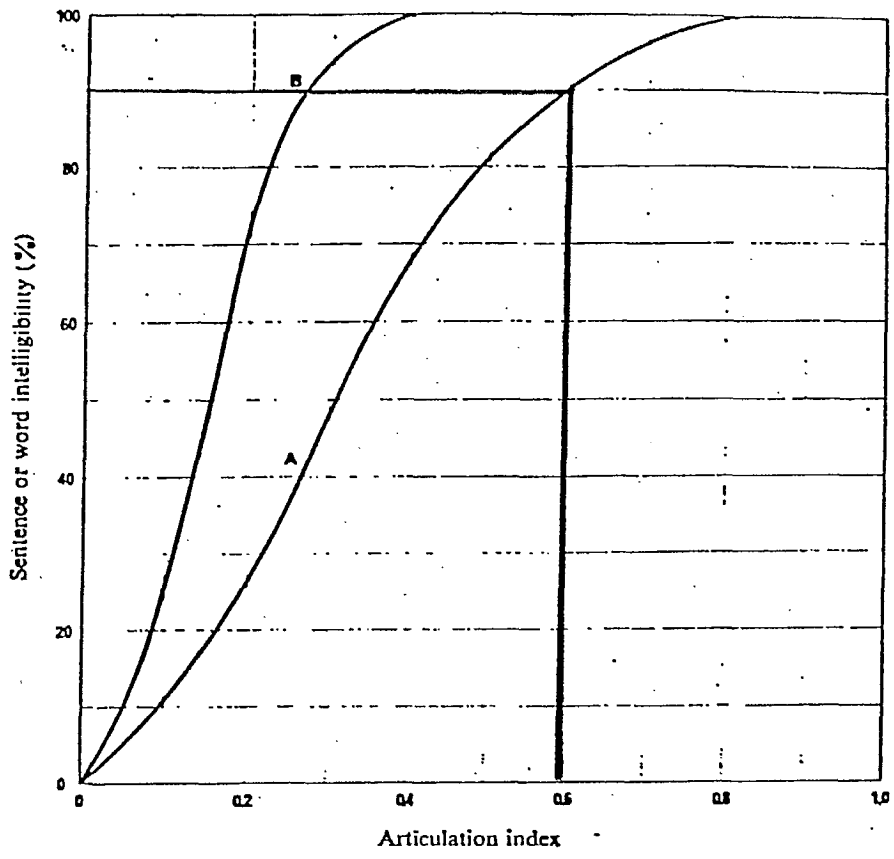

FIGURE 1

Percentage intelligibility as a function of articulation index

A: modified rhyme tests

B: air traffic control message tests

TABLE 4-1

FIGURE 1

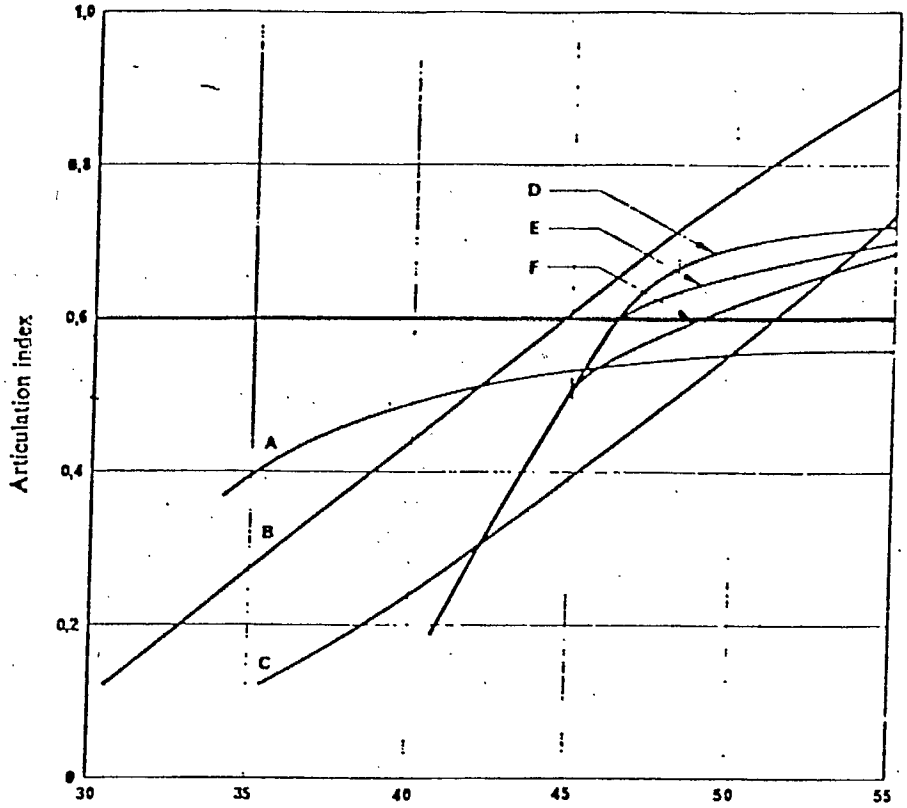

FIGURE 2

Comparison of analogue voice modulation techniques

A: FRENA (Frequency and amplitude)
B: 5 kHz single sideband-mean radio-frequency power
C: 5 kHz single sideband-peak radio-frequency power
D: frequency modulation (18 kHz)
E : frequency modulation (10 kHz)
F : frequency modulation (8 kHz)

TABLE 4-1

FIGURE 2

4.2 Interference Calculation 806 - 890 MHz Band

4.2.1 Interference To and From UHF T.V.

4.2.1.1 Interference Levels to Satellite From T.V. Transmitters

Assuming a maximum expected ERP for high-band UHF transmitters of 1000 KW and a flat, 64 MHz wide spectrum, power density equals -7.8 dBW Hz.

In an 18 KHz wide band, corresponding to a single satellite channel power P_o equals 34.8 dBW.

Since the TV interference should be at least 12 dB below the ground station signal at the satellite and given that the ground station power is about 1 dBW, minimum required antenna rejection is -49.9 dB relative to the centre of the main beam. This assumes that the ground station is at the beam edge or 4.1 dB down from the centre and that the satellite is in the main beam of the TV antenna.

As seen in Figure 3-5, the pattern nulls are well below the -49.9 dB level. With an improved antenna design, null steering should not be required near the edges of the earth. Although the antenna rejection is less for TV transmitters near the satellite main beam, the ERP of the TV station may be less, due to the typical TV antenna vertical pattern, where the maximum gain is at the horizon. In the region of the video carrier, additional rejection may be required. Since the antenna pattern is generally constant over the frequency bands, the rejection requirements will be determined by the channel with the most interference.

Figures 4.6 and 4.7 show plots of the interference level in each channel produced by a single TV transmitter. Figure 4.6 displays the level where the transmitter is located on the first side lobe of the main beam and Figure 4.7 shows the level when the transmitter is located at the limb of the earth.

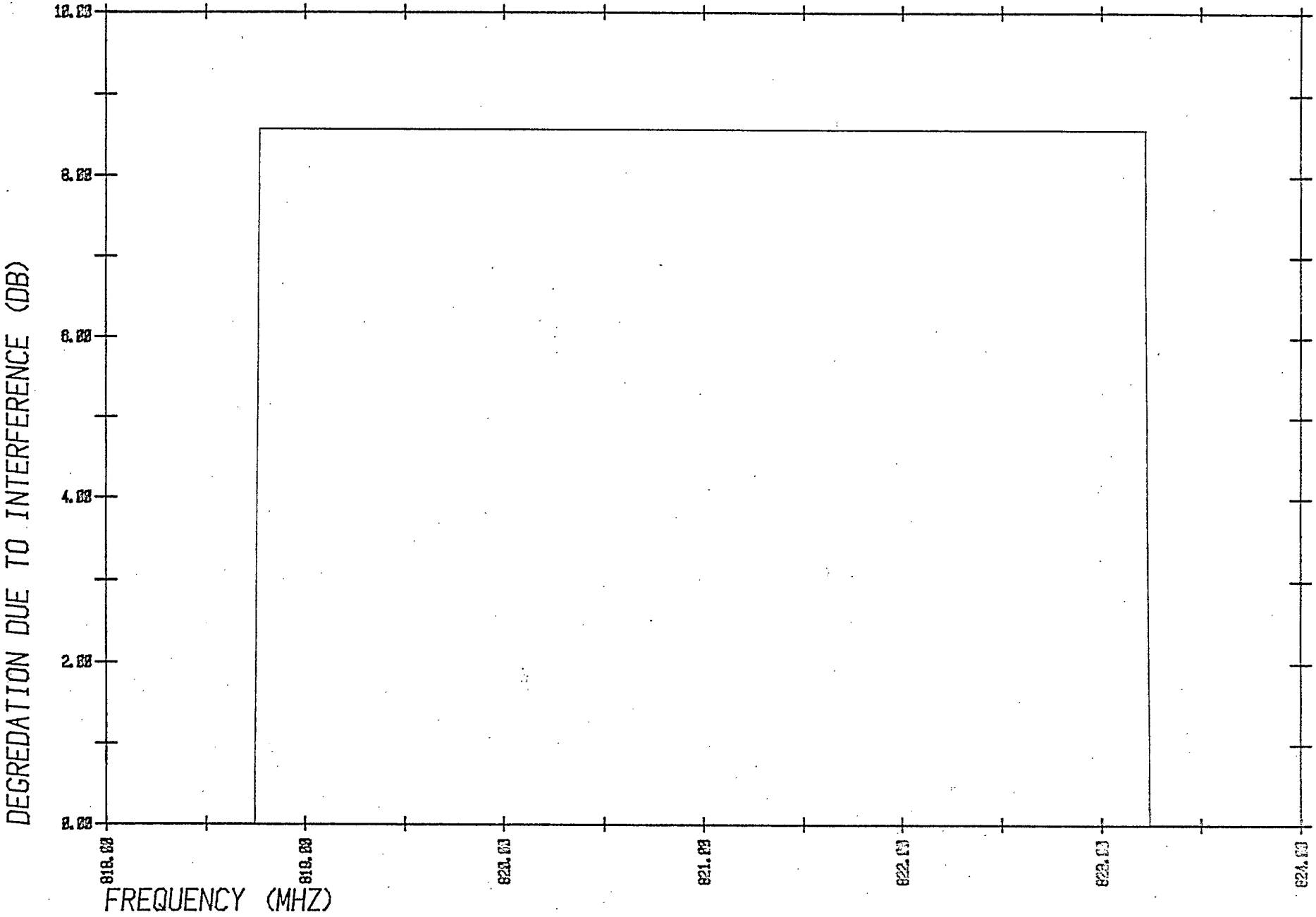

INTERFERENCE FROM TV TRANSMITTER IN 1ST SIDELOBE

FIGURE 4.6

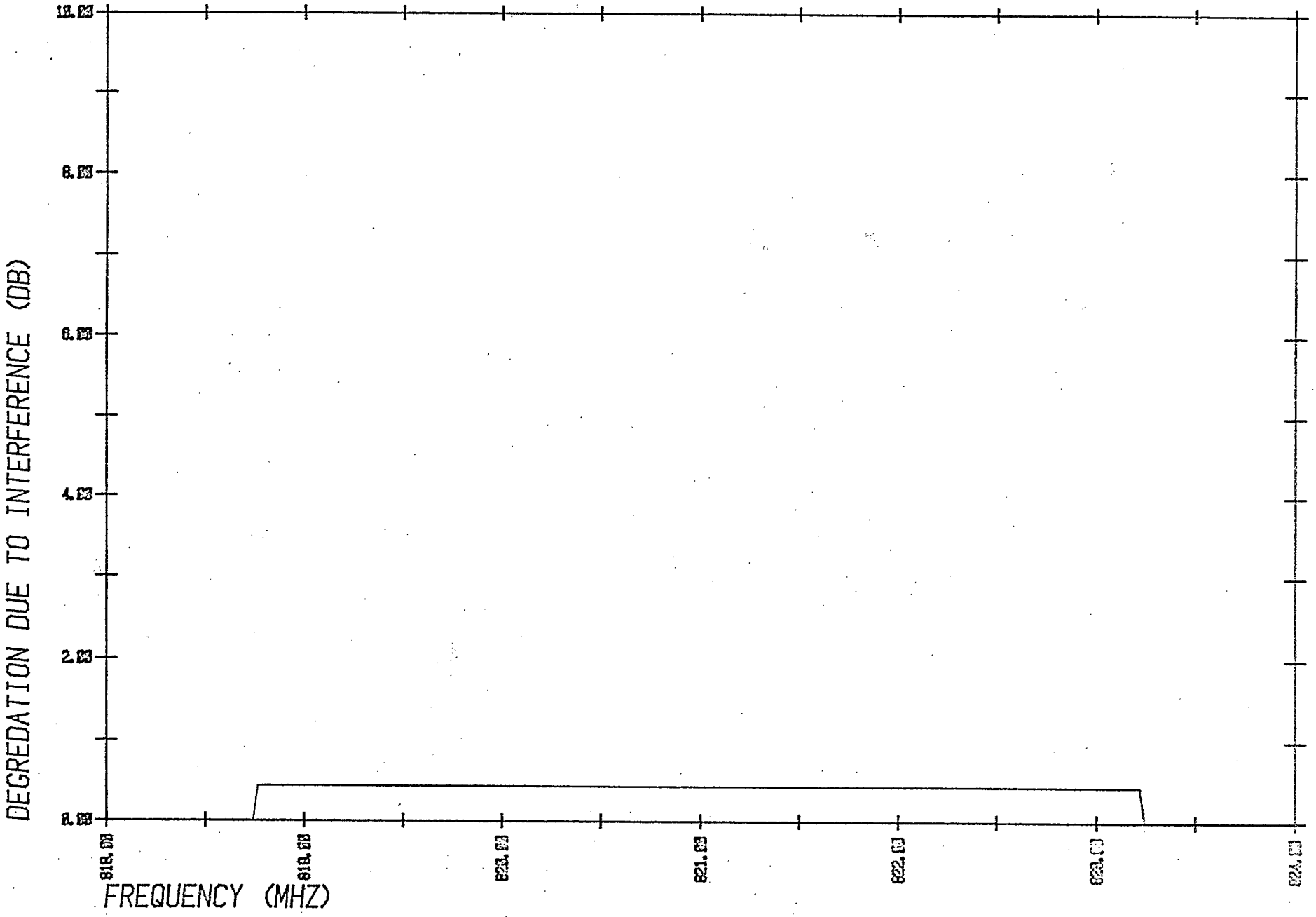

INTERFERENCE FROM TV TRANSMITTER AT EQUATOR

FIGURE 4 .7

4.2.1.2 Present Sources of UHF TV Interference

At present, there is only one TV station operating on Channel 72 (uplink frequency band), which is a low power repeater station in Enderby, B. C. There are no Channel 72 stations in the U.S. There are only 2 stations (Channel 69) in the upper UHF band in the U.S. There are several potential interfering UHF TV stations in France and England. There are no other known sources of TV interference in the world for the 818 - 824 MHz uplink band. France and England are not within range for the satellite longitudes considered.

4.2.1.3 Interference Levels to TV Receivers From Satellite

Assuming a satellite down-link ERP of 40 dBW per channel, 56 channels per band, the total ERP for 3 bands is 62 dBW. With space losses of 183 dB, the signal level at the ground is -120.7 dBW, over a 6 MHz band. The standard signal level for CATV, which corresponds to a minimum level for good quality colour reception, is about -78.8 dBW. A signal of -120.7 dBW signal corresponds to a 7.9 μV signal for 75 Ω, well below a typical TV receiver noise level. Hence it is expected, even under worst case conditions, that the satellite will not produce a detectable signal in a TV receiver.

4.2.2 Cellular Mobile Interference

The frequency allocations for the cellular mobile system do not overlap with the proposed up and down-link frequency bands for the satellite system. The frequency bands allocated to cellular mobile are 825 - 845 MHz and 870 - 890 MHz. The two systems cannot store the same frequencies in the same coverage region, however frequencies could be reused in beams covering regions remote from the cellular system coverage area.

4.2.3 General Land Mobile Radio Service

Frequency allocations for the land mobile service are from 806 to 881 MHz. In particular, an FCC allocation has been made for the multi-channel trunked repeater system. The trunked system will initially combine 5 transmitters and 5 receivers to use the same antenna. A 1 MHz spacing between transmit frequencies will be used initially. The transmit band is from 865.9875 to 860.9875 MHz and the receive band is from 820.9875 to 815.9875 MHz. This is almost a complete overlap with the proposed satellite frequency bands. However, the satellite uplink corresponds to the repeater receive frequencies. Interference will result to and from mobile stations and not the repeater.

In the main beams of the satellite downlink, the expected interfering signal level to mobile stations for a given FM channel is -150 dBW. A typical receiver sensitivity (for a 0 dB gain antenna) is about -161 dBW. Hence as long as the mobile is outside the main beam, where the maximum gain (highest sidelobe) is -25 dB, the satellite will have no effect on the mobile receiver.

The most critical interference arises from the mobile transmitters which typically have a power of 14 dBW or 13 dB greater than the satellite ground stations. The satellite antenna must have a rejection of at least 28 dB for an intering mobile. If several interfering mobiles are to be present, most of them must be far removed (at least 3°) from the main beam. This may be a problem since the entire U.S. is within 3° of at least one beam. The simplest solution to this problem is to change the system frequencies to be outside the trunked system allocation.

4.3 Interference 608 - 614 MHz

The 608 - 614 MHz band corresponds to channel 37 where no UHF TV stations exist. This band is reserved primarily for aero-navigation and in Canada - for radio astronomy. It would be possible to use this as an up-link for regions away from the radio telescopes location. (Say a 200 mile radius.) The band could not be used as a down-link, however the band could handle the uplink and another frequency band used for the downlink.

4.4 Interference 1.5 - 1.6 GHz

If the satellite antenna is scaled down according to frequency ratios, the antenna pattern will be identical to the 800 MHz pattern. The scale factor is about 1.8. If the satellite and ground station transmit powers are increased by the same factor (2.6 dB), the interference levels and performance are exactly the same as the 800 MHz case. However, at 1.5 GHz, there are fewer interferers. The MARISAT system using this frequency band would not be an important source of interference (as the land mobiles were for the 800 MHz case) since the earth coverage areas for the two systems are mutually exclusive. The MARISAT ship/satellite L-band uplink band is 1.6385 - 1.6425 GHz and the downlink is 1.537 - 1.541 GHz. If the mobile satellite system was to share the same frequency allocations with MARISAT, the best arrangement would be to use complementary up and downlink frequencies (opposite up and downlink and bands for the two satellites) which would result in no interference. If the up and downlink bands were common to both systems, some interference would result, particularly since the MARISAT antenna beam covers the entire earth and has no spatial selectivity. The EIRP of a ship station at 1.6 GHz is 37 dBW in contrast to about a 1 dBW EIRP of a land mobile station. Hence the interference is minimal. However, the ship may receive some interference since MARISAT only has an EIRP of 15.6 dBW

and hence the ship's antenna would require at least 50 dB of interference rejection.

5.0 SYSTEM COSTS AND REVENUES

The system costs have been estimated by comparison to similar existing ground-based equipment and by using a modified version of the communications satellite cost modelling program for the space segment equipment.

5.1 Space Segment Costs

The modelling program is not able to model the baseline system on a link-by-link basis. This is because the link matrix alone would require:

$$(24 \times 58 \times 19) = 26,448 \text{ entries,}$$

and the program then exceeds the core capacity of the computer. The system was thus modelled on a band basis, where each band was assumed to contain 58 channels. This has the effect of requiring one output stage (of 58 times the power) for each beam. The array and antenna sizing remains the same. As the output stage model in this frequency range is linear with power, the output of the program is nearly the same as if an output stage per channel assumed.

Figure 5-1 is a summary description of the space segment as modelled by this cost program. The estimated cost of the space segment is broken down in Figure 5-2. It is to be noted that these costs are projected 1990 Canadian dollar costs for the space segment. The calculation assumes a base year of 1978 for the cost data (in US dollars), then adjusts for inflation at 7% per year, and for exchange at 1.15 Can. $ equals 1 U.S.$. It further assumes a program duration of three years. Figure 5-3 shows the change in space segment total cost if the launch date assumption is changed from 1984 to 1990.

```
**** COMMUNICATION SATELLITE COST MODEL ****
     PREPARED BY: CANADIAN ASTRONAUTICS LTD.
     VERSION NO.   02    MARCH 1979
     SOFTWARE SUPPORT: 1-613-820-8280
```

MODEL NAME: LARGE ANTENNA MODEL
DESCRIPTION:
24 1X1 DEGREE BEAMS
800 MHZ BAND
WFP JUNE 79

SYSTEM PARAMETERS SUMMARY

```
* - LAUNCH IN 1990 ON A SHUTTLE  LAUNCH VEHICLE
    WITH A IUS       UPPER STAGE
* - SYSTEM HAS    2 SPACECRAFT COMPRISED OF
      1 IN ORBIT OPERATING
      1 IN ORBIT SPARE
      0 ON GROUND SPARE
* - SPACECRAFT DESIGN LIFE IS 10.0 YEARS
* - SPACECRAFT MASS IS     1323.  KG
    OF WHICH PAYLOAD IS      590. (KG)
             BUS     IS      732. (KG)
* - PAYLOAD LENGTH IS        24. (FT)
* - PROGRAM COST IS     306.340 MILLION DOLLARS(CANADIAN)
* - 3 AXIS STABILIZED SPACECRAFT WITH EXTENDABLE RIGID SOLAR PANELS
    EQUIPPED WITH BLACK SOLAR CELLS
* - HYDRAZINE MONOPROPELLANT AUXILIARY PROPULSION
* - NICKEL CADMIUM BATTERY
* - CONVENTIONAL STRUCTURE DESIGN
* - ANTENNA TYPES USED
    OPEN PARABOLA(DEPLOYABLE)    26.202  DIAM.(M)
    PRECISION PARABOLA(DEPLOYABLE)     6.117  DIAM.(M)
* - POWER REQUIREMENTS(WATTS)
        247.  BEGINNING OF LIFE
        182.  END OF LIFE
        182.  ECLIPSE
```

FIGURE 5.1

ADJUSTED COST MODEL
LAUNCH YEAR= 1990 CANADIAN DOLLARS

COSTS(THOUSANDS OF $)	OVERALL
HARDWARE COSTS	126553
S/C INTEGRATION	22190
UPPER STAGE COSTS	46109
LAUNCH VEHICLE COSTS	81276
MANAGEMENT FEES	12655
PROFIT	13920
MISSION ANALYSIS	2576
T&L	1058
TOTAL COSTS	306339

THE EXCHANGE RATE IS TAKEN AS $1 U.S.= 1.150CANADIAN

ESTIMATED COST OF SPACE SEGMENT
IN 1990 CAN. DOLLARS.

FIGURE 5.2

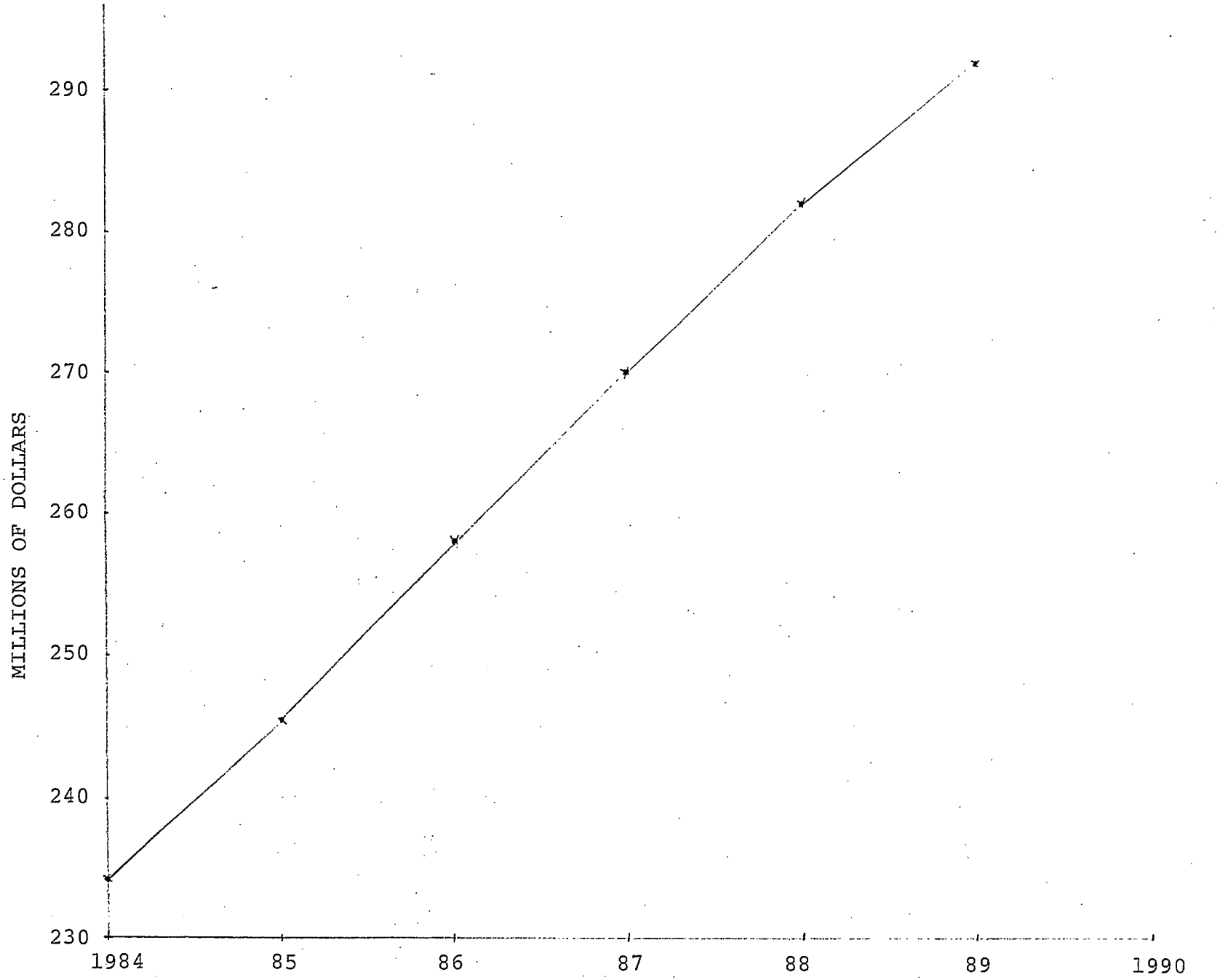

FIGURE 5-3 PROJECTED SPACE SEGMENT COST AS A FUNCTION OF YEARS OF LAUNCH

5.1 Space Segment Costs (Cont'd.)

As a basis of comparison, a model for an L Band system was also run, this is shown in Figure 5-4. Note that the cost remains nearly the same because as the antenna size is reduced, the solar array size increases.

5.2 Ground Segment Costs

5.2.1 Pilot Beacons

The cost of pilot beacons is expected to be similar to the cost of the data collection platforms for LANDSAT. These have in the past cost about $5K in 1976 Canadian dollars. The 1990 cost is thus estimated as

$$1.07^{(1990-1976)} \times 5000 \quad \$12,892 \text{ each.}$$

Assuming six spares, a complement of 30 beacons will thus cost $386,780.00 in 1990.

5.2.2 Regional Ports

The regional ports are similar in size and complexity to the thin route stations used by TELESAT Canada. Currently, one of these stations costs about $3M. Using the same inflation factor as the previous section,

$$1.07^{(1990-1979)} \times \$3M = \$6.31 \text{ M per station.}$$

Thus a system equipped with ten of these stations would cost $63.1 M in 1990.

MODEL NAME: LARGE ANTENNA MODEL
DESCRIPTION:
24 1X1 DEGREE BEAMS
1.5 GHZ BAND
WFP JUL 79

SYSTEM PARAMETERS SUMMARY

* - LAUNCH IN 1990 ON A SHUTTLE LAUNCH VEHICLE
WITH A IUS UPPER STAGE
* - SYSTEM HAS 2 SPACECRAFT COMPRISED OF
1 IN ORBIT OPERATING
1 IN ORBIT SPARE
0 ON GROUND SPARE
* - SPACECRAFT DESIGN LIFE IS 10.0 YEARS
* - SPACECRAFT MASS IS 1233. KG
OF WHICH PAYLOAD IS 530. (KG)
BUS IS 703. (KG)
* - PAYLOAD LENGTH IS 24. (FT)
* - PROGRAM COST IS 305.715 MILLION DOLLARS(CANADIAN)
* - 3 AXIS STABILIZED SPACECRAFT WITH EXTENDABLE RIGID SOLAR PANELS
EQUIPPED WITH BLACK SOLAR CELLS
* - HYDRAZINE MONOPROPELLANT AUXILIARY PROPULSION
* - NICKEL CADMIUM BATTERY
* - CONVENTIONAL STRUCTURE DESIGN
* - ANTENNA TYPES USED
OPEN PARABOLA(DEPLOYABLE) 13.988 DIAM.(M)
PRECISION PARABOLA(DEPLOYABLE) 6.117 DIAM.(M)
* - POWER REQUIREMENTS(WATTS)
348. BEGINNING OF LIFE
256. END OF LIFE
256. ECLIPSE

ADJUSTED COST MODEL
LAUNCH YEAR= 1990 CANADIAN DOLLARS

COSTS(THOUSANDS OF $)	OVERALL
HARDWARE COSTS	126435
S/C INTEGRATION	22150
UPPER STAGE COSTS	46109
LAUNCH VEHICLE COSTS	80834
MANAGEMENT FEES	12643
PROFIT	13907
MISSION ANALYSIS	2576
T&L	1058
TOTAL COSTS	305715

THE EXCHANGE RATE IS TAKEN AS $1 U.S.= 1.150CANADIAN

FIGURE 5.4

5.2.3 Central Control Station

The central control station is fitted with the same RF equipment as a regional port and in addition has the necessary computers and peripherals to support the mission. The present cost is estimated at $12M and thus in 1990 dollars is $25.2M.

5.2.4 User Terminals

The present user terminals for the GLMRS cost between $1900 and $3400 to buy, the cost spread depending upon the options. A reasonable cost for a typical user terminal is thus taken as $2500 present-day dollars, or $5,262 in 1990 dollars.

As initial start-up, it is assumed that 10% of the terminals are required in 1990. The remainder of the terminals are procured as the user base grows. The capital cost of the start-up group of terminals in 1990 is thus:

$$2,680 \times \$5262 = \$14,100,000.$$

For the purpose of estimating the system capital cost, it is assumed that the first 10% of the terminals are capitalized upon initiation of the service. As the user base grows, additional terminals are either bought or leased by the individual users and thus do not factor directly into the system procurement cost.

5.3 Operating Costs

A quick estimate of the operating costs can be made by estimating the man years required to support the operating system. A man-year of 1990 technical/engineering labour is estimated to cost $138K/yr based on $50K/man years

5.3 Operating Costs (Cont'd.)

in 1975 and 7% per year inflation to 1990.

Regional Ports will require 2 men per shift and will operate 24 hrs/day. Thus the complement of staff for each regional port will require a minimum of 8 operators and one supervisor so the ten regional ports will require 90 man-year/yr or a labour cost of $12,420 K/year.

Central Control station labour can be similarly estimated as requiring 5 men/shift or a staff of 20 plus two supervisory personnel for a requirement of 22 man years/yr and a labour cost of $3,036K/yr.

The Pilot beacons must be serviced and repaired on a continuing basis, this is estimated as a 3 man/yr task costing $414K/yr.

These labour costs are fully burdened and thus cover the cost of overhead staff which support the system. However, as this system is scoped to be operational, it is reasonable to include an additional element of direct charge labour which provides the clerical, marketing and accounting services for the system. Using a labour cost of $70K per man year in 1990 dollars, and an estimate of a staff of 50 to perform these tasks, the cost of this element is taken to be $3,500K/yr.

The total operating cost for labour is thus estimated to be $19,370K/yr. To this must be added replacement equipment, which is taken as 7% of the capital cost of the regional ports, central control station and pilot beacons, or $9,155K/year.

The total operating cost is then $28,525K/year.

5.4 Summary of Costs

The system cost is summarized in Table 5.1. In the table the system cost elements are summed and the interest cost on a decreasing balance is then added and the result divided by the design life of the spacecraft. The yearly capital cost is added to an estimate of the yearly operating cost to arrive at a figure for the total yearly system cost.

5.5 Revenue Projection

A projected revenue curve was generated from the user growth curve presented in Figure 5.5. This curve assumes an initial user population of 10% of the end of life projection and a typical growth curve of users. The number of minutes used per year were then estimated for the same growth curve.

The revenues from the system were calculated assuming $100/month rental for the initial 2680 user terminals and charges of $1, $1.50 and $2 per minute toll charge. These revenue projections are plotted in Figure 5.6. The revenues increase as the number of users grows and at some point, each curve crosses the line showing the yearly expense curve. (This line is shown sloping as the interest payments actually diminish as the outstanding principle is reduced.)

The breakeven point is approximately six years for the lowest per-minute revenue of one dollar. This breakeven point at half the spacecraft life means that the system will not quite pay for itself in ten years. The higher rates of course result in return on the money invested in the system. For example a charge of $1.50/minute results in a total revenue after 10 years of $1,167,500 K for total

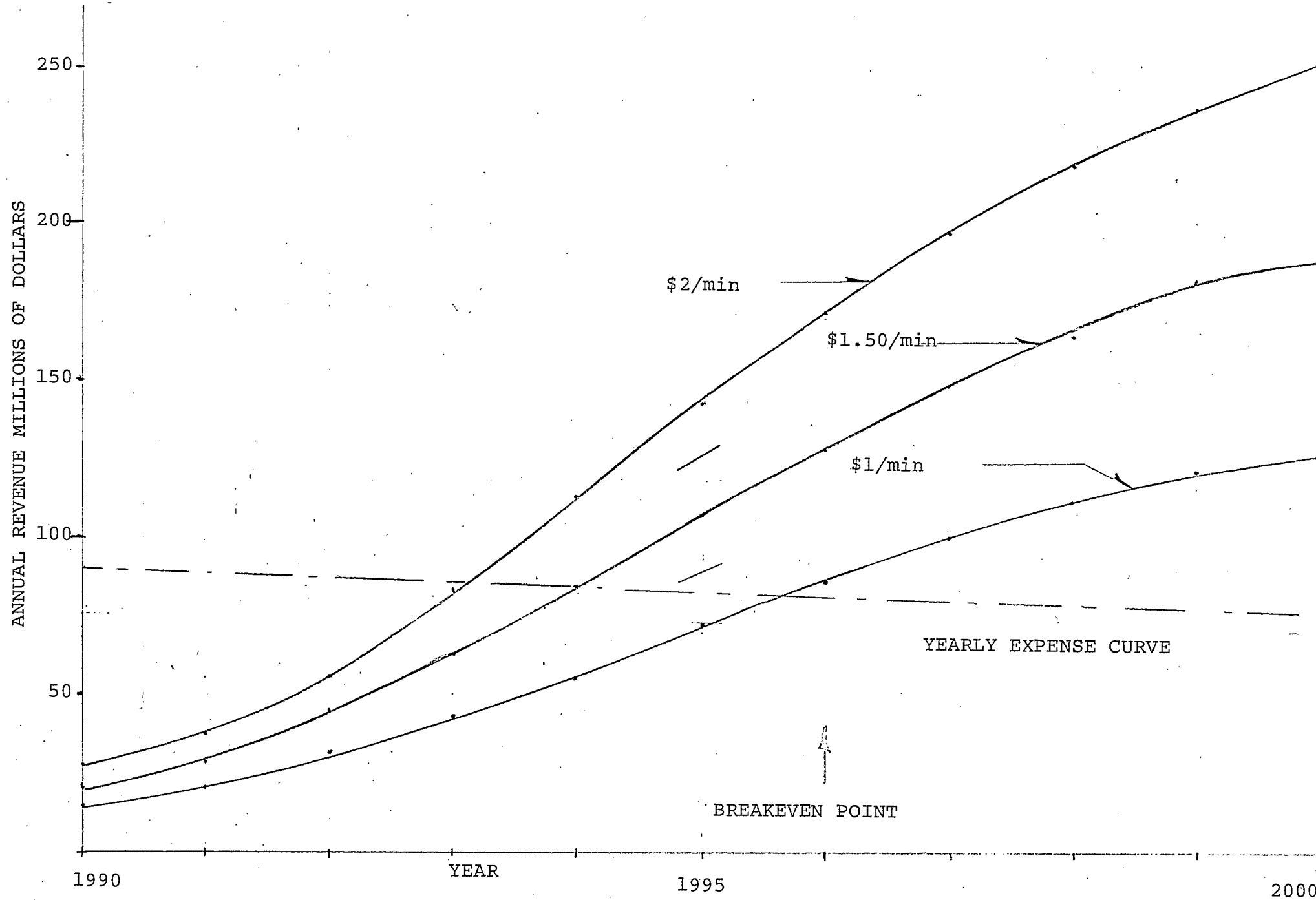

FIGURE 5.6 REVENUE PROJECTIONS

AMENDED

108

AMENDED

		$K
1.	Space Segment	306,339
2	Pilot Beacons (30 off)	387
3.	Regional Ports (10 off)	63,100
4.	Central Control Station	25,200
5.	Initial 10% User Terminals	14,100
	TOTAL CAPITAL COST OF SYSTEM	409,126
	Interest for capital @ 10%/yr (amortized over design life of 10 years.)	204,563
	TOTAL ACQUISITION COST OF SYSTEM	613,689
	Acquisition Cost/yr.	61,368
	Estimated Operating Cost/yr	28,525
	TOTAL COST/YEAR	89,893

SUMMARY OF SYSTEM COSTS

TABLE 5-1

CANADIAN ASTRONAUTICS LIMITED

AMENDED

5.5 Revenue Projection (Cont'd.)

expenses of $898,930 K. This represents a return on capital of $268,857 K in ten years, which is equivalent to a return of 3.7% per annum, compounded annually.

6.0 CONCLUSIONS AND RECOMMENDATIONS

6.1 Conclusions

This report defines the performance requirements for a typical communications system utilizing large aperture antennas. It then presents a conceptual design which meets these requirements. The system is capable of providing two-way voice communications for 26,800 users equipped with mobile transceivers located anywhere in Canada. The technology required for this system exists today, or is a straight-forward modification of existing designs. Baseline system performance can be improved by implementation of advanced modulation formats and more sophisticated antenna designs.

It is shown that, for the beam size and antenna patterns used for the baseline, only six frequency bands are sufficient to provide full duplex service. Each of the bands is 1.35 MHz wide, with three bands used for uplink, and three for downlink. Co-channel interference is minimized by remodulating the signals. This remodulation may be accomplished on-board the spacecraft or in the central control station. By 1990, spacecraft technology will be sufficiently advanced that both the switching and remodulation could be done on-board.

Rough cost estimates show that it is feasible to procure and operate the system profitably assuming use charges similar to those for the existing land mobile systems.

Interference analyses lead to the conclusion that the system can operate in conjunction with existing land mobile systems. However, the baseline system is interfered with by TV broadcast transmitters in the upper UHF band. For this reason, either exclusive use of the 806-890 MHz band for mobile, mobile-satellite service is

6.1 Conclusions (Cont'd.)

required, or the system must operate with a 609-614 MHz uplink or in the 1.5 to 1.6 GHz region. The only reason that the latter frequencies are undesirable is the anticipated higher cost for the ground-based tranceivers.

6.2 Recommendations

This preliminary study has described a conceptual system capable of a unique augmentation to Canada's communication facilities. In the course of the study, a number of areas requiring study were identified. These are listed here in random order:

- Attitude Control Studies
  Much work must be done regarding the dynamics of large, flexible structures. This is an area where extensive expertise exists in Canada.

- Adaptive Nulling and Electronic Steering of Antenna Beams
  Novel methods for nulling interferers and for real-time electronic steering of multi-beam antennas should be investigated. One such system is described in this report. Computer simulation and engineering hardware tests should be done.

- Modulation Formats
  A detailed study should be done of the optimum format for voice transmission for this application. Trade-offs between analogue and digital schemes should be made. Simulated links should be established and bit error rates and intelligibility criterion evaluated.

6.2 Recommendations (Cont'd.)

- Antenna Design - Electro-Mechanical

  An Engineering trade-off should be made for various reflector configurations. Cassegrain and off-set feed systems should be further evaluated for cost, ease of manufacture, integration and test.

- Conceptual Design Study

  A detailed conceptual design study of a specific system should be performed. This would include the results of other preliminary studies and would result in an accurate mass-estimate and a detailed evaluation of subsystem costs. Preliminary mission analysis and launch vehicle compatibility would be performed. The final report of this study would form the basis for an engineering design phase which would precede a flight program.

REFERENCES

2-1 Projected Population of Canada, Statistics Canada Publication 91-514.

2-2 Communications Statistics, Statistics Canada Publication.

2-3 Summary of Land Mobiles 1972-1976 by Region, Band and Year, Telecommunications Economics Branch, Statistical Information Services Division of the Department of Communications.

2-4 Information Transfer in 1990, Roger W. Hough, AIAA 3rd Communications Satellite Systems Conference, April 6-8, 1970.

2-5 Man on the Move, Study Performed for the Department of Communications by C. Roger Schindelka, Institute for Northern Studies, University of Saskatchewan, August 1977.

2-6 Communications Satellite Systems, James Martin, Prentice-Hall, 1978.

2-7 Multi-purpose UHF Communication Satellite System Vol. 2, June 1975.

2-8 Pearce, Can. Elec. Eng. J, Vol. 2 #4, 1977.

3-1 Conference Proceedings; AIAA/NASA Conference on Advanced Technology for Future Space Systems; May 8-10, 1979; NASA Langley; Hampton Virginia.

3-2 Industry Capability for Large Space Antenna Structures; JPL Report 710-12; R. E. Freeland; 25 May, 1978.

3-3 Technology Survey of Deployable Parabolic Antennas and Extendible Helical Antennas for Spacecraft; Spar R.673; April 1975.

3-4 Report on Visit to West Coast, Sept, 26-29, 1978; H. R. Warren; DOC Memorandum WI-7-15 PRO/B/1.8, 17 October, 1978.

3-5 Product Brochure; Harris Corporation; Communications and Data Handling.

3-6 Deployable Reflector Design for k_u Band Operation; Harris Corporation; NAS-CR-132526; September 1974.

3-7 Product Brochure; TRW Defense and Space Systems Group; Large Expandable Structures.

3-8 Deployable Box Truss Space Structure; Martin Marietta Aerospace; Wm. Tobey; MMA Report No. 78-52411-01; Dec. 1978.

3-9 Summary Report of Hybrid Antenna Reflector Concept; Coyner & Riead; Astro Research Corporation; NASA CR-145075; September 1976.

3-10 Space Deployable Large Aperture Flex Rib Reflectors; LMSC Report No. LMSC-A946613-1.

3-11 Considerations on the Use of Graphite Reinforced Plastics for Space Erectable Antennas; AA Woods and M. Kural; LMSC.

3-12 ATS-6 Experimental Communications Satellite Report on Early Orbital Results; W. A. Johnston Jr; J of S/C and Rockets; February 1976.

3-13 The Communications Technology Satellite Flight Performance; H. R. Raine.

3-14 Astromasts for Space Applications; Astro Research Corporation Brochure; Aug. 1978

5-1 Study of Feasability of Access to a Portion of the Radio Frequency Spectrum 406.1 to 410 MHz for the Mobile Satellite Service.
CAL Report December 1977.

5-2 Sinclair Radio Laboratories, 'Sinclair Base Station Antennas 108-512 MHz', 1975.

5-3 Taub and Schilling, 'Principles of Communication Systems, P. 134, McGraw Hill 1971.

5-4 'Reference Data for Radio Engineers' ITT, March 1969.

APPENDIX A

TRAFFIC MODEL ANALYSIS

APPENDIX A

Traffic Model Analysis

This Appendix outlines the preliminary traffic model used for the Large Antenna/Mobile-Satellite study. The time period of interest is the late 1980's and the 1990's.

A.1 Introduction

In predicting future traffic, one can plot historical data on semilog paper and extrapolate. This method works reasonably well with communications services already in existence for some time. It is, however, of little value for services that have not yet come into being, such as mobile-satellite communications.

Technical forecasters have classified prediction periods into three groups:

Inertia Period:	0-5 years, predictions are based on trends (i.e. semilog extrapolation), predictions are reasonably accurate, and intervention in this period if difficult.
Choice Period:	5-20 years, predictions are difficult due to new developments, and intervention in this period is relatively easy.
Uncertain Period:	over 20 years, uncertainties are overwhelming, and only general goals can be examined.

A.1 Introduction (Cont'd.)

The period 1985 - 2000 falls into the latter two categories and projections are less accurate. Particularly in this field, new technological developments (such as large aperture space-borne antennas) may accelerate the growth of a particular service.

Some data are available giving a rough indication of the extent of communications usage in general and mobile radio usage in particular. This data will be used as a basis for predicting future growth in requirements for mobile radio. The future mobile traffic will likely be shared between ground based systems and a satellite based system and this sharing must also be estimated. As an output of the work described in this section, a range of possible traffic densities will be used to estimate the satellite communications capacity needed.

A.2 Growth Rates

Population (1971-2001): According to Statistics Canada (Ref. 2-1) the population of Canada will grow to about 27.6 million in the year 1990 or 30.4 million in the year 2000 assuming a moderate birth rate (See Figure A.2.1, Projection B). For a high birthrate (Projection A) the population could be about 10% higher. For a low birth-rate (Projection C, D), the population could be about 6% lower.

Telephone Toll Calls (1967-1976): According to Statistics Canada (Ref 2-2), the growth in numbers of telephones installed in Canada has grown at the rate of 5.8% per year (See Figure A.2.2). During the same time period the number of telephone toll calls increased by 11.0% per year (See Figure A.2.3). The population grew at the rate of 1.4%/year during the same period. No information was available on the length of telephone calls or the aggregate total number of minutes of toll calls.

Number of Land Mobiles (1972-1976): According to figures available from the Canadian Government Department of Communications (Ref. 2-3) the growth in number of Land Mobiles licensed by DOC was 17.8%/year during this time period (See Figure A.2.4). No information was available on other types of mobiles or on total number of minutes used.

Unfortunately none of the above growth rates start at the time of introduction of the service. Ref. 2-4 is an attempt to look at information transfer in 1990. Reproduced from this reference is Table A.2.1 showing average annual growth rate (number of units in service) for telephone, telegraph, television, computer and automobiles in the first 1, 2, 5, 10 and 20 years since their introduction. These growth rates for the first 10 years ranged from 13 to 210% and in the first 20 years, from 11 to 84%. For the telephone

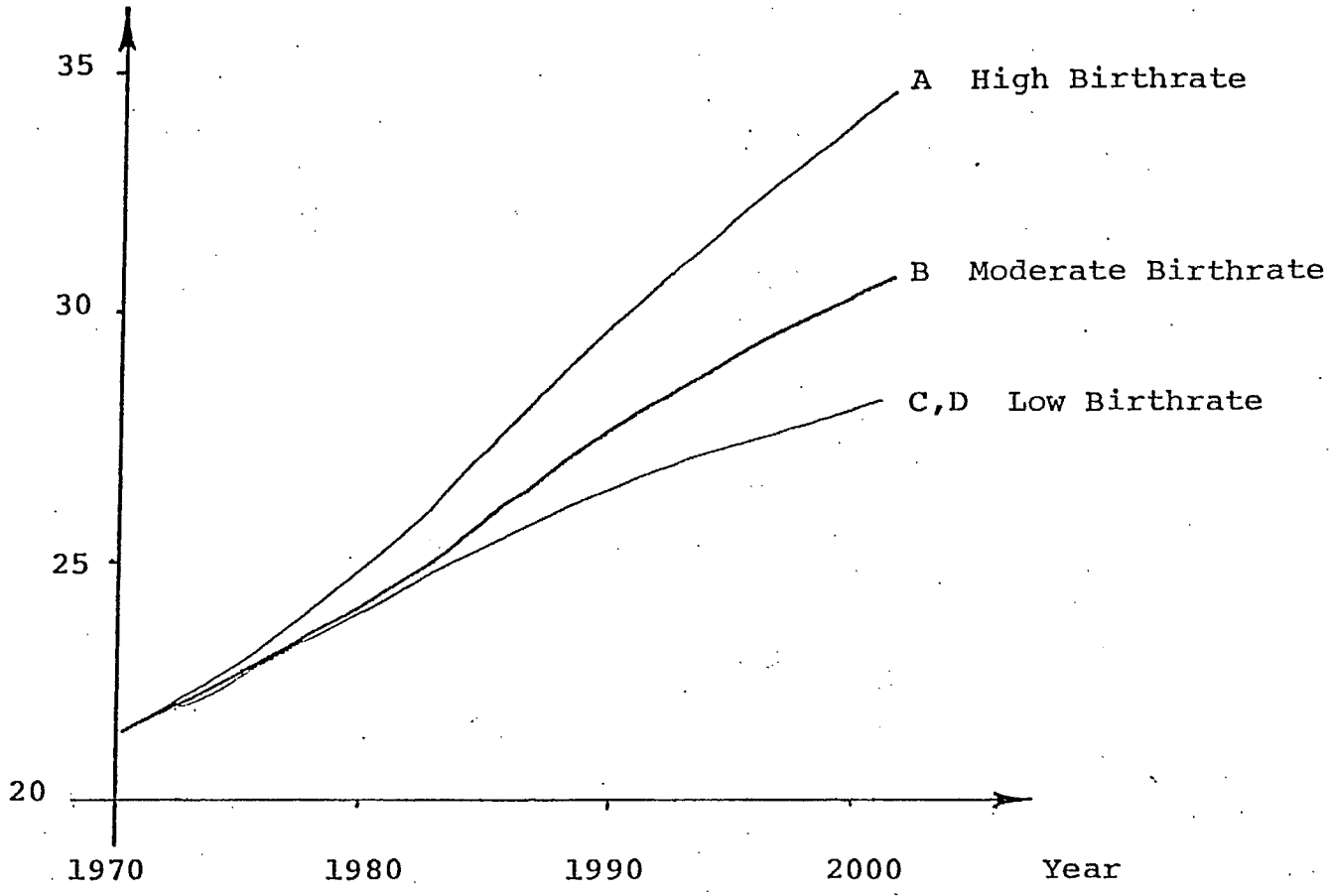

PROJECTED POPULATION OF CANADA

(From Ref 2-1)

FIGURE A.2.1

Average annual rates of early growth

		Growth Rate (%/yr)				
		First year	First 2 yrs	First 5 yrs	First 10 yrs	First 20 yrs
Telephone	1876-1896	300%	200%	80%	50%	28%
Telegraph	1867-1887	10	17	12	13	11
Television	1946-1966	75	370	320	190	58
Automobile	1900-1920	85	70	60	50	41
Computers	1951-1971	700	400	300	210	84 (est.)

Average Rates of Early Growth

Table A.2.1

A.2 Growth Rates (Cont'd.)

and telegraph, the two items most directly related to mobile communications, the average annual growth rates ranged from 12 to 80% for the first 5 years (Geometric mean 31%), 13 to 50% for the first 10 years (G.M. 25%), and 11 to 28% for the first 20 years (G.M. 18%). As a first guess then, it will be assumed that the number of mobile satellite communications units will grow at the rate of the geometric means stated above (and shown in Figure A.2.5). It will further be assumed that the volume of traffic will also grow at this rate (conservative assumption).

A.3 Traffic and Number of Users in Base Year

A.3.1 Government (DND and Civilian)

For the purposes of this study, it is assumed that government mobile satellite communications service begins in 1985 on an experimental system.

In a study performed for the Multipurpose UHF Satellite Communications System, estimates were made for National Defence and Civilian Government requirements, assuming a 1980 service date. It was estimated that the total traffic would be 4×10^6 minutes per year, split equally between the DND and civilian applications. The estimated number of users is 365 for the civilian side and 200 for the military. Adding a contingency to these numbers, to allow for some inaccuracy for the projections, the total number of users and total traffic for a 1985 start of experimental service are:

TABLE A.2

	ESTIMATED	WITH CONTINGENCY
Number of Stations	565	749
Traffic (minutes)	4×10^6	6.74×10^6

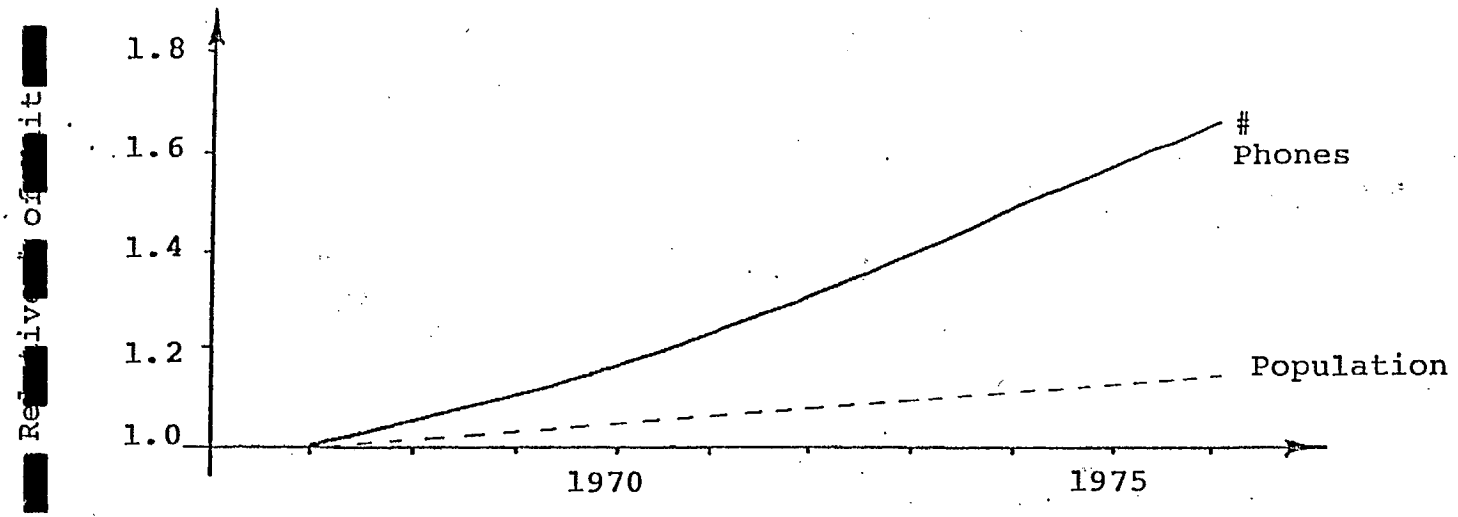

NUMBER OF PHONES RELATIVE TO NUMBER IN 1967

FIGURE A.2.2

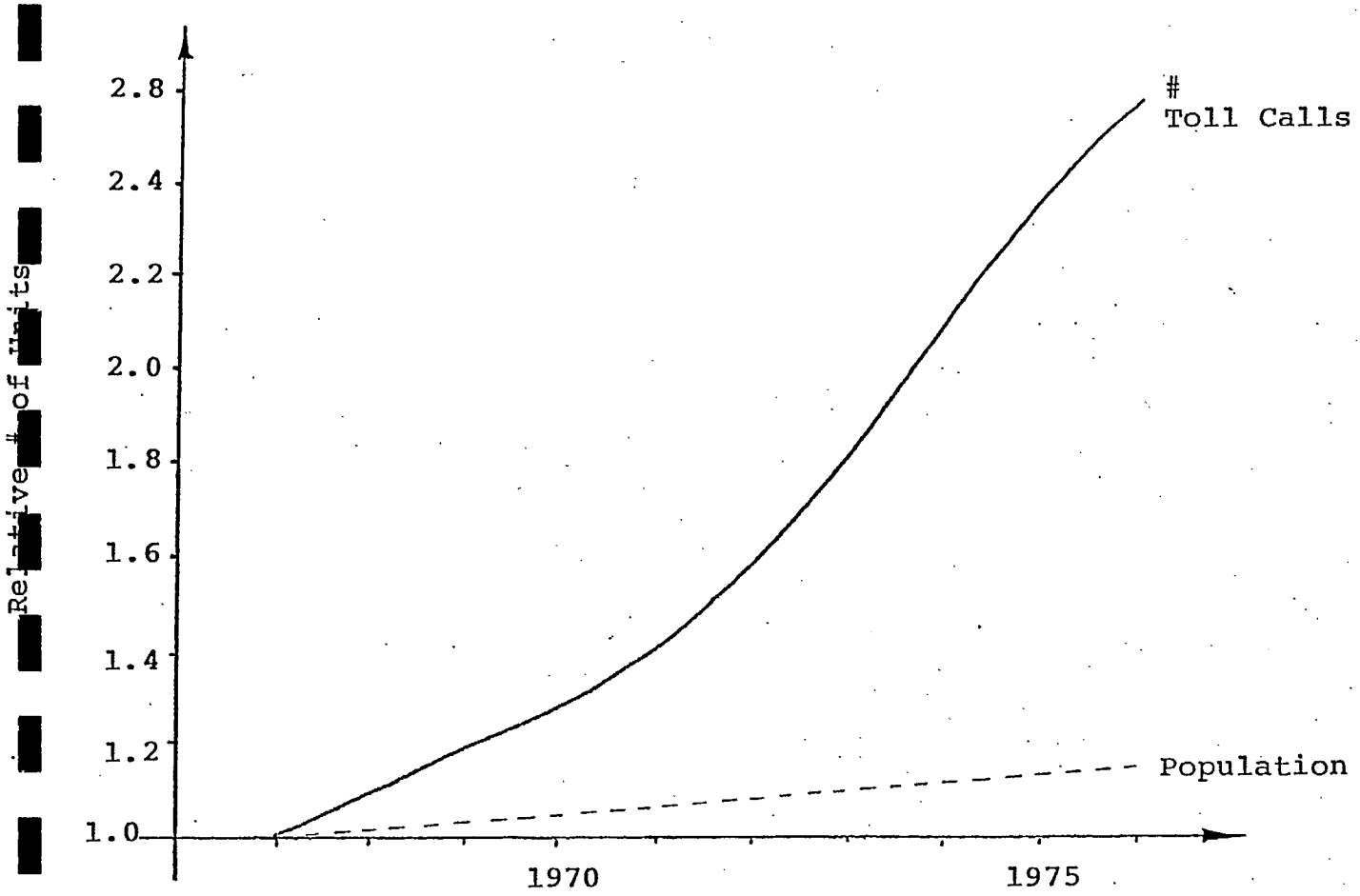

NUMBER OF TOLL CALLS RELATIVE TO NUMBER IN 1967

FIGURE A.2.3

Projected
Average Growth Rate

	# Units	Traffic
0-5 Yrs	16.5%	16.5%
5-10 Yrs	8.1%	11.0%
10-15 Yrs	6.2%	11.0%

Projection for # Mobiles

1976	264,968
1990	715,000
2000	1,248,000

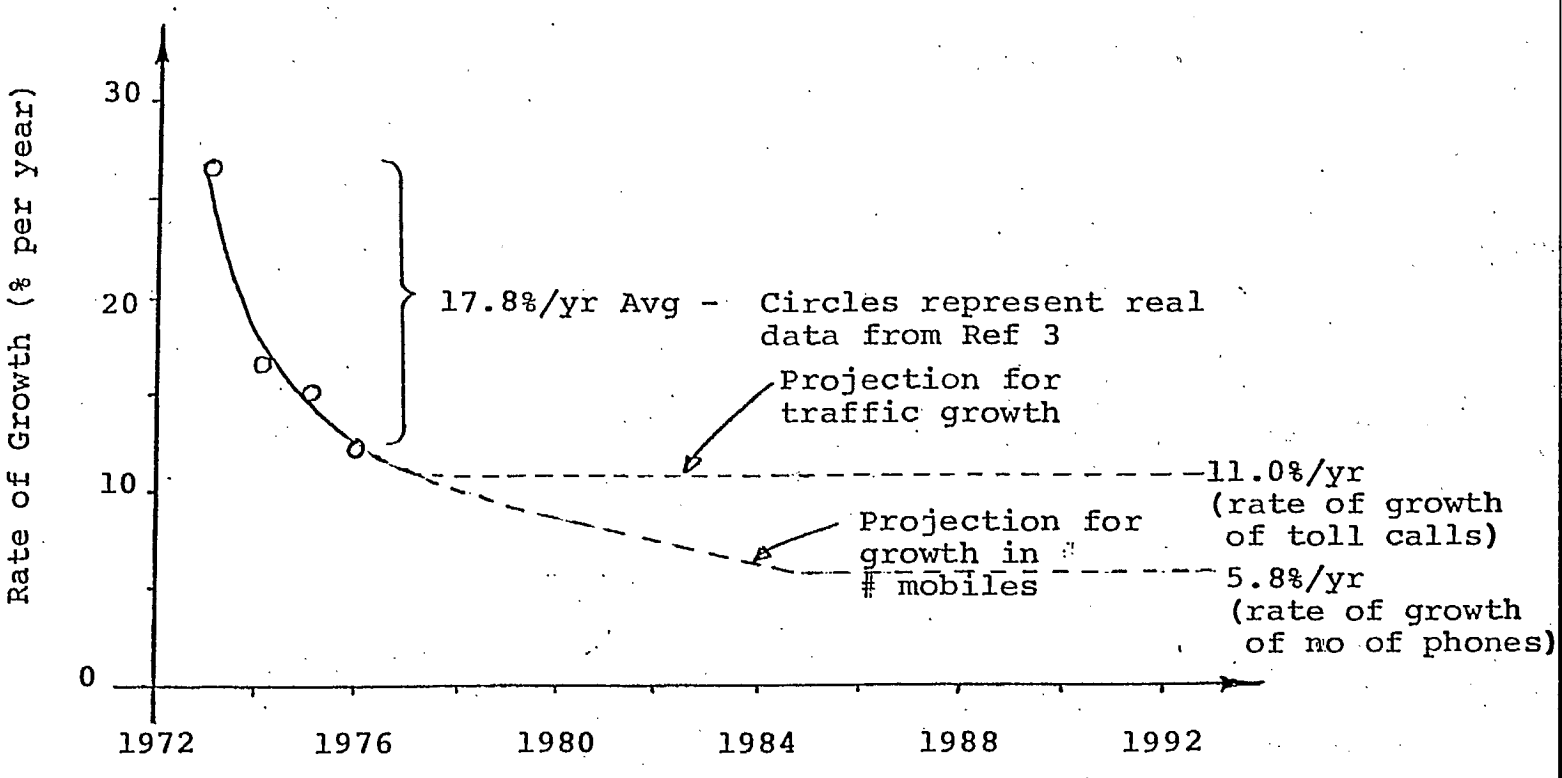

RATE OF GROWTH OF NUMBERS OF LAND MOBILES AND MOBILE TRAFFIC

FOR ALL OF CANADA

FIGURE A.2.4

A.3.2 Commercial Users

For the purposes of this study, it is assumed that commercial mobile communications traffic begins in 1990.

Based on the rate of growth of number of land mobiles (Figure A.2.4), it is estimated that there will be 2.7 times as many units in 1990 and 4.7 times as many units in the year 2000 as there were in 1976 (last year for which data is available). The projection, based on 264,968 units licensed in 1976 (ref. 2-3), is then 715,400 units in 1990 and 1,245,000 units in 2000.

According to a study done on rural use of mobile communications in Alberta, Saskatchewan and Manitoba (Ref. 2-5), 7.3% of all mobiles in these provinces (both Private and General Land Mobile Radio Service (GLMRS)) are used in rural areas which would be a prime target for a mobile satellite communications service. An additional 19.4% of Private and GLMRS units are licensed to users living in population centres under 5000. A substantial fraction of these users are also potential mobile satellite communications users. These three provinces had 24% of all Canadian licensed land mobiles in 1976, and their annual growth rate (1972-1976) was 22.4% per year compared to 17.8% for the country as a whole.

As a starting point for 1990, it will be assumed that, as a minimum, 1% of users classified as residing rurally, or in centres under 5000 are the initial customers for the system. Therefore, the minimum number of commercial users in 1990 is assumed to be 0.01 x (0.073 + 0.194) x 715,400 or 1910. As an upper limit, it will be assumed that 1% of all users are the initial customers. Therefore the maximum number of commercial users in 1990 is assumed to be 0.01 x 715,400 or 7154. No data was found for the total usage time, although, according to Ref. 2-5, the typical length of call for Private and GLMRS is under 2 minutes and 95%

A.3.2 Commercial Users (Cont'd.)

are under 5 minutes. For this study, it is assumed that the typical commercial user will use the mobile for 5 (minimum) to 10 (maximum) minutes per day. Therefore the minimum traffic in 1990 is 3.5×10^6 min/year the maximum is 26.1×10^6 min/year.

	Minimum	Maximum
No. Users	1910	7154
Traffic (minutes)/year	3.5×10^6	26.1×10^6

As a comparison, the total number of telephone calls in Canada in 1976 was 22,219,161,000. Assuming an average duration of 3 min/call, the traffic for that year was 6.6×10^{10} minutes.

A.4 Projections for 1990-2000

A.4.1 Projection for Number of Mobile Units

Two projections are provided for estimating the number of user mobiles for each of the government and commercial users, these are shown in Figure A.2.6.

For the government stations, Projection A (lower bound) is based on the estimated 749 users in the 1985 base year with a continued 5.8%/yr increase. Projection B (upper bound) is also based on 749 users in 1985, but assumes that the number of users grows according to the schedule of Figure A.2.5.

The curve shows the average growth rate per year averaged over periods of 5 to 20 years. The data is based on figures from Ref 4.

Derived from this curve are the following growth rates:

Period	Rate
0-5 yrs	31.0%/yr
5-10 yrs	20.2%/yr
10-15 yrs	11.9%/yr

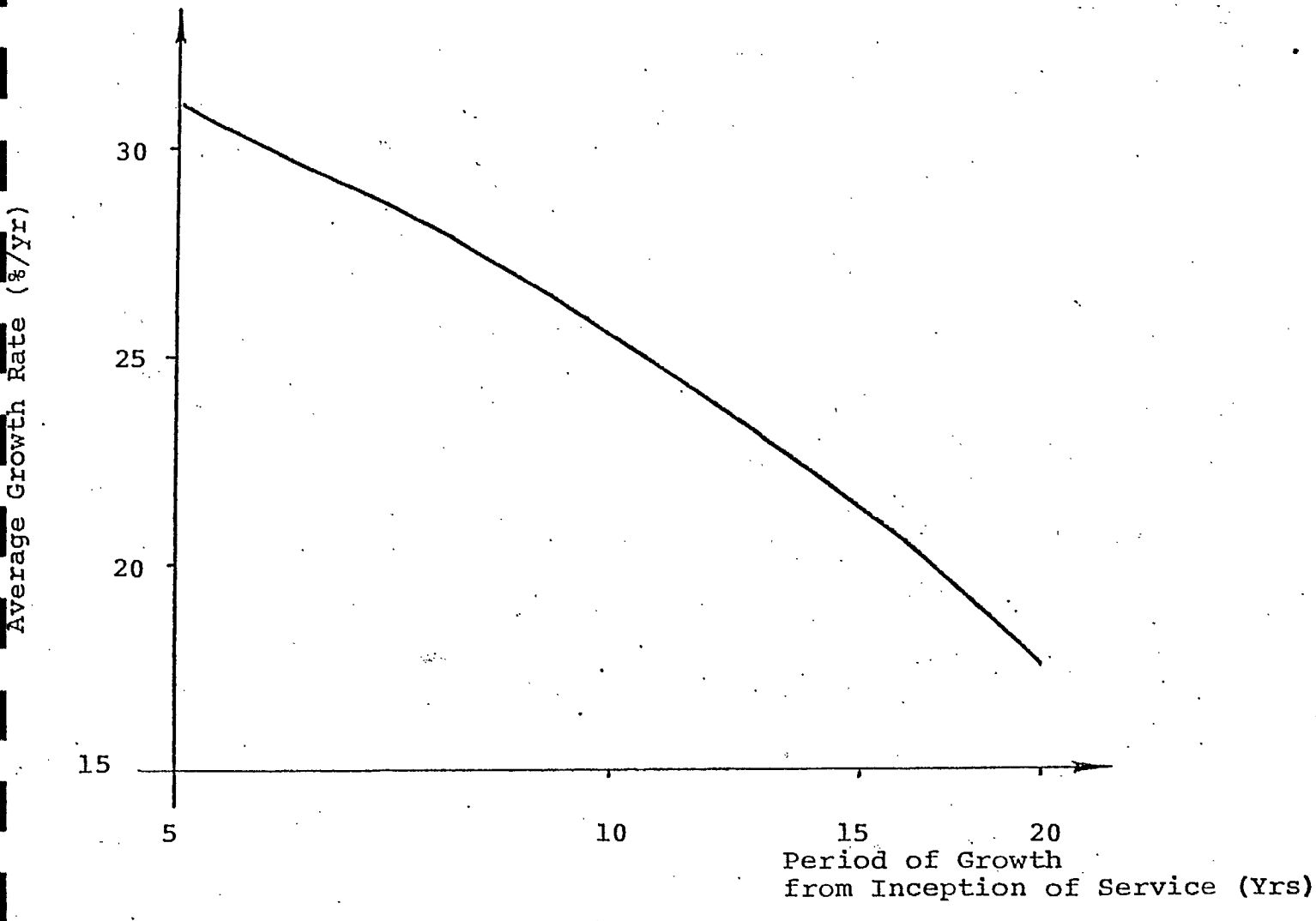

PROJECTED AVERAGE GROWTH RATES
FOR MOBILE SATELLITE COMMUNICATIONS

FIGURE A. 2.5

A.4.2 Traffic Projections

Two projections were also used to predict the government traffic and two more for commercial traffic, these are shown in Figure A.2.7.

For government traffic, Projection A (lower bound) assumes that traffic continues to grow at 11%/year and Projection B (upper bound) assumes traffic grows according to the schedule of Figure A.2.5.

For commercial traffic, Projection C (lower bound) assumes that the traffic starts with the minimum 3.5×10^6 minutes/year and grows according to the schedule of Figure A.2.4. Projection D (upper bound) assumes that the traffic starts with the maximum 26.1×10^6 minutes/year, according to the schedule of Figure A.2.5.

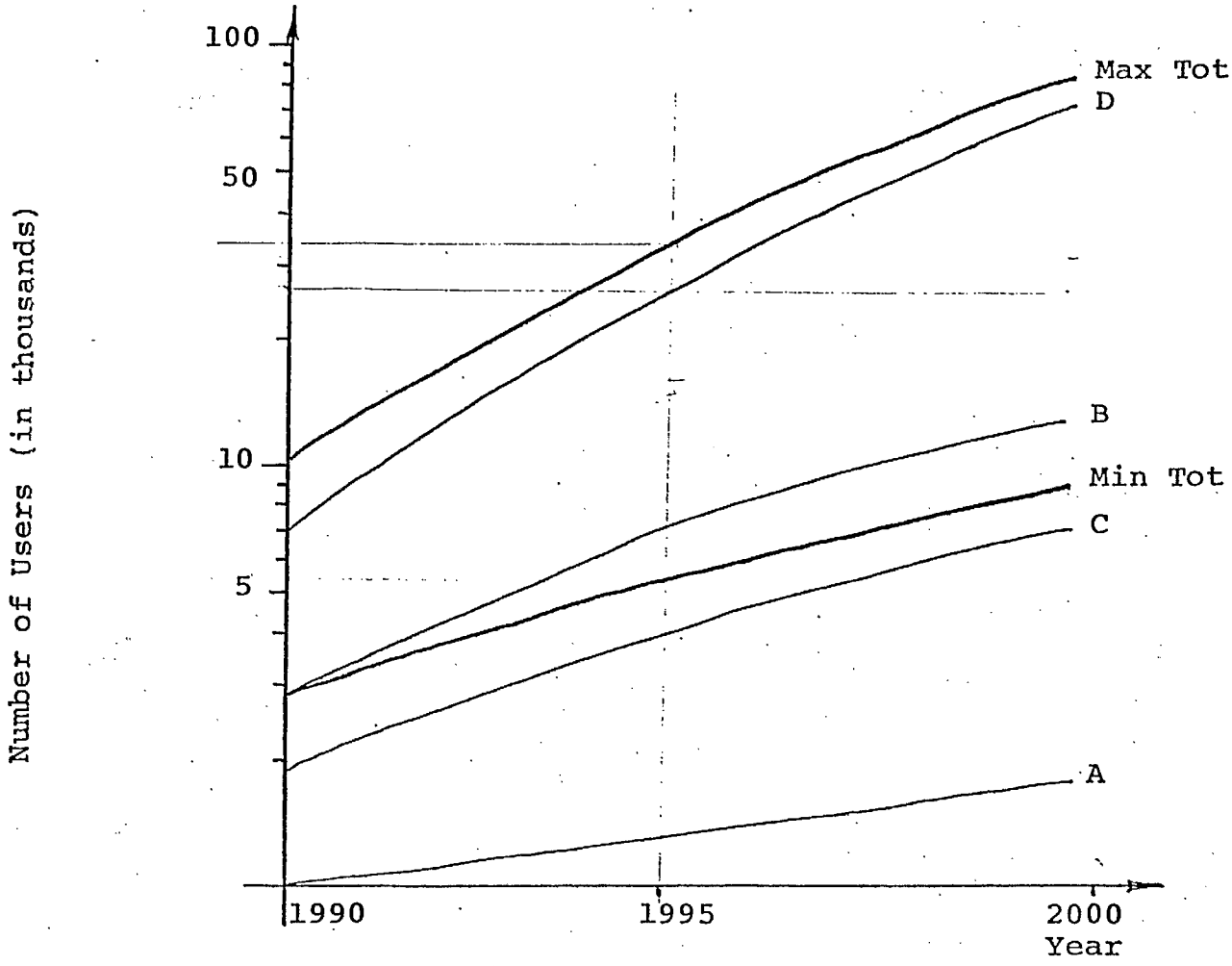

PROJECTED NUMBERS OF MOBILE UNITS

FIGURE A.2.6

Curve A - Government, Lower Bound
B - Government, Upper Bound
C - Commercial, Lower Bound
D - Commercial, Upper Bound

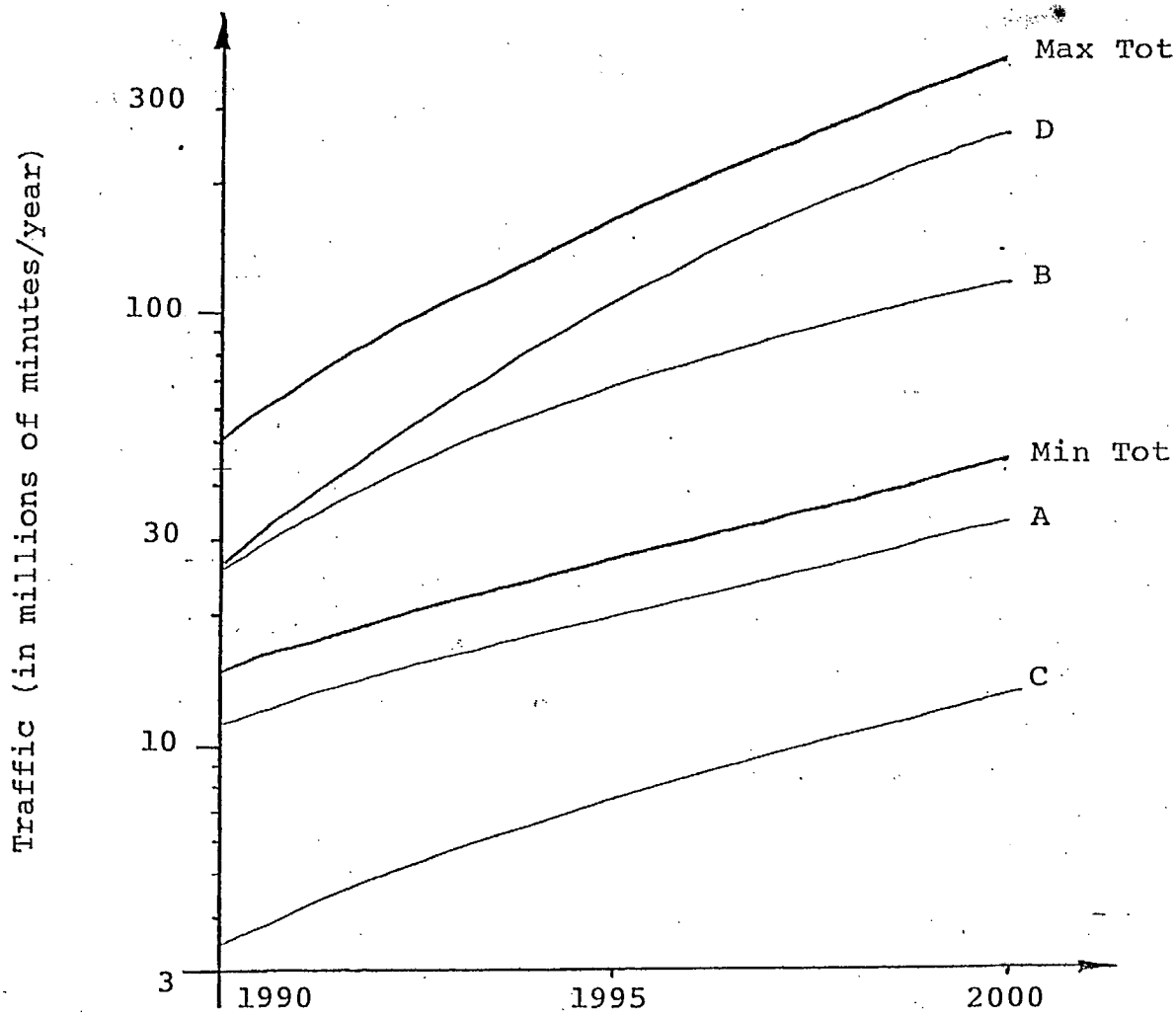

PROJECTED MOBILE-SATELLITE TRAFFIC

FIGURE A.2.7

Curve A - Government, Lower Bound
B - Government, Upper Bound
C - Commercial, Lower Bound
D - Commercial, Upper Bound

APPENDIX B

SYSTEM SIZING BASED ON CAPACITY

APPENDIX B

SYSTEM SIZING BASED ON CAPACITY

Introduction

This section describes the approach taken to establish the system channel capacity needed to support the projected traffic of the Appendix A.

B.1 Estimate of Number of Channels/Beams

In order to provide a specified system availability it is necessary to have extra channels accessible to the users. The number of extra channels is proportional to the number of users and to the required availability.

According to Figure 13.1 of Ref. 2.6, the average usage during peak hours for a commercial telecommunications system is about 2.9 x average usage and the peak usage on a peak day is about 4.5 x average use. Ref. 2.6 also states that about 75 to 85% of the total daily capacity of a telephone network is unused since the network is designed to provide good availability during peak hours.

According to figures from a previous study (reference 2-7), in 1980 the civilian users make during the 8 hr peak period, 219 calls/hr from 365 stations, the mean call being 5.04 minutes long. In the off-peak 16 hour period, the 365 users make 117 calls/hr, the mean call being 5.09 minutes long. Therefore, the average user is classified by the following model:

B.1 Estimate of Number of Channels/Beams (Cont'd.)

Peak usage	0.60 calls/hr (219/365),	5 minutes/call
Off-peak	0.32 calls/hr	5.1 mins/call
Average	0.41 calls/hr	5.1 mins/call

Peak usage is 0.60/0.41 1.46 x average usage.

For the purposes of this study, it will be assumed that the figure for peak usage of a commercial system (4.5 times average usage) (ref. 2-6) is to be used in order to provide good service. This assumption appears to provide some margin for the civilian government requirements mentioned in the second paragraph above. It will also be assumed that the civilian government model of 0.6 calls/hour 5 minutes/call represents the typical user during peak hours. This assumption is also conservative in that the average commercial user has been assumed to use the system only 5 to 10 minutes per day.

B.1 Estimate of Number of Channels/Beams (Cont'd.)

It is anticipated that the system will have the communications links broken into a number of different beams and these will be allocated so that approximately the same number of users are served by each beam.

In any one beam, then, the mean number of channels is given by:

$$T_m = \frac{T_y}{365 \times 24 \times 60 \times k}$$

T_y = total estimated yearly traffic in minutes

k = number of beams

The number of channels required to service the peak hours of transmission is:

$$T_p = 4.5\ T_m$$

where 4.5 is the peak-to-average duty ratio

B.2 Estimate of Excess Capacity/Beam

If it is desired to have 99% probability of getting a free channel, then a number of extra channels must be available above the peak loading. The following outlines an approximation made to calculate the overcapacity required.

Let:

Probability that a user is transmitting $= p = \frac{5 \text{ min/call} \times 0.6 \text{ calls/hr}}{60 \text{ min/hr}}$

$= 0.05$

B.2 Estimate of Excess Capacity/Beam (Cont'd.)

Number of users/beam = N

Number of channels/beam = n

Probability that (n-1) or fewer users are occupying the system } = 0.99 (+2.33σ)

$$\text{then } \sum_{i=o}^{n-1} {}^{N}C_{i} (p)^{i} (1-p)^{N-i} = 0.99$$

In this case, the cumulative binomial distribution above can be approximated by the normal distribution with:

mean = Np

and S.D. = $\sqrt{Np\ (1-p)}$

% overcapacity required is $H = \frac{\sqrt{Np\ (1-p)} \times 2.33 \times 100\%}{Np}$

$$= \frac{1015.6}{\sqrt{N}} \%$$

Figure B.1 shows the % overcapacity required as a function of number of users/beam.

The total number of channels per beam may then be calculated as:

$$T = (1 + H/100)\ T_p$$

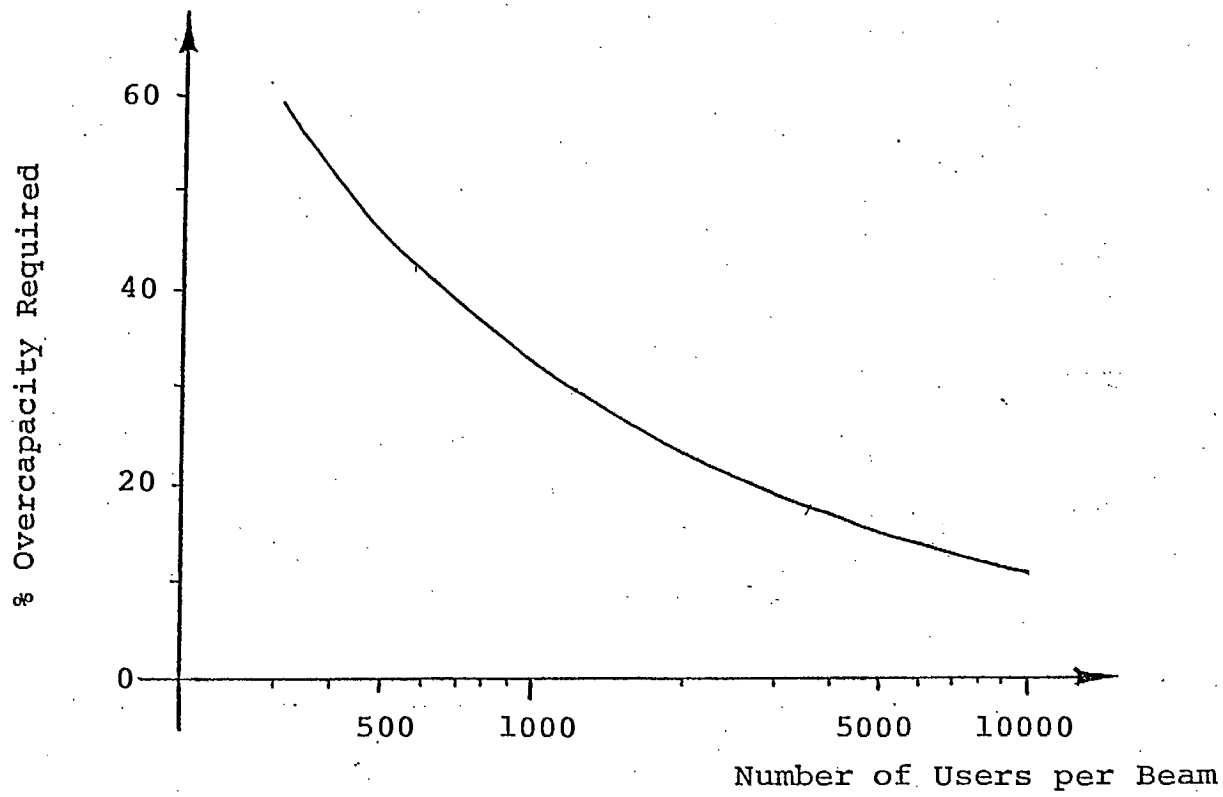

% OVERCAPACITY REQUIRED FOR 99% AVAILABILITY

FIGURE B.1

B.3 Capacity for Baseline System

Using the results of the previous two sections, an estimate can be made of the required system channel capacity for the coverage patterns described in Section 2.2.3.

A launch year of 1990 is chosen and a satellite design life of 10 years is assumed. Thus, it is required that the system support projected traffic for the year 2000.

For the year 2000 the estimated total number of users was projected, (figure 2.2.6) to be from 9000 (min) to 80000 (max). The mean number of users is taken as 26,800. These are assumed distributed evenly over the available channels.

In the same way, the total traffic in the year 2000 was projected (Figure 2.2.7) to be from 44 x 10^6 min/yr (min) to 350 x 10^6 min/yr (max). The mean value of these projections is 124 x 10^6 min/yr.

The number of beams that the large aperture antenna must support is simply estimated by the ratio of the coverage area to the individual beam size. Here the coverage area is assumed to be 3^o North-South by 8^o East-West.

Beam Size	# of Beams
$3^o \times 8^o$	1
$3^o \times 4^o$	2
$3^o \times 2^o$	4
$1^o \times 1^o$	24
$\frac{1}{2}^o \times \frac{1}{2}^o$	96

From these numbers, Table 2.4 has been constructed showing some of the trade-offs between beam size, required bandwidth and number of channels/beams. It can be seen that for the two smaller beam sizes at least, the bandwidth is less than a standard UHF TV broadcast channel.

APPENDIX C

RF LINK BUDGETS

Required C/N_o	53	dB-Hz
IF Bandwidth (18 KHz)	42.6	dB-Hz
RCV CNR	10.4	dB
Noise Power Density ($400^{\circ}K$) $N_o = kT$	-203.6	dBW/Hz
Total Receive Noise Power	-161.0	dBW
Required Signal Power	-150.6	dBW
Pol Loss	-3	dB
Off Boresight	-4.1	dB
RCV System Losses	-1	dB
RCV ANT Gain	30.4, 33.4, 36.4, 44.2, 50.3	dB
Free Space Loss	-183	dB
ATM Loss	0	dB
TX ANT Gain	3	dB
TX System Loss	-1	dB
TX Power	8.1, 5.1, 2.1, -5.7, -11.8	dBW

LINK BUDGET
900 MHz Uplink

Required C/N_o	53	dB-Hz
IF Bandwidth (18 KHz)	42.6	dB-Hz
RCV CNR	10.4	dB
Noise Power Density (350° K) N_o fcT	-204.2	dBW/Hz
Total Received Noise Power	-161.6	dBW
Required Signal Power	-151.2	dBW
Pol Loss	-3	dB
Off Boresight Pointing	-4.1	dB
RCV System Loss	-1	dB
RCV ANT Gain	30.4, 33.4, 36.4, 44.2, 50.3	dB
Free Space Loss	-175.5	dB
ATM Loss	-0.1	dB
TX Antenna Gain	3	dB
TX System Loss	-1	dB
TX Power	0.1, -2.9, -5.9, -13.7, -19.8	dBW

LINK BUDGET
380 MHz Uplink

Required C/N_o	53	dB-Hz
IF Bandwidth (18 KHz)	42.6	dB-Hz
RCV CNR	10.4	dB
Noise Power Density (450° K) N_o fcT	-202.1	dBW/Hz
Total Received Noise Power	-159.5	dBW
Required Signal Power	-149.1	dBW
Pol Loss	-3	dB
Off Boresight Pointing	-4.1	dB
RCV System Loss	-1	dB
RCV ANT Gain	30.4, 33.4, 36.4, 44.2, 50.3	dB
Free Space Loss	-188	dB
ATM Loss	0	dB
TX Antenna Gain	3	dB
TX System Loss	-1	dB
TX Power	14.6, 11.6, 8.6, 0.8, -5.3	dBW

LINK BUDGET
1600 MHz Uplink

Required C/N_o	53	dB-Hz
IF Bandwidth (18 KHz)	42.6	dB-Hz
RCV CNR	10.4	dB
Noise Power Density (380° K) N_o fcT	-202.8	dBW/Hz
Total Received Noise Power	-160.2	dBW
Required Signal Power	-149.8	dBW
Pol Loss	-3	dB
Off Boresight Pointing	-4.1	dB
RCV System Loss	-1	dB
RCV ANT Gain	30.4, 33.4, 36.4, 44.2, 50.2	dB
Free Space Loss	-179.5	dB
ATM Loss	0	dB
TX Antenna Gain	3	dB
TX System Loss	-1	dB
TX Power	5.4, 2.4, -0.6, -8.4, -14.5	dBW

LINK BUDGET

600 MHz Uplink

Required C/N_o	53	dB-Hz
IF Bandwidth (18 KHz)	42.6	dB-Hz
RCV CNR	10.4	dB
Noise Power Density		
(400° K) N_o fcT	-203.6	dBW/Hz
Total Received Noise Power	-161.0	dBW
Required Signal Power	-150.6	dBW
TX ANT Gain	30.4, 33.4, 36.4, 44.2, 50.3	dB
TX Losses	-1	dB
Pol Loss	-3	dB
Off Boresight	-4.1	dB
Free Space Loss	-183	dB
ATM Loss	0	
RCV ANT Gain	3	dB
RCV Loss	-1	dB
TX Power	8.1, 5.1, 2.1, -5.7, -11.8	dBW

LINK BUDGET
900 MHz Downlink

Required C/N_o	53	dB-Hz
IF Bandwidth (18 KHz)	42.6	dB-Hz
RCV CNR	10.4	dB
Noise Power Density		
(350^o K) N_o Pct	-204.2	dBW/Hz
Total Received Noise Power	-161.6	dBW
Receiver Signal Power	-151.20	
TX Amt Gain	30.4, 33.4, 36.4, 44.2, 50.3	dB
TX Losses	-1	dB
Pol Loss	-3	dB
Off Boresight	-4.1	dB
Free Space Loss	-172	dB
ATM Loss	-0.2	dB
RCV ANT Gain	3	dB
RCV Loss	-1	dB
TX Power	-3.3, -6.3, -9.3, -17.1, -23.2	dBW

LINK BUDGET

250 MHz Downlink

Required C/N_o	53	dB-Hz
IF Bandwidth (18 KHz)	42.6	dB-Hz
RCV CNR	10.4	dB
Noise Power Density (450^o K) N_o Pct	-202.1	dBW/Hz
Total Received Noise Power	-159.5	dBW
Receiver Signal Power	-149.1	
TX Amt Gain	30.4, 33.4, 36.4, 44.2, 50.3	dB
TX Losses	-1	dB
Pol Loss	-3	dB
Off Boresight	-4.1	dB
Free Space Loss	-187.5	dB
ATM Loss	0	dB
RCV ANT Gain	3	dB
RCV Loss	-1	dB
TX Power	14.1, 11.1, 8.1, 0.3, -5.8	dBW

LINK BUDGET
1500 MHz Downlink

APPENDIX D

CO-CHANNEL INTERFERENCE ANALYSIS

APPENDIX D

CO-CHANNEL INTERFERENCE ANALYSIS

The assumption is made that all stations have the same transmission power.

Let:

n_i	=	the number of beams (interfering stations) in each level of neighbour i.
G_i	=	maximum gain of antenna within limits of neighbour i
G_o	=	Gain of antenna at edge of desired (main) beam
C/N_o	=	Carrier to noise density, one-way link
B_T	=	Transmission bandwidth (I.F.) of each F.M. signal (Hz)

Co-channel Interference Analysis (Cont'd.)

W	Base-band bandwidth of each channel (maximum frequency response)
Δf	maximum carrier deviation from centre
SNR_I	Signal to noise ratio at input (I.F.) of F.M. demodulator (after I.F. filters of width B_T)
SNR_o	Signal to noise ratio at output of F.M. demodulator after low-pass filter of width W.

One-way link co-channel interference referenced to centre of main beam

$$I_o = \sum_{i=1}^{3} n_i G_i$$

Interference to station (one-way) of edge of main beam (point A)

$$I_A = I_o - G_o = \sum_{i=1}^{3} n_i G_i - G_o$$

For one-way receiver noise only

$$SNR_I = \frac{C/N_o}{W}$$

Co-channel Interference Analysis (Cont'd.)

For one-way total effective noise (interference plus noise)

$$SNR_I = \frac{C/N_o}{W} \pm \frac{1}{I_A}$$

From Carson's Rule

$$B_T = 2(\frac{\Delta f}{W} \pm W)$$

Relationship between SNR_o and SNR_I

For above 'FM threshold' $SNR_o \simeq 3.SNR_I(\frac{B_T}{2W})^3$

S.O. Rice ('Noise in F.M. Receivers', Proc. Symp. Time Ser. Anal., Brown University, June 11-14, 1962) derived an expression for SNR_o for below threshold (≃10 dB)

$$SNR_o = \frac{3\ SNR_I\ (B_T/2W)^3}{SNR_I\ \ 3\ (1-erf(\ SNR_I))\ .\ (B_T/W)^2 \pm 1}$$

where erf is the 'error function'

$$erf(z) = \frac{2}{\pi} \int_o^z e^{-t^2}\ dt$$

This expression for SNR_o is valid for SNR_I > 2 dB

This function is plotted in Figure D-1 for various B_T, with W = 4 KHz.

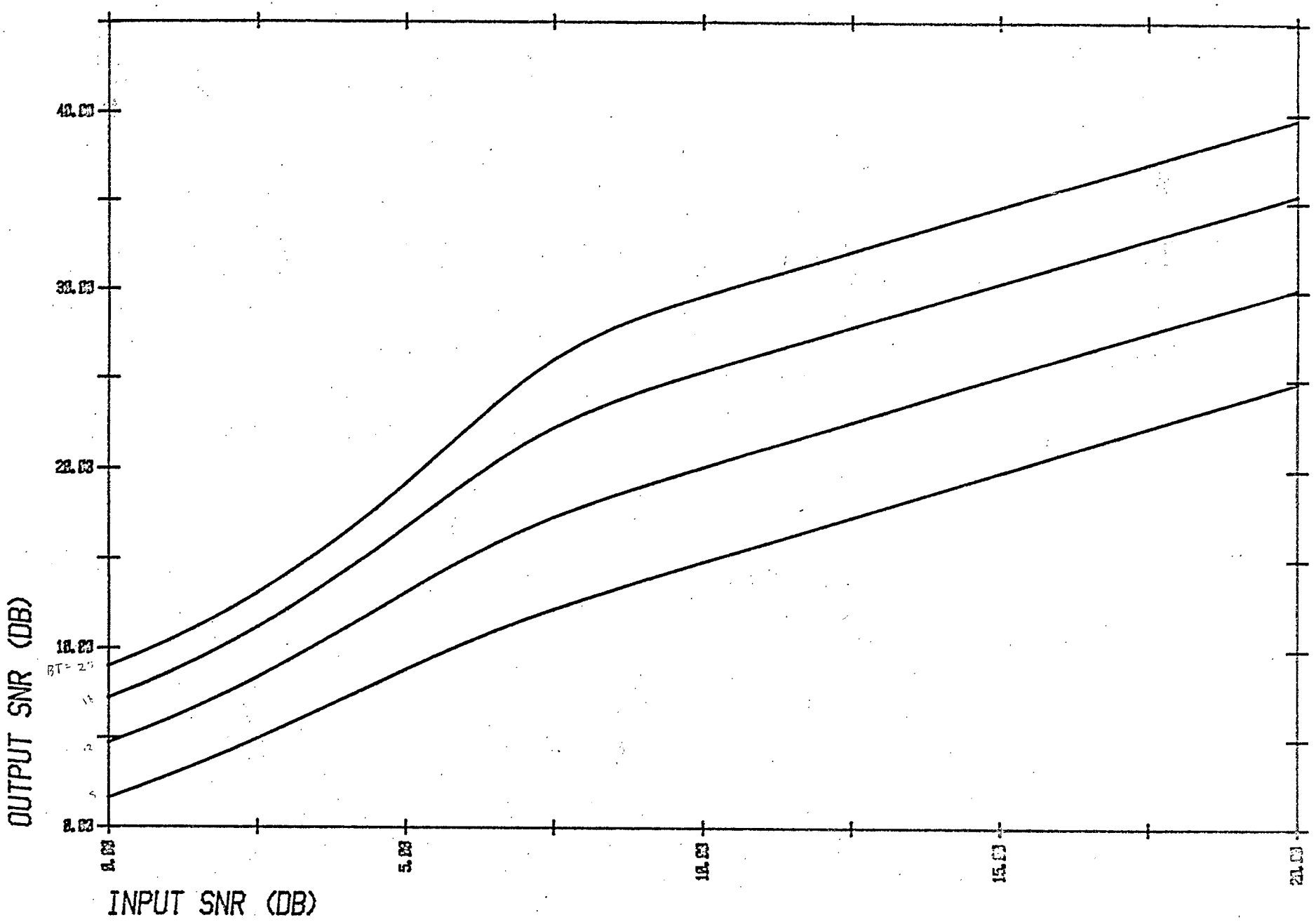

FM DEMODULATOR SNRO VS SNRI FOR W=4 KHZ

FIGURE D-1

Co-channel Interference Analysis (Cont'd.)

If the signals are demodulated and remodulated (regenerated) at the master control station via the SHF links, the transmitted signal for the UHF downlink will have an initial SNR_o'. As received at the ground station,

$$SNR_I^2 = \frac{1}{\frac{1}{SNR_o'} \pm \frac{1}{\left(\frac{C/N_o}{W} \pm \frac{1}{I_A}\right)}}$$

C/N_o and I_A are the same for both up and down-link due to equal C/N_o and antenna reciprocity.

The signal is demodulated for the second time, giving a final SNR_o^2.

TABLE 3-2

Neighbouring Beam Level - i	MIN Distance	MAX Distance	n_i	G_i	$n_i G_i$
1	1^o	2^o	5	-25 dB	-18.0 dB
2	2.17^o	3.03^o	2	-31 dB	-28.0 dB
3	3.5^o	4.44^o	2	-41.5 dB	-38.5 dB
				I_o =	-17.6 dB

Since G_o = - 4.1 dB
I_A = -13.5 dB

Assuming for noise density C/N_o of 53 dB Hz
and B_T = 18 KHz = 42.6 dB
receiver (I.F.) SNR_I = 10.4 dB

This produces an SNR_o = 25.7 dB for noise without interference.

For a co-channel interference level I_A = -13.5 dB
and noise level (w.r.t. signal) = -10.4 dB
combined noise and interference SNR_I' = -8.7 dB

This produces an SNR'_o = 23.7 dB

As received at the ground station

SNR'_I = 8.6 dB $\qquad$ C/N_o = 51.2 dB Hz

and the final SNR_o^2 = 23.6 dB

There are several important results. Comparing the total co-channel interference level I_o of -17.6 dB to the n_1 G_1 of -18.0 dB, the conclusion is that the interferers in the level -1 neighbouring beams (the closest beams) contribute almost all the interference. For this assumed antenna pattern, the receiver noise level of -10.4 dB is larger than the interference level of -13.5 dB. With the regeneration at the control station, the combined two-way link performance is almost the same as the one-way link performance (23.6 dB SNR vs 23.7 dB SNR). If the central control station acted as a simple linear transponder, the SNR_I^2 at the ground station would be a mere 5.6 dB which results in an SNR_o^2 of 18.0 dB. This SNR_I^2 is operating significantly below receiver threshold and hence the system performance would be sensitive to additional link losses.

Figure D-2 compares the demodulated SNR_o for a one-way link and the two-way link. Above the threshold of 8 dB SNR_I, the regeneration at the end of the up-link essentially completely recovers the up-link losses. The SNR_o^2 curve without regeneration shows that there is considerable degradation in SNR in the below threshold region. Figure D-3 shows the effect of changing the co-channel interference level with a fixed SNR_I for noise of 10 dB.

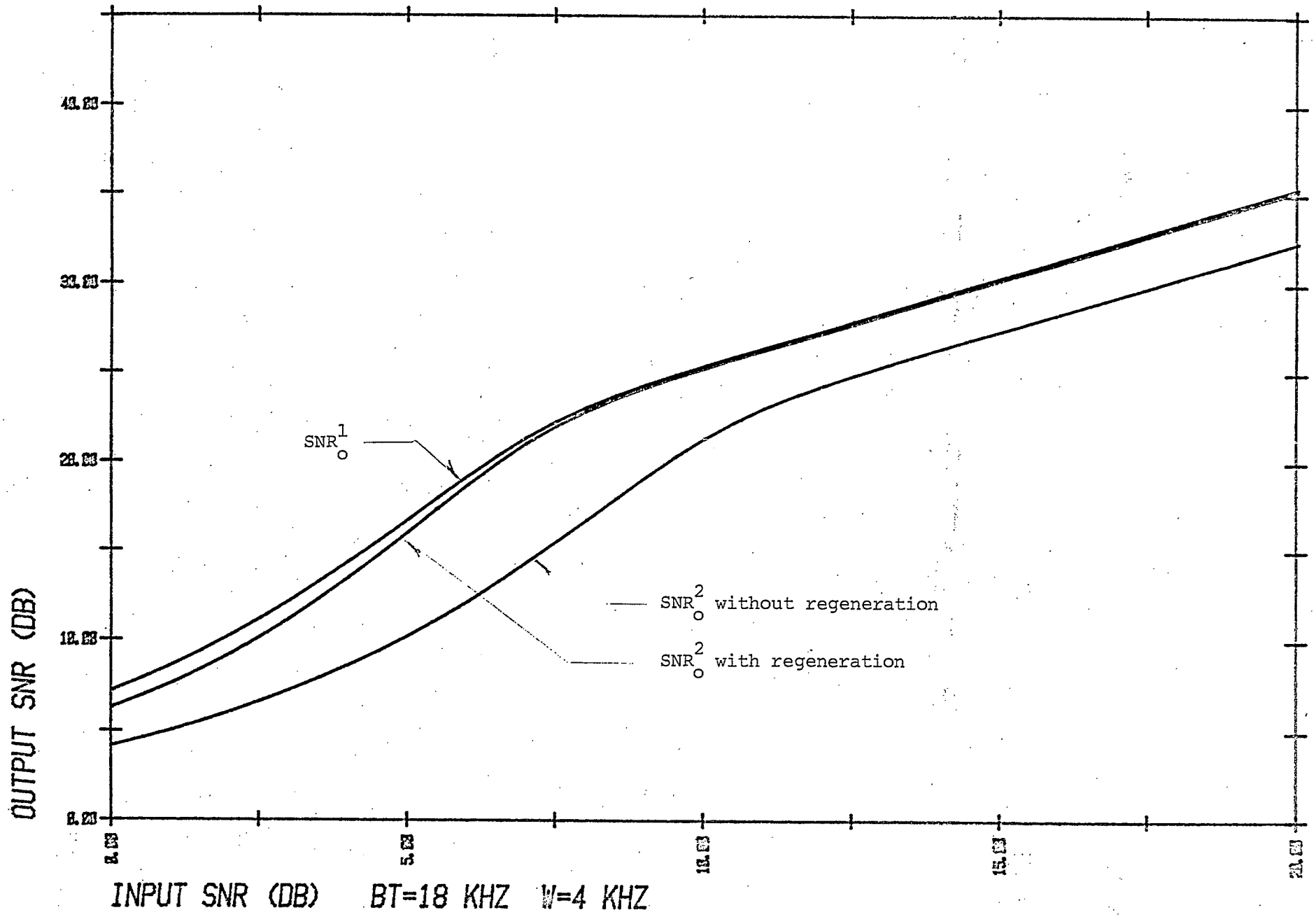

FM SNRO VS SNRI FOR 1-WAY, 2-WAY WITH, WITHOUT REGENERATION

FIGURE D-2

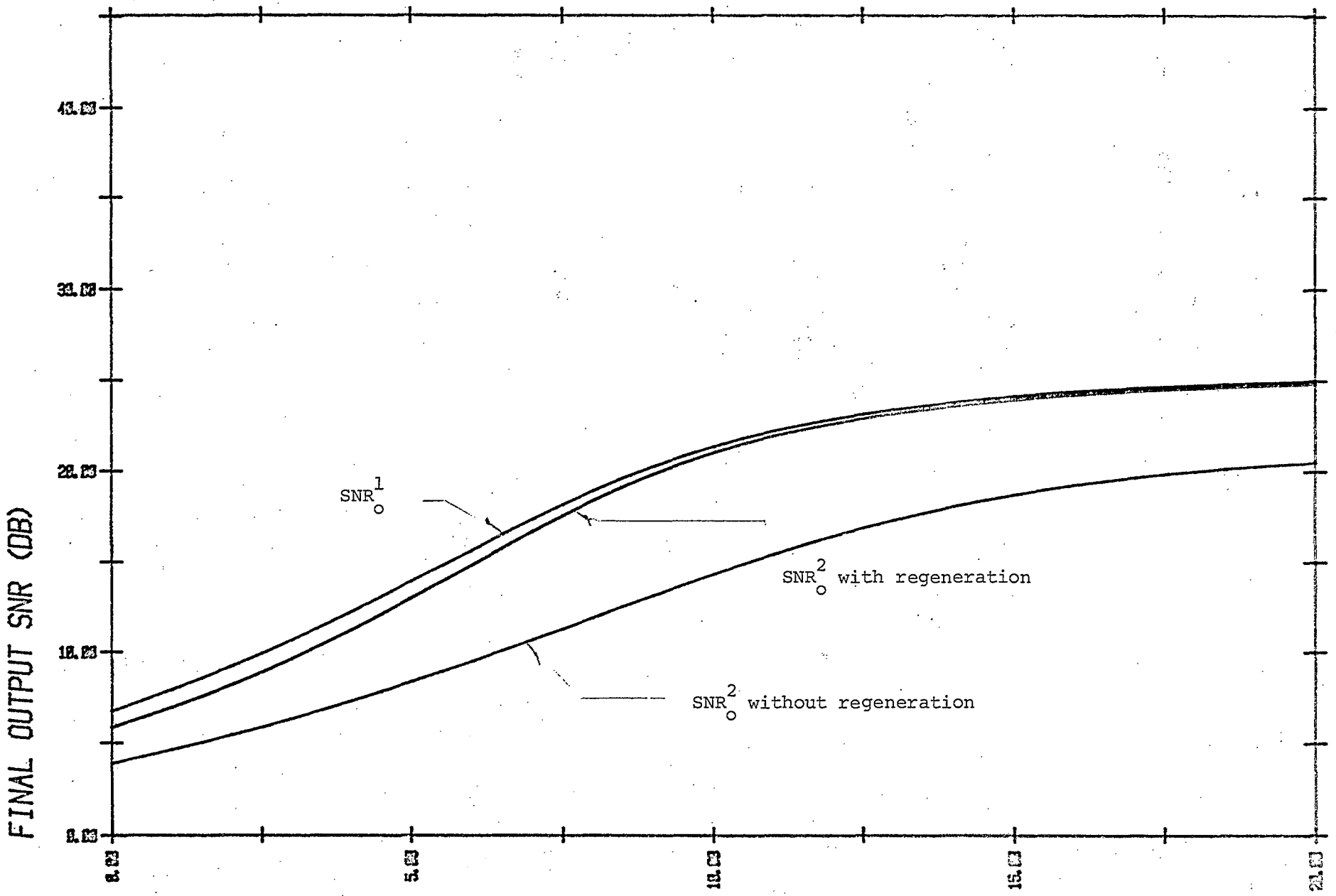

SNRO PERFORMANCE ON INTERFERENCE FOR SN=10 DB

FIGURE D-3

In conclusion, for the assumed unoptimized antenna pattern, the worst-case co-channel interference in addition to the system noise produces a C/N_o at the ground station receiver of 51.2 dB Hz which produces a receiver output SNR of 23.6 dB. If no co-channel interference was present, the C/N_o would be 52.8 dB Hz. C/N_o for a one-way link is assumed to be 53 dB Hz.

APPENDIX E

TWO PAPERS ON LARGE DIAMETER DEPLOYABLE ANTENNAS

AN APPROACH TOWARD THE DESIGN OF LARGE DIAMETER OFFSET-FED ANTENNAS

A. A. Woods, Jr.,* and W. D. Wade**
Lockheed Missiles & Space Company, Inc.
Sunnyvale, California

ABSTRACT

A desire for maximum efficiency in space antennas is placing emphasis on the application of offset fed antennas. Lockheed Missiles & Space Company has been investigating the application of the wrap-rib design in the offset geometry antenna configuration. The basic technology developed over the previous 15 years on deployable antennas is directly applicable with relatively minor modifications required in the area of rib, or surface support, manufacturing and constraints on feed tower/reflector support booms. This basic wrap-rib design approach for large apertures as applied to both the symmetric and offset configurations is discussed and performance/growth capability presented.

INTRODUCTION

NASA, specifically Langley, Marshal and JPL, have announced their plans to place large, high efficiency parabolic antennas in space for use as public services platforms. Specific uses have been identified for solar power transmission, radio astronomy and communications. The system demand for high efficiency has placed emphasis on offset-fed antenna geometry. For a selected aperture size an offset aperture has a clear advantage in aperture efficiency, higher beam efficiency and lower interference susceptibility. These advantages result from the placement of the feed system and feed support structures completely outside of the antenna field of view. A penalty is paid for the increased efficiency with depolarization effects resulting from the geometric assymmetries. These effects usually include a high cross-polarization level for linearly polarized systems and a beam squint for circularly polarized waves. With due consideration to the electrical impacts, offset-fed antennas are prime concepts for providing the desired high efficiency for the emerging missions.

Lockheed Missiles and Space Company, Inc., has been involved in the design and development of space deployable antenna systems for over a decade. In recent years, considerable effort has been placed on advancing the flight proven wrap-rib concept to support large diameter mission requirements. Through the development and incorporation of graphite epoxy materials the wrap-rib design can support the surface figure stability requirements of 30 to 300 m diameter apertures. Since the successful extrapolation of the design to the large aperture class antennas was achieved it was only logical to investigate adaptation to offset geometry systems. This application of the wrap-rib reflector design to offset-fed antennas is discussed here. Design and performance parametric data, materials for use in construction, descriptions of hardware and projections to the large sizes are provided.

WRAP-RIB DESCRIPTION

The wrap-rib parabolic reflector is based on an approximation to a paraboloid of revolution. The wrap-rib antenna is comprised of radially emmanating gores between the ribs which take the form of parabolic cylinders. The parabolic cylinders more closely approximate a true paraboloid of revolution as the number of gores is increased. The point of diminishing returns for this reflector in terms of antenna performance is a function of both the radio frequency wavelength of interest and the reflector diameter. Figure 1 illustrates the physical appearance of the resulting reflector.

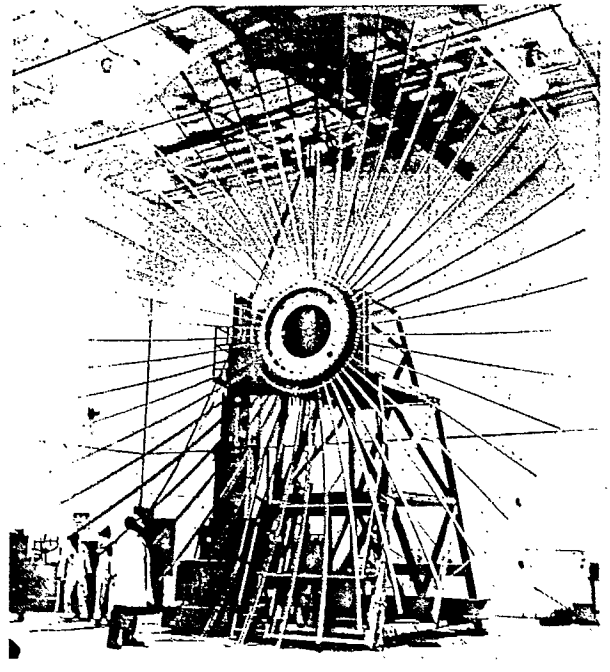

Figure 1. 9.1m Parabolic Wrap-Rib Reflector

*Staff Engineer, RF/Antenna Systems
**Design Specialist, RF/Antenna Systems

The gores are fabricated from a flexible membrane material which is usually a knitted or woven fabric of electrically conductive material. The gores are sewn to parabolically curved cantilevered ribs terminated at the central hub structure in a hinge fitting. For launch the antenna must be folded into a package size which will fit into the shuttle transportation system. For stowage the ribs are rotated on the hinge pin, then elastically buckled and wrapped around the hub. Once in space, the reflector is deployed either by sudden release of the stored rib energy or through a deployment restraint mechanism which simply controls the rate of energy release and therefore the deployment rate. The choice of these deployment schemes depends on the particular spacecraft requirements and the reflector overall deployed diameter. Figure 2 shows deployment of a wrap-rib antenna, including some details of the hub assembly.

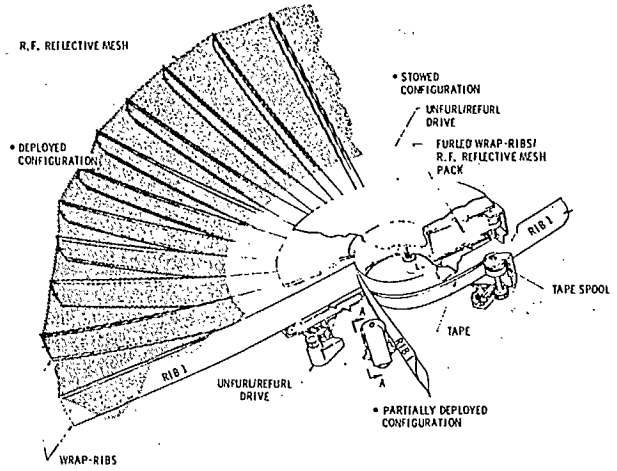

Figure 2. Deployment Mechanism of Reflector

Rib Design

There have been two rib design configurations applied to the wrap-rib reflector concept, i.e., the open or C-shaped rib cross section and the closed or lenticular cross section, both of which are illustrated in Figure 3.

Figures 4 and 5 are photographs of actual hardware fabricated into the two shapes. The choice between the two is dictated generally by the diameter of the reflector. The C-section can be employed up to about 45 m in diameter while the lenticular section application is theoretically useful from about 15 m to above the 300 m class.

Regardless of the cross-sectional shape used, the design requires that the ribs provide a dimensionally stable structure in the space environment for the reflective mesh surface, and the ribs must be capable of being wrapped into the allowable storage envelope for an indefinite length of time without appreciable dimensional changes occurring.

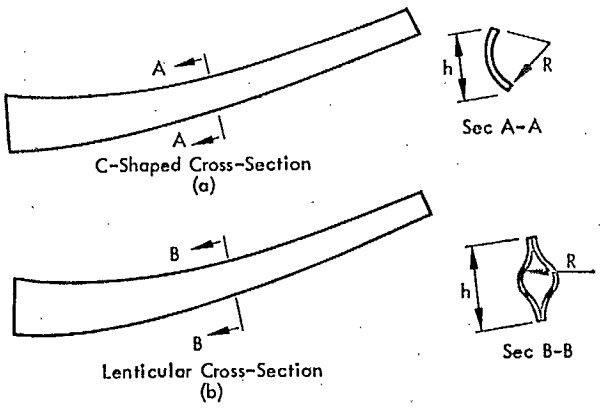

Figure 3. Developed Rib Designs

Reflective Surface

The reflective mesh surface is comprised of an electrically conductive knitted or woven fabric. The strands or yarns in the fabric can be of several basic materials either organic or metalic in nature. For most materials adequate reflective properties are obtained through the use of either electroless plating or electroplating with a good conductive material, e.g., gold, silver, aluminum etc. The diameter of the wires and the distance between them are dictated by the highest antenna radio frequency.

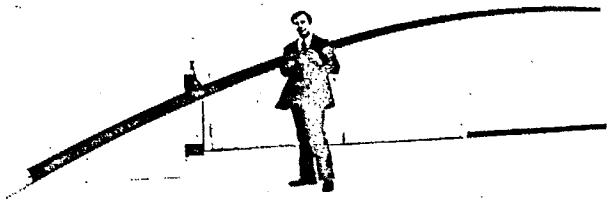

Figure 4. 7.0m Graphite Epoxy C-Rib

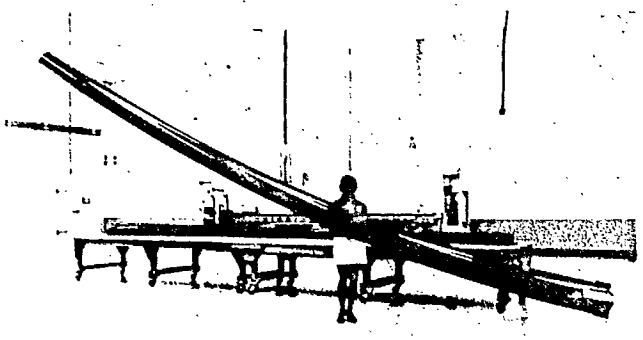

Figure 5. 6.9m Graphite Epoxy Lenticular Rib

OFFSET DESIGN APPROACH

Geometrically an offset reflector is described by a paraboloid where the geometric centerline is not coincident with the parabolic axis of symmetry. In order to gain the electrical advantages of reduced blockage the parabolic axis and therefore the focal point must in fact be located external to the section aperture. This section can most easily be visualized by forming a large paraboloid of diameter D and then passing a cylinder, with a parallel axis of symmetry, through the paraboloid (Figure 6). If the cylinder has a diameter (d) less than D/2 and its radius is common with the radius of the parabola, the section of the paraboloid bounded by the cylinder is representative of the desired offset reflector surface. Further if D/2-d is larger than the radius of the feed and the feed support structure is attached external to the radius of the offset section there is no blockage of the electrical field of view.

This new surface can be described mathematically with a simple coordinate transformation and rotation of the equations for the parent paraboloid. The result is a planar symmetric structure as opposed to the original axisymmetric structure with impacts in manufacturing and assembly costs due to the added geometrical complexity.

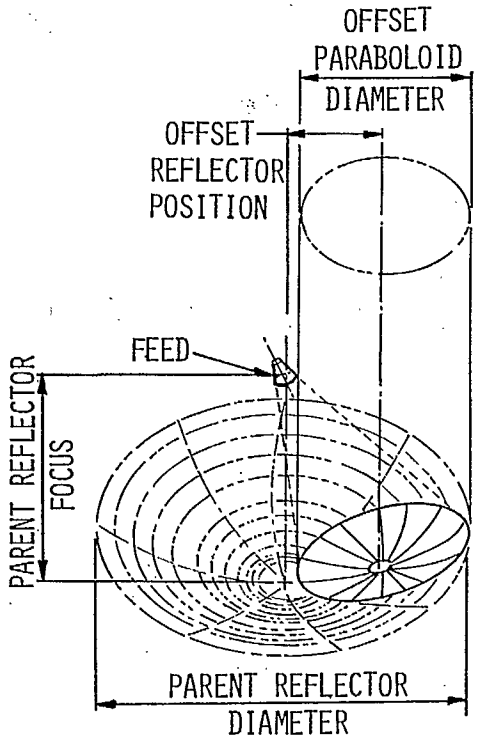

Figure 6. Offset Reflector Geometry

Initial Design Approach

As a result of the manufacturing considerations the initial adaptation of the wrap-rib design for use as an offset paraboloid retained as much of the structural symmetries as possible. In fact, the reflector section was constructed as a section of the parent parabola. This design, known as the fan-flex, was fabricated and tested in 1975. Figure 7 presents a picture of a stowed antenna system containing two deployable fan-flex reflectors and Figure 8 shows the system deployed during range testing.

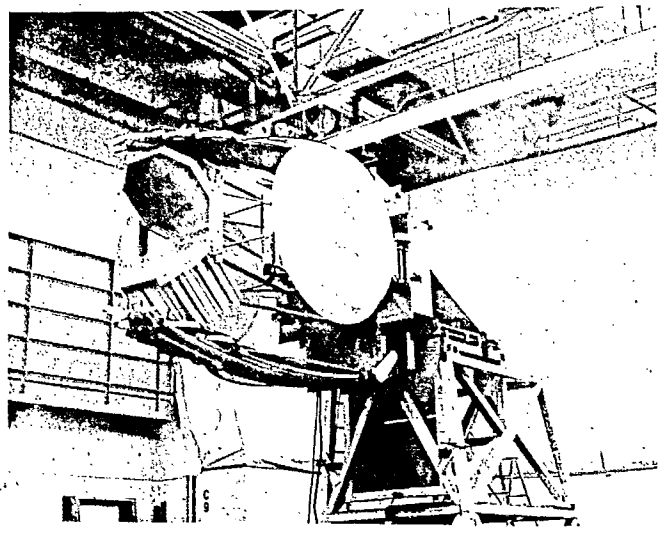

Figure 7. Stowed Offset Fan-Flex Antenna

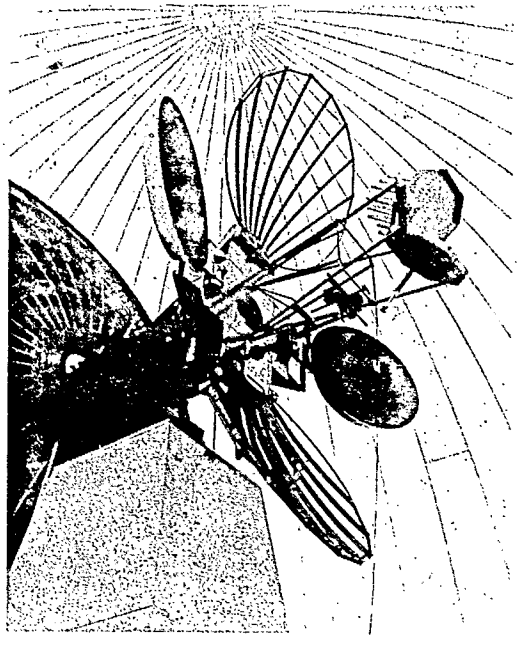

Figure 8. Deployed Fan-Flex During Range Testing

The fan-flex, although successful in the aforementioned design application presented some serious growth limitations. These were a large stowed envelope relative to the wrap-rib, a long and therefore heavy rib since the rib was edge mounted and had to be designed for ascent loading, and a surface approximation ill-conditioned to the illumination function of the surface. The end result was a design with limited growth compared to the wrap-rib from a size and weight standpoint.

Offset Wrap-Rib

The logical design solution was to adapt the wrap-rib and minimize the cost impact in the manufacturing and assembly areas. The offset wrap-rib uses the radial rib system attached to a central hub as in the axisymmetric design except that the hub is now located in the center of the offset section with the plane of the hub parallel to the local slope of the section. The significant benefits of the adaptation are:

- o Rib length is reduced to approximately D/2 which reduces weight and thermal distortions
- o Ribs can be wrapped around the central hub for storage during ascent preserving a low volume package
- o Rib and surface designs developed and proven with the axisymmetric wrap-rib are useable
- o The radially increasing surface approximation error is well conditioned with the offset reflector illumination function distribution which minimizes the required number of ribs
- o A shaped cover can be used over the central hub to preserve the surface contour.

As with any adaption there are compromises. In this case the reflector must be attached through the hub to a support structure (Figure 9) and the stability of this support structure must be considered as a degrading effect on antenna performance. Further multiple rib tooling is necessary to contour the ribs due to the reduction in symmetry with a manufacturing cost impact of approximately five percent.

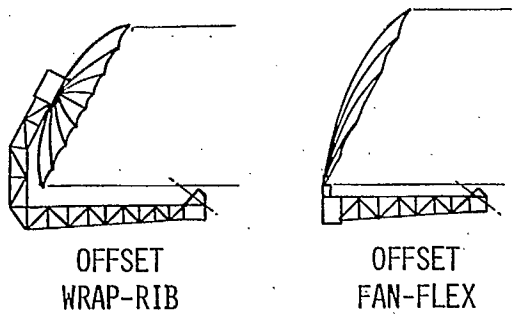

Figure 9. Typical Antenna Configurations

PERFORMANCE PROJECTIONS

For determining the growth potential for the offset wrap-rib two design limits were investigated. These were the thermally distorted surface figure and the parabolic approxmation error. The thermal distortions dictate the maximum aperture diameter from an orbit performance view while the surface approximation drives the stowed volume and weight parameters.

The parametric evaluation of distortions of the surface were estimated as random surface errors. The actual performace is a very complex issue, related to the actual distribution of errors and many other factors. The only correct method for achieving final antenna performance data is to use surface integration methods with a complete description of the distorted geometry. For the approximate errors, a resonably well accepted and accurate interelationship between gain in the ideal case and that achieved in the case of the structural distortions is represended by the relationship

$$G_d = G \exp^{-\left(\frac{4\pi\delta}{\lambda}\right)^2} \qquad (1)$$

Where λ is the wavelength and δ is the RMS surface error.

In the case of thermal distortions, previous detailed analysis of an orbit performance have shown that the worst case surface figure can be resonably well estimated by the expression

$$\delta_T \propto \left[\frac{\alpha_l a_R h}{K_t t} + \frac{\alpha_m a_m E_m}{E_r I_r}\right] d^2 \qquad (2)$$

where:

δ_T = surface error
α_l = rib longitudinal (radial) coefficient of thermal expansion
a_R = rib surface solar absorbitivity
h = average rib height
K_t = rib transverse thermal conductivity
t = rib thickness
α_m = mesh circumferential thermal coefficient of expansion
a_m = mesh surface solar absorbitivity
E_m = mesh modulus of elasticity
E_r = rib modulus of elasticity
I_r = rib moment of inertia
d = reflector section diameter

Thermal Diameter Limits

This surface error was investigated to determine the relationship between reflector section diameter and operating frequency for three performance loss levels identified as those which would typically be tolerated. The resulting data are displayed in Figure 10. Material properties

used in the parametric evaluation were consistent with the previously developed and element test validated graphite epoxy lenticular rib and molybdenum/gold knit mesh surface.

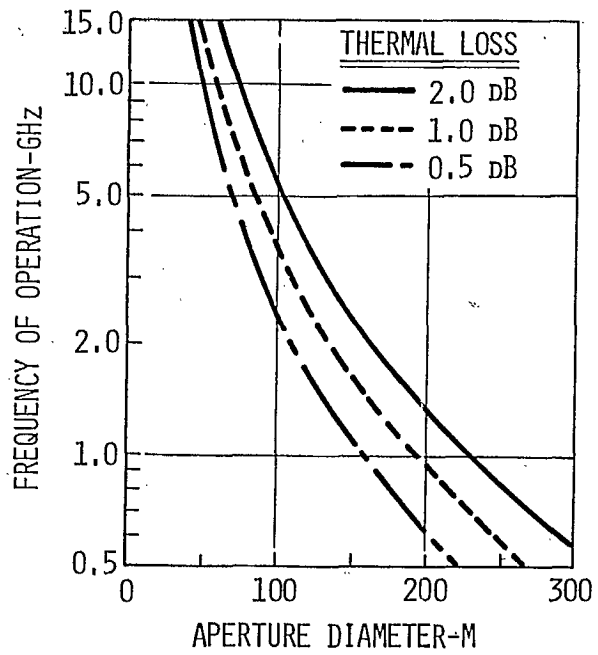

Figure 10. Thermal Aperture Limits

Approximation Error Limits

The number of ribs required to support operation at a given frequency are determined by the allowable surface approximation error loss. In the case of the wrap-rib reflector the area weighted RMS error is defined by

$$\epsilon = \left\{ \frac{N\left(\frac{d}{2}\right)^4}{48\pi F^2} \left[\frac{\pi}{N}\left(1 - \frac{A}{2} + \frac{3B}{2}\right) + \frac{B-A}{4}\sin\left(\frac{2\pi}{N}\right) + \frac{B}{32}\sin\left(\frac{4\pi}{N}\right) \right] \right\}^{\frac{1}{2}} \quad (3)$$

Where

$$A = \frac{2N}{\pi}\tan\left(\frac{\pi}{N}\right)$$

$$B = \frac{A^2}{2}$$

and N = number of ribs
d = diameter of reflector section
F = equivalent focal length of offset section

This error function was illumination weighted by a standard function $f(r) = \overline{A} + \overline{B}\,(1-Y^2/a^2)^2$ with the peak of the illumination at the center of the offset aperture and a -10dB edge illumination assumed. The resulting surface error relationship was then used to determine the number of ribs required to provide a -0.5 dB surface approximation error in an offset reflector. A focal length to diameter ratio of 0.7 was assumed and the size/frequency envelope described by the -2.0 dB curve of Figure 10 was used. The resulting data are presented in Figure 11.

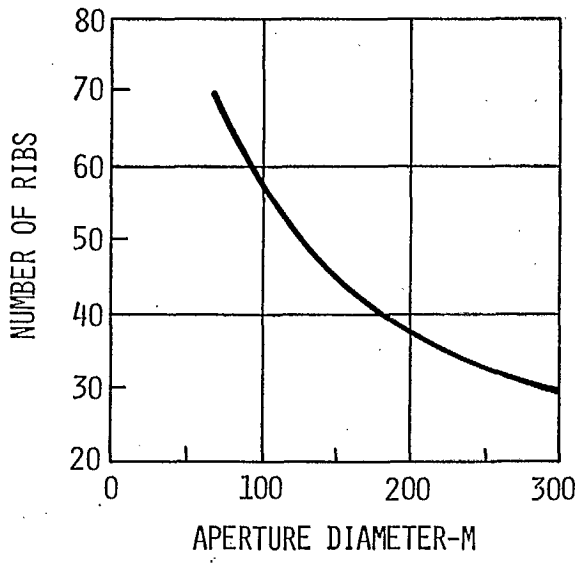

Figure 11. Required Number of Ribs

Stowed Design Parameters

The reflector stowed diameter and weight are readily determined with the diameter and number of ribs defined. The resulting stowed parameters are presented in Figure 12. This data shows a maximum stowed diameter of 3.4m associated with a 300m diameter reflector which would support operation up to 500 MHz. The 300 m diameter reflector would have a mass of 6850 Kg. In all cases the stowed length is less than 1m due to the geometry of the stowed package and the rib height.

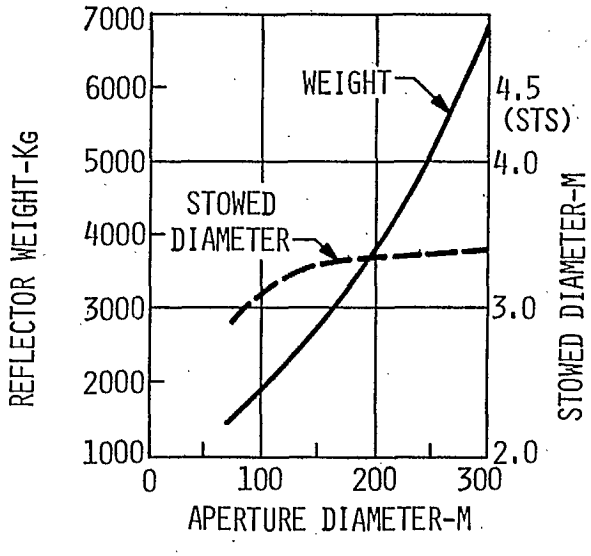

Figure 12. Stowed Reflector Weight and Diameter

Deployed Natural Frequency

As a final parameter of interest, the deployed reflector natural frequency was identified. These results are presented in Figure 13 for reference purposes. Two modes were identified; the torsional mode which tends to cause reflector defocus, and the rocking mode which produces antenna beam shift.

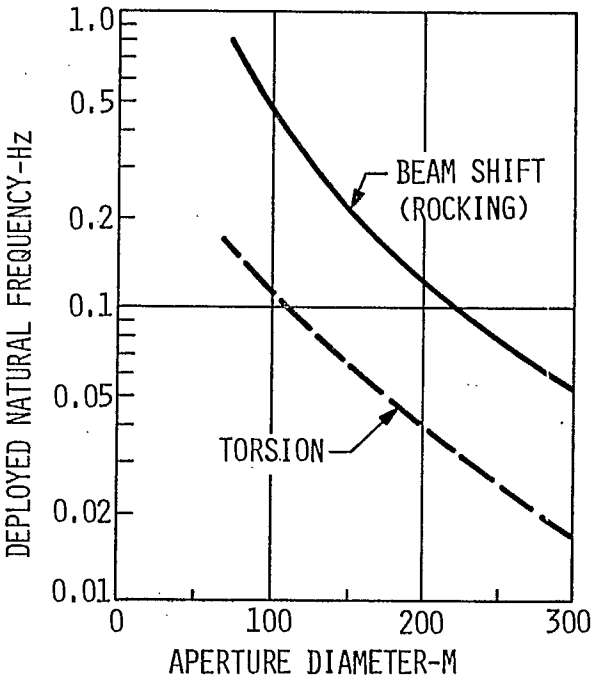

Figure 13. Deployed Reflector Natural Frequencies

SUMMARY AND CONCLUSIONS

The design and analyses performed to date indicate that the proven wrap-rib reflector design can be readily adapted to an offset reflector geometry with a manufacturing cost impact of approximately 5%. The adaptation retains the benefits of high density packaging and light weight. Growth potential exists for deploying offset-fed reflectors of the wrap-rib concept in sizes up to 300m. Vehicle interfacing requires a separate support boom to attach the central hub of the offset wrap-rib reflector to the vehicle. This boom must be designed to satisfy stability requirements of the antenna system since deformations will be additive to the reflector errors.

TRACKING AND DATA RELAY SATELLITE SINGLE ACCESS DEPLOYABLE ANTENNA

Dr. B.C. Tankersley and H.E. Bartlett
Harris Electronic Systems Division
Melbourne, Florida

Summary

The Tracking and Data Relay Satellite (TDRS) (Figure 1) utilizes two 4.8 meter deployable antennas for accessing and communicating with high data rate user satellites. These single access antennas operate at the dula frequencies of S- and Ku-band, with full tracking capability at Ku-band. The stringent gain and tracking requirements at Ku-band require state-of-the-art designs in the deployable reflector and the dual frequency feed system. To meet these requirements special surface shaping techniques and thermally stable materials were developed for the deployable reflector. A unique dual frequency cassegrain feed system utilizing sidelobe cross-over for tracking was developed to meet the tracking requirements. The feed system tracking performance is essentially insensitive to reflector distortions. This paper summarizes the design and performance of the TDRS single access antenna design.

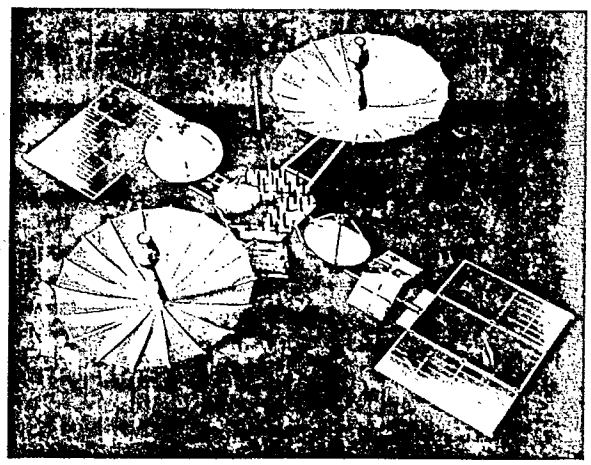

Figure 1. Tracking and Data Relay Satellite (TDRS)

I. Reflector Design

Figure 2 illustrates the deployable reflector design. The reflector utilizes eighteen graphite fiber reinforced plastic (GFRP) ribs to shape and support the reflective mesh surface. The number of ribs is based on a trade-off considering surface tolerance and weight. As the number of ribs increases, the surface error decreases, while weight increases. The minimum number of ribs consistent with the surface tolerance requirements is, therefore usually selected. The ribs are circular in cross-section tapering from 1.5-inches diameter at the root to 0.75-inches at the tip. The rib is constructed of 4 plies of HMS graphite oriented in a 90^{o}, 0^{o}, $\pm 45^{o}$ configuration. The resulting wall thickness is 0.016-inch. The reflective mesh surface is attached to the ribs by

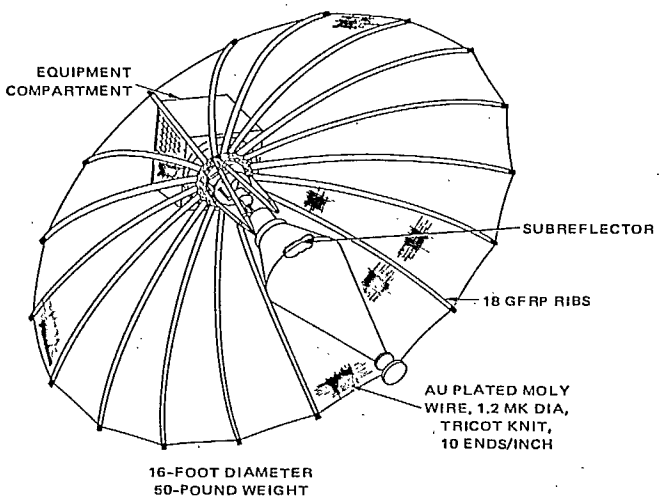

Figure 2. TDRS Single Access Antenna

adjustable standoffs and therefore the tolerance on rib shape is not a critical parameter. The ribs are typically fabricated to a constant radius of curvature rather than a parabolic shape.

The reflective mesh (Figure 3) consists of 1.2 mil diameter, gold-plated, molybdenum wire which is knitted into a soft (low spring rate), elastic mesh. The mesh opening size

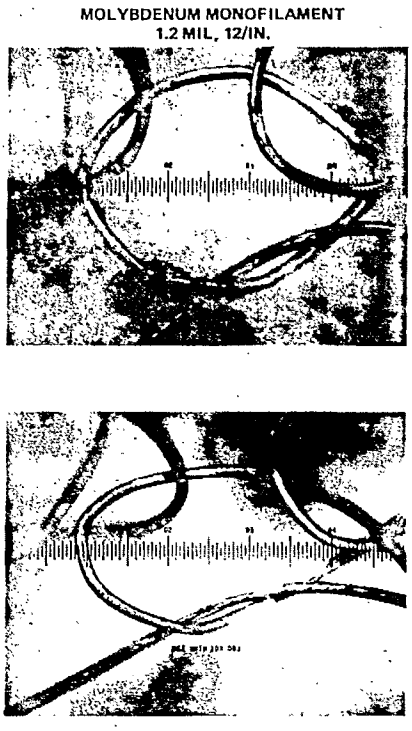

Figure 3. Molybdenum Wire Mesh

can be varied to ensure adequate RF reflectivity for a given requirement. The mesh opening size for the TDRS reflector is 0.1 inches. The required reflector surface tolerance is achieved with minimum weight through the use of a secondary drawing surface technique. This technique is illustrated in Figure 4. A series of circumferential quartz cords is attached to the back of the ribs by adjustable standoffs. A second series of quartz cords is attached to the front mesh surface as shown in Figure 5. These "front" cords run parallel to the "back cords". The front and back cords are connected by a series of beta glass tie wires (see Figure 4 and 5). By properly adjusting the rib stand-off heights, the back cord geometry, and these individual tie wires, a very accurate surface contour is achieved.

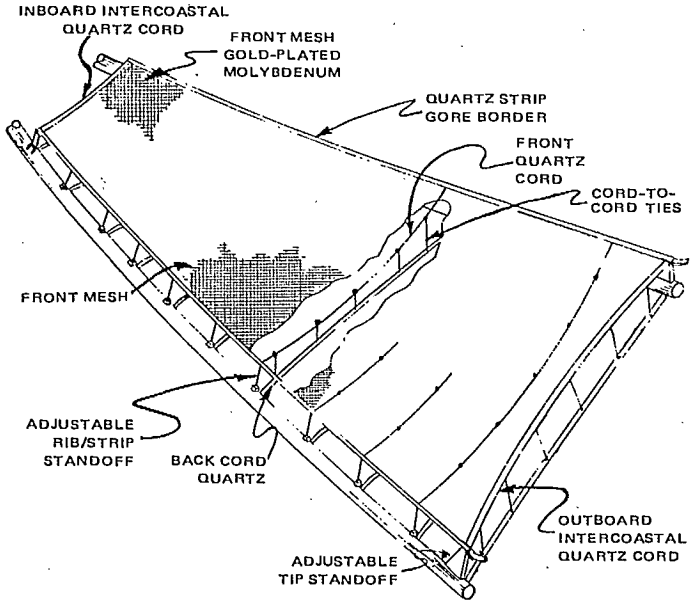

Figure 4. Dual Surface Design

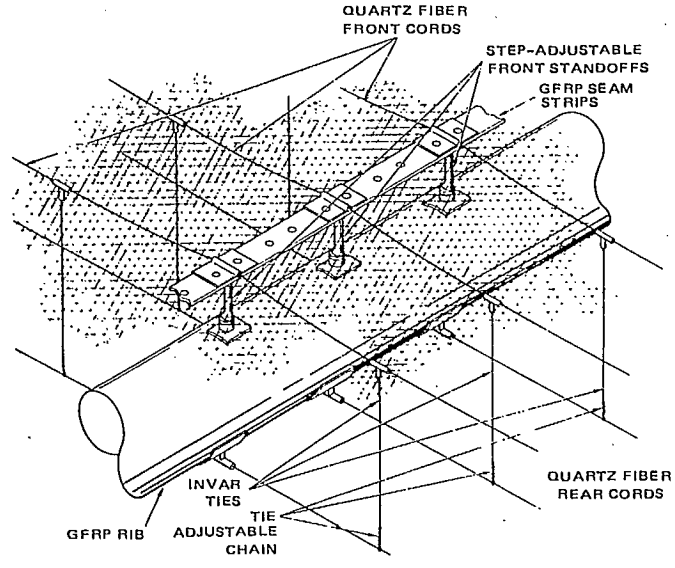

Figure 5. Surface Design Details

Setting the reflector surface is illustrated in Figure 6. The reflector contour is measured in the face-up and the face-down positions. The measured face-up and face-down positions are then averaged to determine the "zero-gravity" surface contour. This contour is then compared on a point-by-point basis with the desired parabolic contour and surface adjustments made as necessary to achieve the desired manufacturing contribution to the total surface tolerance budget. The setting process is iterative, with each setting iteration requiring approximately one

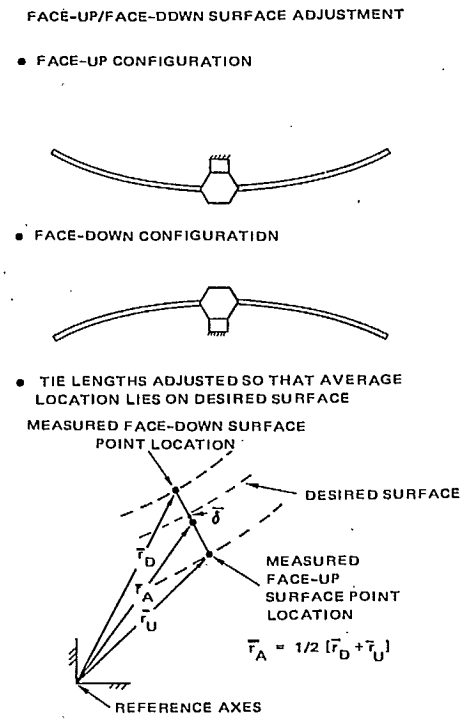

Figure 6. Surface Setting Technique

week. Two to three setting iterations are usually required to achieve a high accuracy contour. As shown in Figure 6, there is an error associated with the above described "averaging technique" due to the non-linearity of the reflector structure. Figure 7 illustrates the magnitude of surface distortions experienced with the 4.8 meter reflector for the TDRS program during the face-up, face-down measurement process. The error associated with averaging these distortions results in an uncertainty of the surface contour of 0.00012 inches RMS. The magnitude of the error is thus sufficiently small to be neglected. With larger reflectors, e.g. 15 meter diameter reflectors, the averaging technique yields equally valid results if the reflector ribs are counter balanced at the tips. This counter balancing limits the distortion range over which averaging is accomplished and results in an acceptably low error.

Deployment of the reflector surface is achieved in a totally controlled manner to

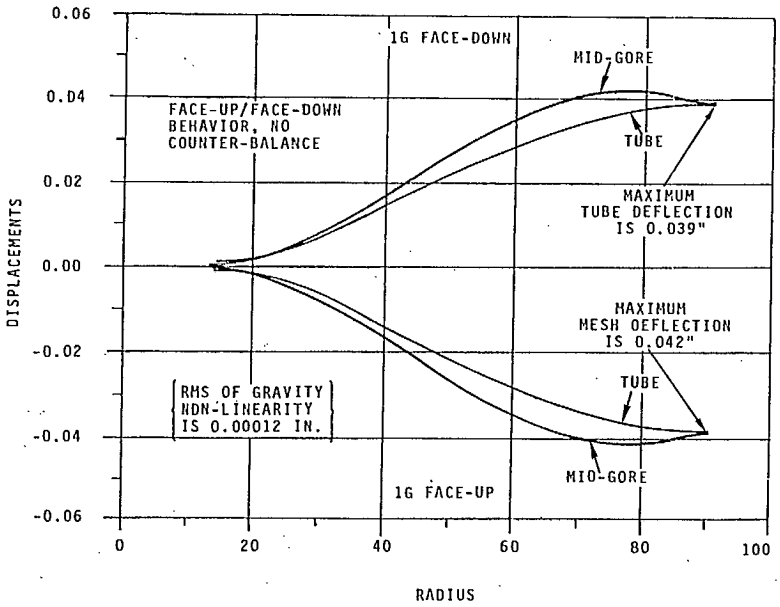

Figure 7. Gravity Distortions Are Sufficiently Small to Allow Averaging

ensure no degradation of the accurate reflector surface occurs and to essentially eliminate any transfer of stored energy to the spacecraft. The mechanical deployment system (MDS) is shown in Figure 8. The MDS consists of a carrier mounted to the moving section of a recirculating ballnut pair on a ballscrew shaft. Connected between the carrier and the ribs are pushrods that transmit the required force and motion to deploy the ribs. As the carrier moves along the screw shaft, the ribs are rotated from their stowed to their fully deployed position. Latching in the deployed position is accomplished by driving the carrier and linkages through an over-center condition (relative to the rib pivot position).

The feed support structure provides the primary structure for the stowed antenna as well as serving as the structure for support of the dual frequency feed and subreflector. This support structure consists of a 6 member GFRP truss structure and a monocoque (single skin) quartz radome structure. The subreflector is a sandwich construction of kevlar skins and a kevlar honeycomb core.

Thermal control of the reflector ribs and feed support structure is accomplished with multi-layered insulation blankets. These blankets utilize inner layers of 0.3 mil embossed aluminized kapton and an outer layer of 1 mil kapton with vapor deposited aluminum striping. The percentage of VDA striping is based on the average solar absorptivity (αs) and emissivity (ϵ) values desired. The number of layers is selected to provide a desired thermal time constant and to minimize distortions due to diametral temperature gradients.

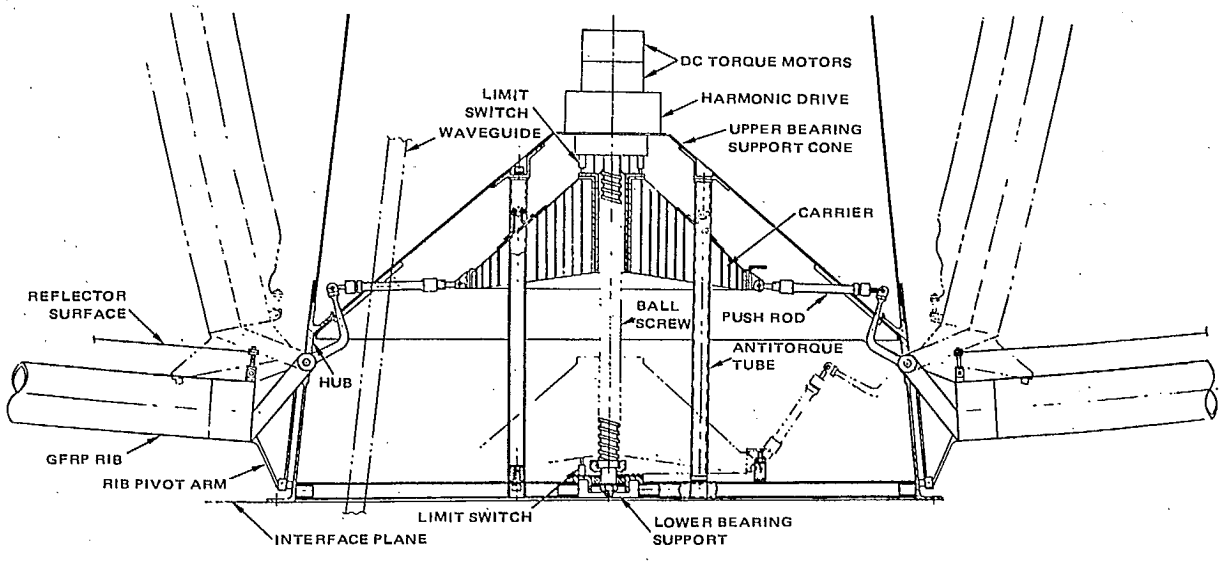

Figure 8. Hub

II. Feed Design

Five-Horn Cassegrain feeds[1] are very desirable for communications antennas for which the tracking requirements are usually not very stringent. The simplicity of the sum channel makes possible greater bandwidth and higher efficiency. The historical problem has been the tradeoff between a sufficiently large sum horn for good illumination efficiency and sufficiently small error horn spacing for adequate error channel secondary pattern crossover. Figure 9a illustrates the problem. When the error horn spacing is fixed so that the error horn secondary pattern crossover is at the first null (or on the main offset beam), the sum horn aperture size is such that large spillover past the subreflector is incurred. In order to make the sum horn larger (to reduce spillover), the error horn spacing must be increased resulting in a crossover on the first sidelobe.[2] Generally, crossover on the first sidelobe or beyond has been avoided because of the sensitivity of the low-level sidelobes to various factors, including reflector distortion, frequency change and blockage. The sensitivity of tracking performance to reflector distortion is especially important for spaceborne antennas.

A Five-Horn Cassegrain feed has been developed for the TDRSS 4.8-meter deployable antenna, which uses the up-taper of the dual shaped reflectors[3] in conjunction with a special error horn design to produce a stable tracking crossover on high-level sidelobes. This permits use of a larger sum horn, as illustrated in Figure 9b, and greater spillover efficiency.

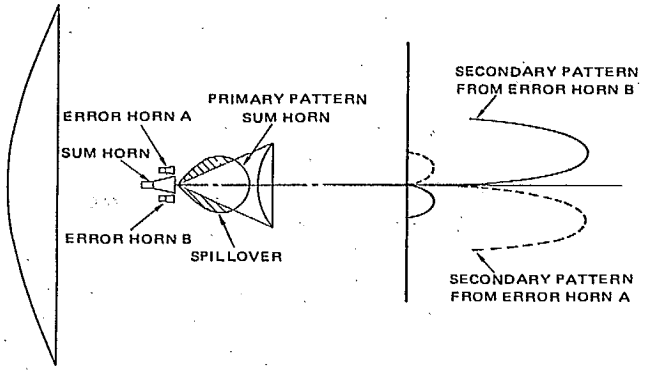

Figure 9a. 5-Horn Feed With Crossover in Null

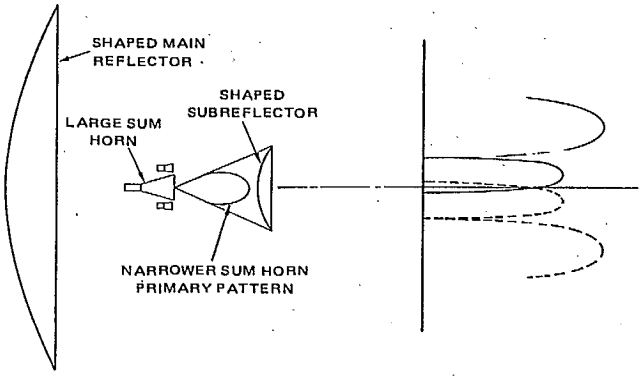

Figure 9b. Crossover on First Sidelobe

The error horns are rectangular with the narrow dimension in the plane of the associated tracking crossover. Because the error horns have a much broader illumination in this plane than the sum horn, the up-taper which produces uniform reflector illumination (maximum gain) for the sum channel results in a highly inversed distribution for the error horns, and hence the desired high sidelobes.

The performance of the five-horn feed was investigated both analytically and experimentally. The analysis consisted of a two-step vector Kirchhoff surface current integration over the dual-shaped Cassegrain antenna. Experimental results were obtained from a breadboard feed mounted in an existing 6 meter shaped reflector. The breadboard feed is shown in Figure 10. Figure 11 shows a comparison of measured and computed secondary offset error horn patterns. The sidelobe is not distinct from the main offset lobe because of phase aberration. The small disparity between the measured and predicted patterns is probably the result of surface errors of the 6 meter reflector. Figure 12 shows measured sum and difference patterns in the 6 meter reflector.

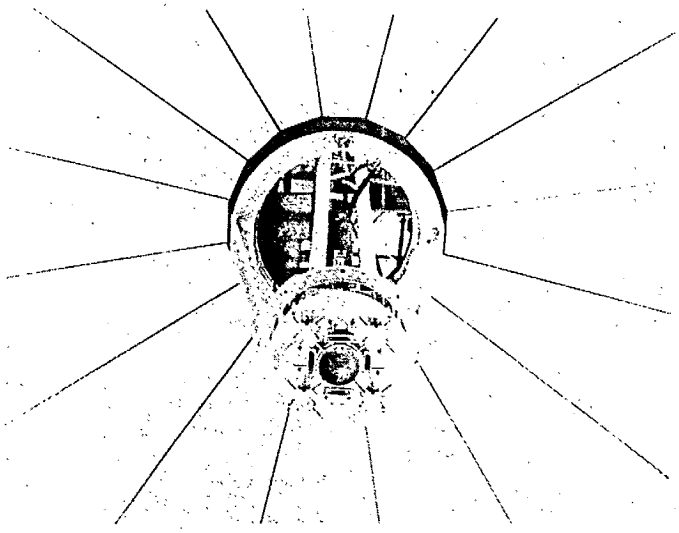

Figure 10. Breadboard Feed

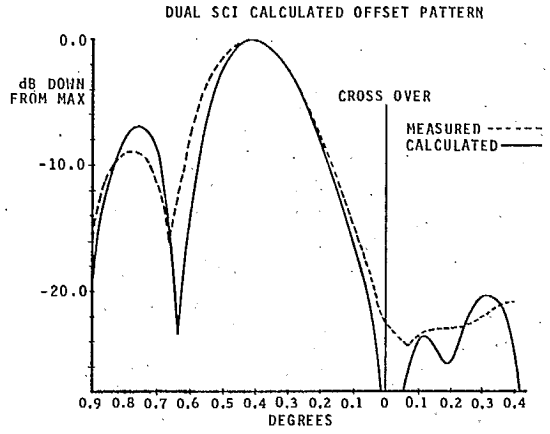

Figure 11. Experimental and Computed Results for the 5-Horn Feed in the 6M Reflector at 15 GHz. Computed Results did not Include the 0.040" RMS Reflector Roughness.

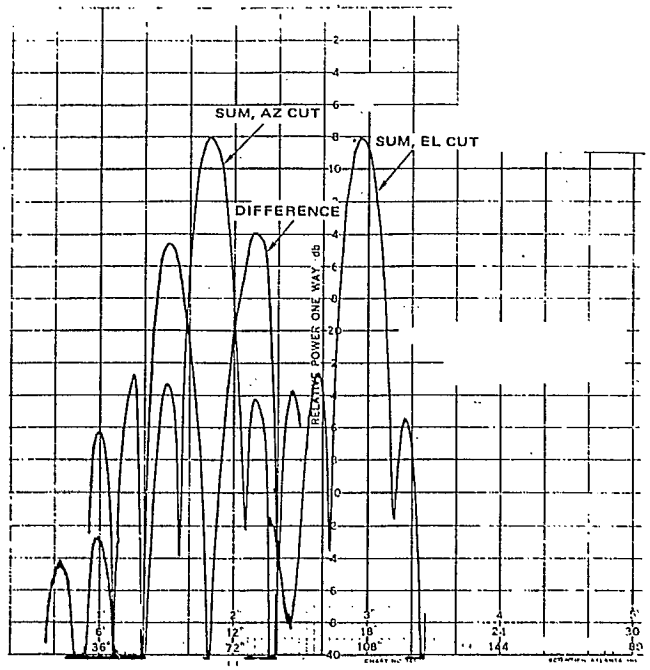

Figure 12. Sum and Difference Secondary Patterns in 20 Ft Reflector, 15.1 GHz

III. Antenna Performance

Orbital Antenna Gain performance is predicted both with loss budgets and with a composite computer math model. Although the composite math model provides a more accurate prediction, the loss budget has a diagnostic advantage in that the significance of the various components is revealed by inspection.

The loss budget for the 4.8 meter antenna is shown in Figure 13. The defocus, roughness, and pointing error losses are based on the budgeted worst case distortions given in Figure 14. The mesh reflectivity loss is based on measured values for the gold-plate estimated based on calculated flat-plate approximations and measurements on similar radomes on previous programs. The blockage loss is based on the aperture blockage resulting from the feed support structure. The feed related losses are based on measured range test results with the breadboard feed.

The defocus, roughness, and pointing error values for the reflector are shown in Figure 14. The pillow effects result from a natural phenomenon. Due to the pretension of the mesh and the doubly curved parabolic surface, the mesh tends to "pillow" toward the focal point. This phenomenon is described by the partial differential equations of membrane theory. The secondary drawing surface technique significantly reduces this error but the mesh between tie points still pillows toward the focal point, forming small "pillows" between adjacent tie points.

By far the largest source of surface tolerance is the manufacturing (or setting) tolerance. This error source represents the physical ability of technicians to adjust the surface and is also constrained by the schedule and dollars available to make iterative settings. Typically 2 to 3 iterations are required to achieve high precision surfaces. The manufacturing tolerance shown is based on actual measured hardware experience.

The thermal distortion effects of the reflector and feed support are determined using analysis techniques. Corc creep results from a slight permanent preset of the quartz cords when they are initially pretensioned. Preconditioning of the cords can be accomplished if this source of error becomes significant. Dryout shrinkage error results from changes in the dimensions of the GFRP ribs and feed support when moisture absorbed by the GFRP outgasses in the orbital environment. Both the cord creep and GFRP dryout error have been verified by element tests of these materials.

As shown, a biasing strategy is used with respect to the defocus effects of the

	2.025	2.2	2.3	11.7	14.0	13.75	14.896	15.121
DEFOCUS	--	--	--	0.11	0.16	0.15	0.18	0.19
ROUGHNESS	0.01	0.01	0.01	0.36	0.51	0.49	0.58	0.60
MESH REFLECTIVITY	0.03	0.03	0.03	0.46	0.53	0.53	0.57	0.58
SCALLOP LOSS	0.23	0.23	0.23	0.19	0.19	0.19	0.19	0.19
RADOME LOSS	0.05	0.05	0.05	0.20	0.20	0.20	0.20	0.20
BLOCKAGE	0.22	0.22	0.22	0.22	0.22	0.22	0.22	0.22
FEED LOSS	0.58	0.58	0.61	0.50	0.30	0.30	0.30	0.30
VSWR	0.15	0.15	0.15	0.10	0.05	0.05	0.05	0.05
SPILLOVER-TAPER	1.78	1.95	2.24	1.11	0.72	0.72	0.72	0.72
	3.05	3.22	3.54	3.25	2.88	2.85	3.01	3.05
100% GAIN	40.08	40.80	41.18	55.31	56.87	56.72	57.41	57.54
NET GAIN	37.03	37.5	37.64	52.06	53.99	53.87	54.40	54.49
SPEC	36.0	36.8	36.8	50.0	52.8	52.6	53.6	53.6
MARGIN/MEASUREMENT TOLERANCE	1.0	0.8	0.8	2.1	1.2	1.3	0.8	0.9

Figure 13. Antenna Loss Budget

	ΔF (IN)	RMS (IN)
PILLOW ERROR	--	0.010
MANUFACTURING ERROR	--	0.018
SURFACE THERMAL	+0.080	0.005
FEED SUPPORT THERMAL	+0.030	--
RIB DRYOUT SHRINKAGE	+0.027	0.001
CORD CREEP	+0.022	--
COMBINATION	+0.159	0.024
BIAS	-0.103	
PREDICTED VALUES	+0.057	0.021
UNCERTAINTIES	±0.057	0.008
WORST-CASE	0.113	0.0226

Figure 14. Reflector Distortions

above error sources. The resulting predicted values shown are then modified by the value of the various uncertainty contributions. The uncertainty budget is shown in Figure 15. The uncertainties include measurement accuracy, deployment repeatability, uncertainties in the thermal and elastic properties of the materials, and variations to account for manufacturing tolerances (e.g. cord and mesh pretension) and analysis uncertainties. Combination of the RSS value of the uncertainties with the predicted values provides the worst-case distortion budget values shown in Figure 14.

The predicted effect of reflector surface errors has good accuracy because the defocus and mispointing values produced by the various contributions are summed before the loss computation.

A more exact calculation of the gain can be made by super-imposing all of the physical surface errors and computing the gain with the surface current integral program. The accuracy of this result depends upon the accuracy of the assumed patterns of error variations over the aperture. On previous programs the gains calculated by the two methods have agreed to within 0.1 dB.

	ΔF (INCHES)	RMS (INCHES)
SURFACE MEASUREMENT	0.003	0.004
ALIGNMENT	0.003	
STRUCTURAL MOVEMENT	--	--
NON-LINEARITY	0.003	0.001
COUNTER WEIGHT LOAD	--	--
DEPLOYMENT NON-REPEATABILITY	0.038	0.006
TEMP. VARIATION AT SETTING	--	--
RIB STIFFNESS	--	--
CORD & INTERCOSTAL STIFFNESS	0.001	--
MESH IN-PLANE STIFFNESS	0.003	--
CORD - CTE	0.009	0.001
INTERCOSTAL - CTE	--	--
MESH - CTE	--	--
RIB - CTE	--	--
MESH TEMP., +25°F	0.002	--
CORD & INTERCOSTAL TEMP., -50°F	0.002	--
TIES +50°F	--	--
RIB AVG. TEMP., -30°F	0.008	--
RIB GRADIENT, +2°F	0.003	--
HUB TEMP UNCERT., ±25°F	0.020	--
CORD & JOINT CREEP/CONDITIONING	0.022	--
MESH & CORD PRETENSION VARIATION	0.002	--
PILLOW-MESH TENSION	--	0.003
RIB DRYOUT SHRINKAGE	0.027	0.001
STRUCTURAL ANALYSES	--	--
RSS	0.057	0.008

Figure 15. Uncertainties, Summary Table

References

(1) Dunn, J.H. et al, "Tracking Radar", Radar Handbook, M.I. Sholnik, ed., McGraw-Hill 1970.

(2) Deerkoski, L.F. and Schmidt, R.F., "Switchable Beamwidth Monopulse Method and System", Patent-3 965 475, June 1976.

(3) Galindo V., "Design of Dual Reflector Antennas with Arbitrary Phase and Amplitude Distributions" IEEE TAP, Vol. AP-12, pp. 403-408, July 1964.

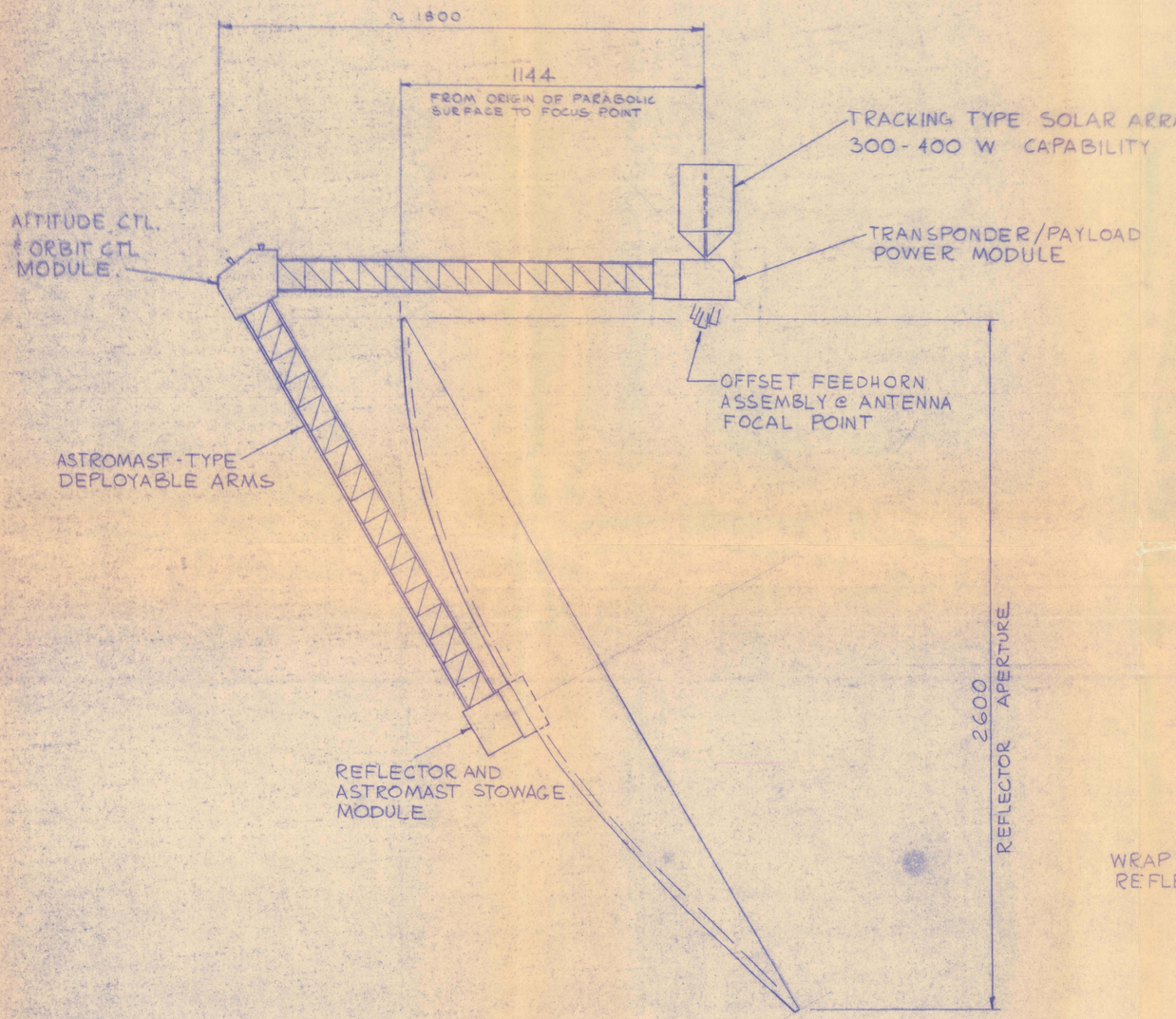

S/C WITH DEPLOYED ANTENNA

VIEW FROM EAST

LMSC WRAP RIB PARABOLIC REFLECTOR WITH MULTIBEAM OFFSET FEED

$f/D = 0.44$

1/100 SCALE

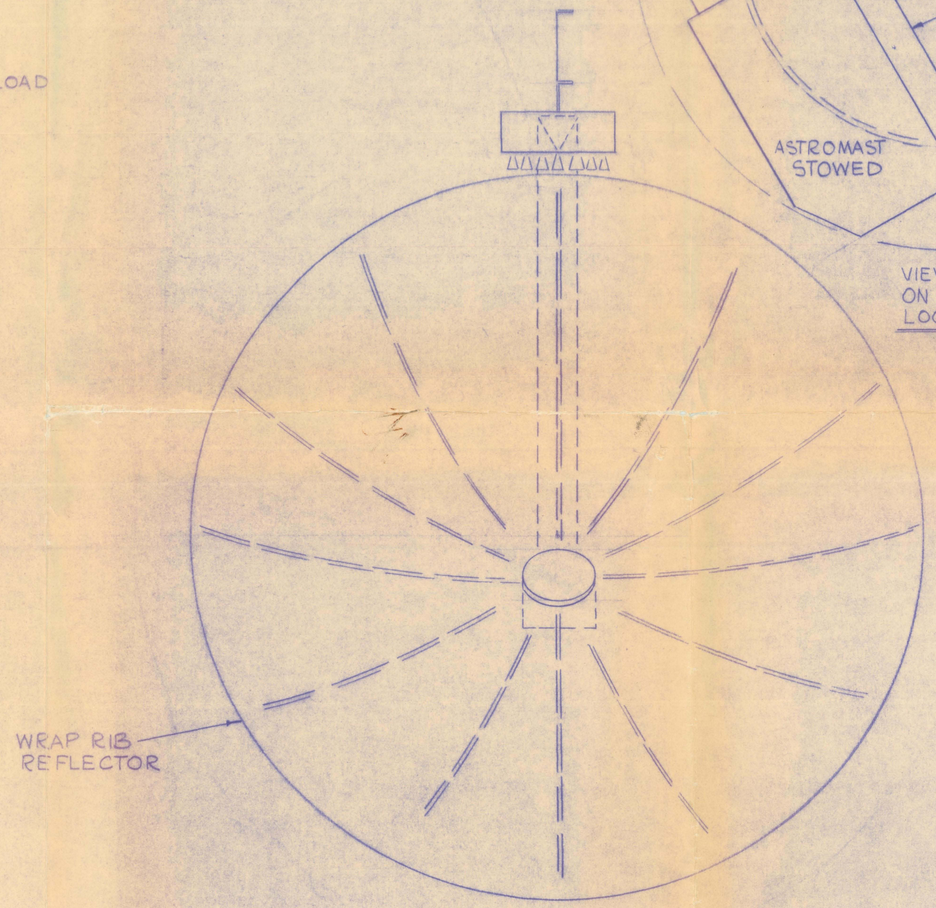

VIEW FROM EARTH

1/100 SCALE

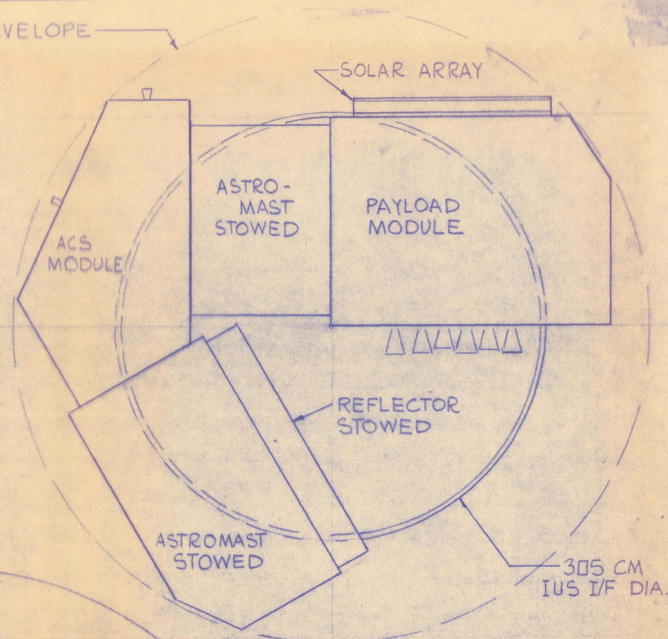

VIEW OF STOWED S/C ON IUS IN STS CARGO BAY LOOKING FORE/AFT

1/20 SCALE

NOTES

1. ELECTRIC PROPULSION CAN BE USED IN ALL 3 MODULES ; IF REQ'D. FOR E/W STA. KEEPING & ATT. CTL.
2. DEPLOYMENT SEQUENCE :
   - SEPARATE FROM IUS @ GEO
   - DEPLOY SA.
   - DEPLOY BOOMS SEQUENTIALLY
   - DEPLOY REFLECTOR
   - ACQUIRE ATTITUDE
3. AUXILIARY SOLAR ARRAYS MAY BE NEEDED @ EACH MODULE
4. WT. MUST BE LESS THAN 5000 LB. FOR IUS LAUNCH
5. MECHANICAL ADJUSTMENT OF REFLECTOR RELATIVE TO FEED ASSY. COULD BE INCORPORATED IF REQ'D.
6. POWER XFER TO ACS & REFLECTOR MODULES IS BY WIRE.
7. REFLECTOR DRAWN AS CIRCULAR, AS VIEWED FROM EARTH - BUT LIKELY WOULD BE OPTIMIZED SHAPE FOR CANADA COVERAGE.
8. NON-CONDUCTIVE BOOM FROM COMM. MODULE DIRECTLY TO CTR OF REFLECTOR IS OPTIONAL CONFIGURATION - IT INTRODUCES SOME BLOCKAGE.

TOLERANCES UNLESS OTHERWISE SPECIFIED		CANADIAN ASTRONAUTICS LIMITED		
☑ METRIC	☐ BRITISH	Suite 201, 1024 Morrison Drive, Ottawa, Ontario K2H 8K7 (613) 820-8280		
DIMENSIONS IN ☐ mm ☑ cm UNLESS OTHERWISE SPECIFIED	DIMENSIONS IN INCHES UNLESS OTHERWISE SPECIFIED FRACTIONS UNDER 6" ± 1/64; 6" - 24" ± 1/32; OVER 24" ± 1/16; DECIMALS XXX ± .005, XX ± .010, X ± .015		NAME	DATE
		DRAWN BY	RB	JULY '79
		CHECKED BY		
		MECHANICAL		
NO DECIMAL ± .5 mm; .X ± 1 mm		ELECTRICAL		
ANGLES ± 1/2°		APPROVED BY		

PROJECT: LARGE ANTENNA

TITLE: MOBILE COMSAT DESIGN CONCEPT USING OFFSET FEED LMSC WRAP RIB ANTENNA

DRAWING NO: FIGURE 3-21

REVISION: —

SCALE: NOTED

SHEET 1 OF 1